
Masters Theses

Student Theses and Dissertations

Spring 2014

An investigation of contaminant metal distribution and mineral speciation in the soil near the Buick Recycling Division smelter, Iron County, Missouri

Krista Nicole Rybacki

Follow this and additional works at: https://scholarsmine.mst.edu/masters_theses



Part of the [Geology Commons](#), and the [Geophysics and Seismology Commons](#)

Department:

Recommended Citation

Rybacki, Krista Nicole, "An investigation of contaminant metal distribution and mineral speciation in the soil near the Buick Recycling Division smelter, Iron County, Missouri" (2014). *Masters Theses*. 7273.
https://scholarsmine.mst.edu/masters_theses/7273

This thesis is brought to you by Scholars' Mine, a service of the Missouri S&T Library and Learning Resources. This work is protected by U. S. Copyright Law. Unauthorized use including reproduction for redistribution requires the permission of the copyright holder. For more information, please contact scholarsmine@mst.edu.

AN INVESTIGATION OF CONTAMINANT METAL DISTRIBUTION AND
MINERAL SPECIATION IN THE SOIL NEAR THE BUICK RECYCLING DIVISION
SMELTER, IRON COUNTY, MISSOURI

by

KRISTA NICOLE RYBACKI

A THESIS

Presented to the Faculty of the Graduate School of the
MISSOURI UNIVERSITY OF SCIENCE AND TECHNOLOGY

In Partial Fulfillment of the Requirements for the Degree

MASTER OF SCIENCE IN GEOLOGY AND GEOPHYSICS

2014

Approved by

David J. Wronkiewicz, Advisor
John P. Hogan
Cheryl M. Seeger

© 2014

Krista Nicole Rybacki

All Rights Reserved

ABSTRACT

Trace metal contamination studies were conducted near the Buick Resource Recycling Division. This study used sequential extraction, total digestion, X-Ray Diffraction (XRD), and Scanning Electron Microscopy-Energy Dispersive Spectroscopy (SEM-EDS) to study trace metals in two soil cores. Sequential extraction analysis of the soil cores revealed that lead was associated with either iron or manganese oxides. Zinc and copper were bound to soil components, extracted mainly from organics, sulfides, and clays. Total digestion results compared favorably to the sum of the sequential extraction results for lead, thus validating the sequential extraction methodology. The highest concentration observed for lead was 4,743 parts per million (ppm) in the Oh soil horizon in the core located 0.72 km NW from the smelter.

Most trace metals were concentrated in the top few inches of each core, a finding consistent with previous studies. However, nickel and copper concentrations increased from 9 to 16 inches of depth in one core. Antimony and cadmium were present in small amounts (<20 ppm) in the upper portion of the soil cores. Iron concentrations increased with depth in both cores.

Samples were analyzed for mineral species and pH. SEM-EDS analysis revealed lead-bearing particles with a subhedral, platy habit, and a composition suggesting the presence of cerussite (PbCO_3). XRD results suggest that the majority of the clay-sized fraction of the soil is comprised of both kaolinite and illite. Smectite was present in small amounts and may influence metal immobilization. Soil acidity increased with depth, which is consistent with previous studies. The data from this study can be added to previous studies conducted in the area to provide nearly a 40 year record.

ACKNOWLEDGMENTS

Thanks to my advisor, Dr. David Wronkiewicz, who provided guidance, patience, and knowledge. Thanks also to my committee members, Dr. John P. Hogan and Dr. Cheryl M. Seeger, for their comments and suggestions that only improved this thesis. Thank you to all those faculty and staff in the Geology and Geophysics department. Thanks to Eric Bohannon and Clarissa Wisner of the Advanced Materials Characterization Laboratory for assistance with XRD and SEM-EDS analyses, respectively. Dr. Honglan Shi of the Environmental Research Center provided assistance with the ICP-OES analyses. I extend my thanks to Dr. Emitt Witt for his assistance in the lab and guidance on the BCR extraction procedure during the project.

I would like to thank the Chancellor's Fellowship and the Geology & Geophysics Radcliffe Trust Fund for financial support.

In the lab, I would like to acknowledge Varun Paul for all his assistance when lab work became a little overwhelming for one person. Thanks to Bobby Swain for his ability to entertain and distract me and Alsedik Abousif deserves thanks as well for helping me out in the lab when necessary. I would like to thank all of my friends who helped me recharge and take a break every so often.

My family has been my support in everything I do. I'd like to thank my mom, grandma, and brother for reminding me that everything is achievable if you set your mind to it and always being there when I needed them.

Finally, I dedicate this thesis to my dad, who wasn't able to see it completed, but was with me all along the way.

TABLE OF CONTENTS

	Page
ABSTRACT	iii
ACKNOWLEDGEMENTS	iv
LIST OF ILLUSTRATIONS	viii
LIST OF TABLES	x
SECTION	
1. INTRODUCTION	1
1.1. LOCATION AND HISTORY	2
1.2. LEAD IN SOIL	4
1.2.1. Lead Minerals	4
1.2.2. Use of Leaded Gasoline	5
1.2.3. Smelting Related Activities	6
1.2.4. Vegetation	6
1.2.5. Factors that Affect Mobility	6
1.3. OTHER METALS IN SOIL	7
1.3.1. Soil pH and Conditions	7
1.3.2. Soil Constituents	9
1.4. GEOLOGICAL BACKGROUND	10
1.4.1. Soils of the Study Area	11
1.4.2. Soil Horizons	13
1.5. PREVIOUS STUDIES OF THE AREA	14
2. EXPERIMENTAL PROCEDURES	17
2.1. SAMPLE LOCATION AND CORING	17
2.2. SEQUENTIAL EXTRACTION	18
2.3. TOTAL DIGESTION	22
2.4. X-RAY DIFFRACTION (XRD)	24
2.5. SCANNING ELECTRON MICROSCOPY - ENERGY DISPERSIVE SPECTROSCOPY (SEM-EDS)	25
2.6. SOIL pH	27
2.7. ICP-OES PROCEDURE AND QUALITY CONTROL	28

2.7.1. Sequential Extraction Quality Control	29
2.7.2. Total Digestions Quality Control	30
2.7.3. Manganese Quality Control.....	31
3. RESULTS.....	33
3.1. TOTAL DIGESTION CONCENTRATIONS.....	33
3.1.1. Core 2 Results	34
3.1.2. Core 4 Results	35
3.2. SEQUENTIAL EXTRACTION RESULTS.....	37
3.2.1. Core 2, Extract A Results	38
3.2.2. Core 2, Extract B Results	38
3.2.3. Core 2, Extract C Results	40
3.2.4. Core 2, Extract D Results	40
3.2.5. Core 4, Extract A Results	43
3.2.6. Core 4, Extract B Results	44
3.2.7. Core 4, Extract C Results	45
3.2.8. Core 4, Extract D Results	46
3.3. SOIL MINERALOGY.....	48
3.4. SEM-EDS RESULTS/MINERAL SPECIES	51
3.5. SOIL pH.....	57
4. DISCUSSION	59
4.1. TOTAL DIGESTIONS.....	59
4.2. SEQUENTIAL EXTRACTION	62
4.3. SEM-EDS	67
4.4. FACTORS POTENTIALLY AFFECTING LEAD MOBILITY.....	69
4.4.1. Clay Mineralogy.....	69
4.4.2. Soil Grain Size.....	71
4.4.3. pH.....	71
4.4.4. Potential Weather Conditions.....	72
4.5. COMPARISON TO PREVIOUS STUDIES.....	74
4.5.1. Lead Concentrations.....	74
4.5.2. Other Metals Comparisons.....	77
4.5.3. Sequential Extraction Comparison.....	78

4.6. COMPARISON TO OTHER SMELTER STUDIES	79
5. CONCLUSIONS	81
APPENDICES	
A. PREVIOUS STUDIES DATASETS.....	83
B. QUALITY CONTROL DATA.....	88
C. SEQUENTIAL EXTRACTION DATASETS	98
D. TOTAL DIGESTION DATASETS	107
E. X-RAY DIFFRACTION (XRD) RESULTS	109
F. pH DATASET AND QUALITY CONTROL	119
BIBLIOGRAPHY.....	121
VITA	125

LIST OF ILLUSTRATIONS

Figure	Page
1.1. Location map of the Buick Resource Recycling Smelter in Iron County, Missouri ...	3
1.2. Locations of the four soil core sampling points of Rucker (2000)	3
1.3. Metal adsorption vs. pH plots	8
1.4. Solubility of lead, zinc, and copper vs. pH plots	9
1.5. Soil survey northwest of the Buick Recycling Smelter	12
1.6. Typical soil horizon profile.....	14
3.1. Concentration trends for core 2 total digestion experiments	35
3.2. Concentration trends for core 4 total digestion experiments	37
3.3. Extract A concentrations (in ppm) for core 2	39
3.4. Extract B concentrations (in ppm) for core 2.....	39
3.5. Extract C concentrations (in ppm) for core 2.....	41
3.6. Extract D concentrations (in ppm) for core 2	41
3.7. Extract A concentrations (in ppm) for core 4	44
3.8. Extract B concentrations (in ppm) for core 4.....	45
3.9. Extract C concentrations (in ppm) for core 4.....	46
3.10. Extract D concentrations (in ppm) for core 4	47
3.11. Percentages of isolated clay-size fraction particles in core 2	49
3.12. Percentages of isolated clay-size fraction particles in core 4	50
3.13. SEM image of a botryoidal-textured particle containing lead in core 2	53
3.14. SEM image and EDS data of a flaky-textured particle containing lead in core 2 ...	53
3.15. SEM image of two particles with lead in core 4.....	53
3.16. SEM image of a smooth particle with lead in core 4.....	55
3.17. SEM image and EDS spectra of a flaky particle containing lead in core 4	55
3.18. EDS spectra for a cerussite ($PbCO_3$) mineral standard in the Hitachi S-4700 Microscope.....	56
3.19. SEM-EDS results of a particle containing lead in core 2	57
3.20. Soil pH profiles for core 2 and core 4.....	58
4.1. Correlation coefficients for zinc, nickel, and copper in core 2 total digestions.....	61
4.2. Correlation coefficients for zinc, copper, and lead for core 4 total digestions	62
4.3. Percentage of lead contained in each extract for core 2 sequential extractions.....	64
4.4. Percentage of lead contained in each extract for core 4 sequential extractions.....	64

4.5. Correlation coefficients for zinc, nickel, and copper in core 2, Extract D	65
4.6. Correlation coefficients for zinc, nickel, and copper in core 4, Extract D	66
4.7. Metal concentration trends for core 2 compared to cores from similar locations in previous studies	75
4.8. Metal concentration trends for core 4 compared to cores from similar locations in previous studies	76

LIST OF TABLES

Table	Page
3.1. Background concentration levels for regional soils.....	33
3.2. Clay distribution in soil cores in percent	49

1. INTRODUCTION

Missouri, host to several lead districts, is familiar with deleterious environmental effects of metals mining, smelting, and recycling smelting processes (Butherus, 1975; Bornstein, 1989; Rucker, 2000). Primary smelting processed several metal sulfides that occur naturally, one of which is galena (PbS). Processes now involve the retrieval of lead from recycled materials. When lead-bearing particles are released from smelter stacks and interact with oxidizing environments, they become unstable due to: the oxidation of sulfur from the sulfide (S^{2-}) to higher valence states (e.g., SO_4^{2-}); reactions with dilute acids present in the soil profile; or solubility constraints between water and the lead-bearing minerals that are present. Both the release of lead into the atmosphere and subsequent reaction of the lead in the soil leads to increased transport, posing a potential health risk to all those who live near smelters.

Elevated levels of trace metals in the soil, including lead, have been noted around the Buick lead recycling smelter for many decades. The four previous studies conducted by Bolter (1974), Butherus (1975), Bornstein (1989), and Rucker (2000) provide a 30 year record of trace metal contamination. Rucker's study included four sample sites northwest of the Buick smelter. The present study revisits two of these four sites.

The purpose of this study is to determine recent levels of metal concentrations in the soils in regards to the distance from the smelter and increasing depth of the soil core. Analysis of the soil for concentrations of zinc, iron, manganese, cobalt, nickel, copper, cadmium, antimony, lead, arsenic, and phosphorus were conducted for comparison to previous studies. This data is compared to previous studies to determine changes in

metal concentrations over time. In addition, studies on soil mineralogy and pH provide valuable information on factors influencing trace metal transport and adsorption.

1.1. LOCATION AND HISTORY

The Doe Run Company's Buick Resource Recycling Division (BRRD) smelter is located 4 miles south of Bixby, Missouri in Iron County. Highway 32 is just north of the facility, while Highway KK is west and southwest of the facility (Figure 1.1). The BRRD and core locations are denoted on the Viburnum West Quadrangle, 7.5 minute series (Figure 1.2). Core 2 is located 0.72 km N 40 W direction of the smelter. Core 4 is located 1.55 km along the same path from the smelter. Both core locations were located on hillcrests to minimize water runoff and erosion. The overall area sees an annual average temperature of 54 to 59°F. Precipitation averages 39 to 49 inches per year (U.S.D.A., 2013).

Originally opened in 1968 as a primary lead smelter for the Buick Mine, the smelter was owned by the AMAX Lead Company of Missouri and Homestake Mining Company (Bornstein, 1989; Jackson and Watson, 1977; Rogers and Davis, 1977; Rucker, 2000). It was originally referred to as the AMAX smelter during AMAX Lead Company ownership; it was subsequently named the Buick Smelter. The smelter had a brief shut down in 1986 and sporadic operations in 1987 and 1988 (Bornstein, 1989; Rucker, 2000). In 1988, the smelter was converted to a secondary smelter, with only the responsibility of recycling lead. A forest fire burned the areas of cores 1 and 2 in 1991 (Rucker, 2000). Rucker (2000) stated during his study that the facility was producing around 120 thousand tons of recycled lead yearly. As reported in the 2012 Sustainability Report

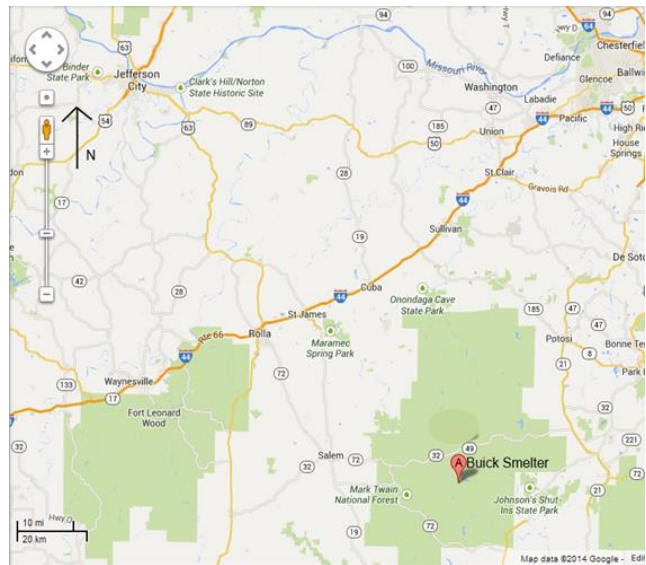


Figure 1.1. Location map of the Buick Resource Recycling Smelter (A) in Iron County, Missouri. The smelter is located about 25 miles east of Salem, Missouri, and just south of Highway 32 (Google Maps, 2014).

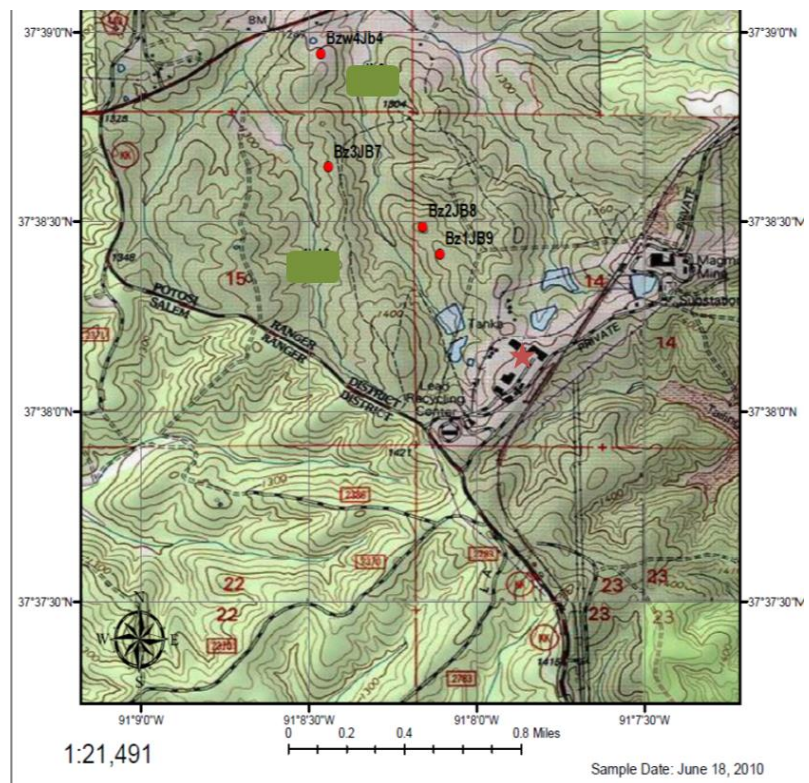


Figure 1.2. Locations of the four soil core sampling points of Rucker (2000). The samples align in the northwest direction from the smelter (denoted by red star). Sample cores for the present study were collected at locations Bz2JB8 and BzW4JB4 (core 2 and core 4, respectively) and were taken as close as possible to those in Rucker's.

published by the Doe Run Company, the secondary smelter has the ability to recover 160 thousand tons of lead from nearly 13.5 million recycled lead-acid batteries yearly. Other lead-bearing materials are also recycled at the facility and it has become one of the world's largest single-site recycling centers (The Doe Run Company, 2012).

1.2. LEAD IN SOIL

Lead is usually introduced to the environment by being weathered from Pb-bearing solids (bedrock), use of leaded gasoline, and mining related activities (Hettiarachchi and Pierzynski, 2004). Additionally, movement of ores, via trains or trucks to a smelting facility, provides the opportunity for metal contaminants to be inadvertently released and introduced into the soil along transit routes. Each of these processes release different phases of lead, all of which have different solubility products and dissolution rates.

1.2.1. Lead Minerals. Ruby et al. (1994) stated that ore lead phase materials are generally galena, anglesite (PbSO_4), and cerussite (PbCO_3) while paint contains a basic lead carbonate ($2\text{PbCO}_3 \cdot \text{Pb}(\text{OH})_2$). The most stable phases are lead phosphates (pyromorphite), which are less soluble than the carbonate, sulfate, oxide, and hydroxide phases of lead (Hettiarachchi and Pierzynski, 2004; Ruby et al., 1994). While galena can be stable in reduced systems with sulfur, exposure to oxygen or other redox sensitive materials may destabilize the S^{2-} ion, and allow lead to complex with other local components to form minerals like anglesite, cerussite, and pyromorphite (Hettiarachchi and Pierzynski, 2004).

McBride (1994) stated that solubilized lead usually exists as Pb^{2+} in soil. This ion becomes less soluble with higher pH conditions in oxidizing conditions. Due to its strong ability to complex with organic material in the soil, lead is often retained in the upper organic-rich layers of soil. Its movement downward is the slowest of all the heavy metals, and is slowest in reduced or nonacidic conditions (McBride, 1994).

Rucker (2000) analyzed a cubic particle isolated from a soil sample in the Scanning Electron Microscope-Energy Dispersive Spectroscopy (SEM-EDS) analysis, which he believed represented the presence of an altered galena grain, with an oxidized coating of anglesite ($PbSO_4$) on the galena crystal. Witt et al. (2013, 2014) in a study of road dusts in southeast Missouri (Viburnum Trend district) near the current study area found a weathered galena particle (2013) and cerussite crystals (2014). The presence of a galena particle in the soil almost 25 years after primary smelting denotes a slow kinetic weathering process.

1.2.2. Use of Leaded Gasoline. Deposition of automotive exhaust from leaded gasoline is another viable source of lead release into the soil. The U.S. Clean Air Act of 1970 has since limited the use of leaded gasoline. Wu and Boyle (1997) studied lead concentrations in the North Atlantic Ocean and noted that the concentrations decreased in the 1980s due to the phasing out of leaded gasoline. Wong and Li (2004) conducted a study of lead in soils in Hong Kong and found that those areas or soils in close proximity to greater traffic volumes were contaminated. This was most likely due to vehicle emissions in the past, since leaded gasoline was phased out in Hong Kong in 1999. Leaded gasoline is likely to play a minimum role in the soil contamination in the current study area, due to the fact that the sample locations are located in a forested area away

from any nearby influence of urban centers and high traffic roads. Core 4 resides the closest to a road, around 0.1-0.2 miles south of Missouri Highway 32.

1.2.3. Smelting Related Activities. There are two separate types of recycling processes that accompany the processing of lead batteries. Sometimes a site will only break the battery and retrieve lead. Other sites also smelt and refine the lead. The latter is responsible for causing contamination via stack emissions (Nedwed and Clifford, 1997). McBride (1994) stated that soils contaminated as a result from aerial emissions do not show significant metal leaching over time spans of years.

Smelting of ore was most likely the reason for the introduction of trace metals into the soil at the BRRD site in the past. Current additions, if any, to those metals are most likely associated with air emissions from recycling processes now underway at the smelting site. Primary smelting is a potential source of lead currently in the soil.

1.2.4. Vegetation. Metals available in the soil also become susceptible to plant uptake. This poses a potentially severe risk to the vegetation and the organisms that live in the soil. Jackson and Watson (1977) studied the effects of heavy metals in soils near what is now the BRRD. They noted depletion of soil and litter nutrient pools, which was supported by the lack of decomposer communities. In regards to vegetation, they found high concentrations of lead in the soil, roots, boles, and leaves of mature oaks. In addition to the direct fallout of metals onto the soil and forest floor litter, the leaves provide a potential source of metals. Metals accumulated on the vegetation canopy can be introduced into the soil each year with the annual litterfall onto the soil surface.

1.2.5. Factors that Affect Mobility. Several other factors affect the mobility of the heavy metals through the soil profile. Stevenson and Welch (1979) speculated that

movement of lead in their study of field soil is due to several factors, one of which is organisms moving downward through the soil. They also suggest that during times of extreme dryness, soils could be transported by physical processes through cracks that may form. Chemical and mineralogical variations within the soil in regards to pH, clay content, and organics play large roles in heavy metal mobility (Martínez-Villegas et al., 2004; Zimdahl and Skogerboe, 1977).

1.3. OTHER METALS IN SOIL

While lead is the primary metal of concern in this study, other metals like zinc, cobalt, cadmium, antimony, nickel, and copper are of interest as they are also present in the lead-zinc ores or lead-acid batteries. Low concentrations are generally not of concern, because organisms and plants can adapt to slight increases of metal concentrations. However, when concentrations increase in soils and waters, organisms may not adapt to such a large variation, and the metal becomes toxic (NIOSH, 2007). Trace metal movement through the soil is influenced by soil conditions and potential adsorption sites in the soil.

1.3.1. Soil pH and Conditions. Soil pH appears to be a major factor in the mobility and solubility of the trace metals as well as the minerals these metals may associate with. For example, manganese oxides show a greater adsorption over a larger pH range than iron oxides (Figure 1.3).

Zinc in acidic and oxidizing conditions is very soluble and mobile when in the Zn^{2+} state (McBride, 1994). Cobalt adsorbs best in oxidizing conditions in soils and mobility is best in acidic soils (McBride, 1994). Cadmium in acidic soils has high

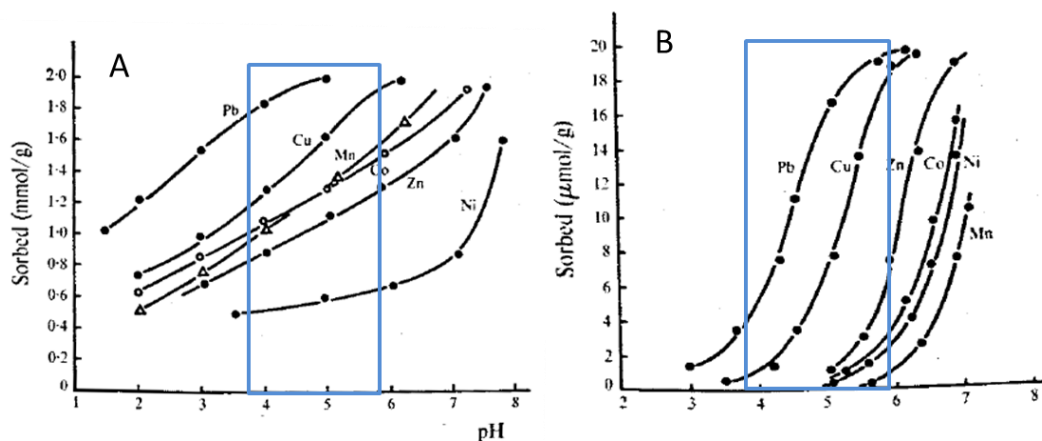


Figure 1.3. Metal adsorption vs. pH plots. On A) manganese oxide (birnessite) and on B) iron oxide (hematite). The blue boxes indicate the range of pH values observed in the soils in the current study. Y-axes have different scales. Modified from McKenzie (1980).

mobility, and is soluble and mobilized by oxidizing conditions (McBride, 1994). Also, when pH increased, solubility of cadmium decreased (Street et al., 1978). Antimony is stable in oxidizing conditions in the Sb^{5+} state, with the Sb^{3+} oxidation state common in reducing environments (McBride, 1994). Hammel et al. (2000) stated that the pH value is a minor factor in the mobility of antimony, and also that speciation of antimony with sulfide can reduce mobility due to its low solubility. Nickel is only found stable in the Ni^{2+} state due to its stability over a wide range of conditions, but in lower pH conditions is soluble and exchangeable, thus giving it a medium mobility in acidic conditions (Adriano, 2001; McBride, 1994).

McBride (1994) assumes copper mobility in acidic soils as the metal has low mobility in near-neutral conditions. A study by Martínez and Motto (2000) found the solubility of copper increased with a decrease in soil pH, as did lead and zinc due to their similar solubility curves in various soils used in their study (Figure 1.4). They suggest similar reactions with the metals and soil components as a potential factor. They also

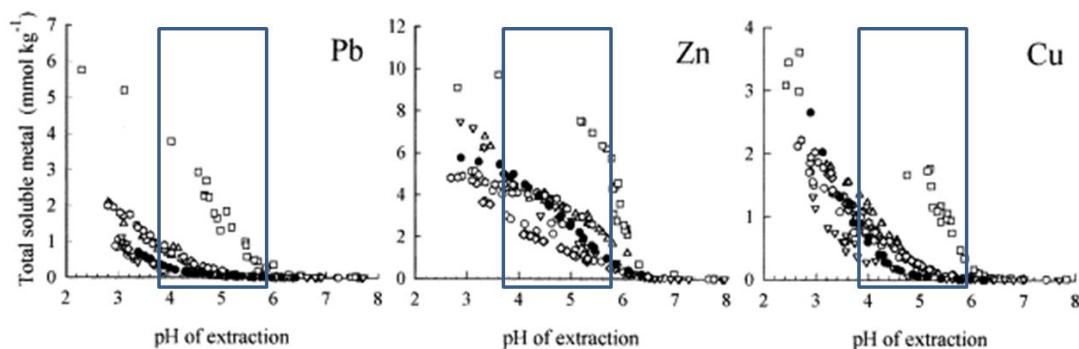


Figure 1.4. Solubility of lead, zinc, and copper vs. pH plots. The blue boxes indicate the range of pH values observed in the soils in the current study. Different symbols denote the different soils from Martínez and Motto's study. Modified from Martínez and Motto (2000).

determined specific pH values where the elements' solubility differed from the noted solubility of the metals at normal values (natural). The pH value for zinc was 6.2, while the pH for copper was 5.5, and the authors suggest pH values below these levels can increase the mobility of the metals in soil.

1.3.2. Soil Constituents. Lindsay (1979) stated that chelating agents are an important factor in zinc mobility. A study by Prokop et al. (2003) revealed that cadmium showed a strong bonding to organics rather than clays within the soil. Antimony associates with sulfides (McBride, 1994). Copper is found in soils mainly as Cu^{2+} , and adsorption onto the oxides, clays, and humus is common in soils (McBride, 1994).

McBride (1994) stated that manganese oxides have strong sorption preferences for elements like Cu^{2+} , Ni^{2+} , Co^{2+} , and Pb^{2+} , while iron and aluminum oxides adsorb Pb^{2+} and Cu^{2+} preferentially. Cobalt associates mainly with iron and manganese oxides, predominantly as the Co^{2+} form. Taylor and McKenzie (1966) noticed that manganese minerals strongly adsorbed cobalt in soil.

While the environment obviously is a large factor in mobility and solubility of an element, the element itself and its speciation does as well. Adriano (2001) lists the elements according to their ionic potential, and thus their ability to bond in the soil. The order is listed as $Ni > Mg > Cu > Co > Zn > Cd > Sr > Pb$ (all considered as 2+ valence ions). A complete table with different factors in soil that can affect mobility of trace elements can be found in Adriano (2001).

1.4. GEOLOGICAL BACKGROUND

The bedrock geology of southeast Missouri is dominated by dolomites that range from early Ordovician to late Cambrian in age. The Gasconade Dolomite of Ordovician-age covers ridge tops within the area and is cherty and light brown dolomite (Thompson, 1995). Below the Gasconade is the Eminence Dolomite, which is a massive bedded, coarsely crystalline, highly burrowed dolomite. The Eminence is upper Cambrian-age, but the contact between it and the Ordovician-age Gunter Sandstone Member of the Gasconade Dolomite is difficult to pinpoint (Thompson, 1995). The Potosi Dolomite lies conformably below the Eminence. The Potosi is a fine to medium grained dolomite that is massively bedded, highly burrowed, and vuggy with quartz druse. Below the Potosi Dolomite is the Derby-Doe Run Dolomite of the Elvins Group. The lower portion of the Derby-Doe Run is thin beds of fine to medium crystalline, argillaceous dolomite, while the upper portion has massive beds and is burrowed. The Davis Formation, also Elvins Group, underlies the Derby-Doe Run Dolomite, and differs as it contains more shale (Mulvany and Thompson, 2013). The Bonneterre Formation conformably lies beneath the Davis Formation and is characterized by a medium bedded, medium to fine grained

dolomite that is light gray (Mulvany and Thompson, 2013). While the Buick Mine was in production, ore was mined from the upper portions of the Bonneterre (Mulvany and Thompson, 2013). The Lamotte Sandstone underlies the Bonneterre Formation and unconformably overlies the Precambrian basement rock. The Lamotte is composed of medium to fine grained quartz that is rounded in the upper portion and becomes angular and coarse with depth. In some of the lower portions, the formation becomes arkosic and in some of the upper portions shale occurs (Mulvany and Thompson, 2013).

1.4.1. Soils of the Study Area. Using the soil map generated for the study area in Iron County, Missouri, the soil types at the sample point locations can be approximated. Both cores are located near the Clarksville-Scholten soil complex and Viburnum silt loam (Figure 1.5).

The Clarksville-Scholten complex is composed of approximately 50 percent Clarksville and 30 percent Scholten. The Clarksville is described as coming from slope alluvium that overlies weathered dolomite. The most limiting layer has the ability to diffuse water in low to higher rates (0.06 to 1.98 in/hr). From 1 to 6 inches depth, the material is a very gravelly silt loam, while from 6 to 13 inches is described as being only a gravelly silt loam. From 13 to 21 inches, the soil goes back to very gravelly silt loam. The Scholten also comes from slope alluvium that ultimately overlies weathered dolomite. The ability to transfer water in the limiting layer is much lower than the Clarksville soil (0.00 to 0.06 in/hr). However, similar to the Clarksville, the Scholten is mainly a very gravelly silt loam from 1 to 13 inches and an extremely gravelly clay loam from 13 to 34 inches. Overall, both are associated with hillside landscaping (U.S.D.A., 2013).

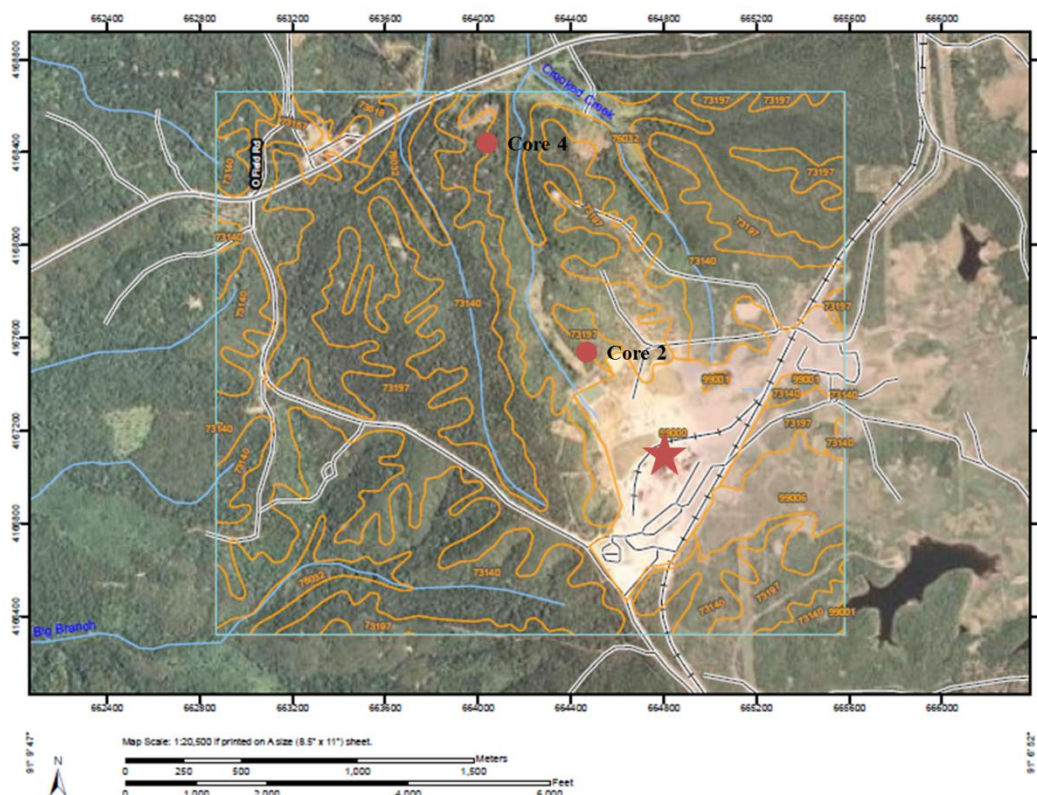


Figure 1.5. Soil survey northwest of the Buick Recycling Smelter (denoted by red star). Both soil cores are near the Clarksville-Scholten complex and Viburnum silt loam, denoted by 73140 and 73197, respectively, on the map (U.S.D.A., 2013).

The Viburnum silt loam (73197) appears to cover many of the hilltops within the area. The Viburnum soil is typically found on ridges and derives from loess over slope alluvium. The most limiting layer can move water at a fast rate (0.20 to 0.57 in/hr). The first 6 inches of depth is characterized by silt loam, with 6 to 18 inches a gravelly, silty clay loam. A gravelly, silty clay occupies the space from 18 to 35 inches.

An earlier study (U.S.D.A., 1991) states the soil in the study area is in the Clarksville-Wilderness Association. This soil is typically characterized as being excessively drained and moderately well drained soils that are cherty and loamy. The hillsides are only classified as Clarksville soils, a very cherty silt loam. For the depth of

the core for the current study, clay content is 14 to 20 percent, and the soil pH is around 3.6 to 6.0. Ridge tops are still mapped as Viburnum silt loam. For 0 to 7 inches depth, the clay content is 15 to 25 percent, and the pH is 5.1 to 7.3. The remaining depth of the core, 7 to 20 inches, clay content is much greater at 30 to 40 percent and pH decreases to 4.5 to 5.5. This report also states that permeability for the Clarksville soil is 2.0 to 6.0 in/hr, while it is 0.6 to 2.0 in/hr for the Viburnum soil.

1.4.2. Soil Horizons. Well defined soil profiles may display up to five separate horizons. The O horizon (referred to as Oh in the current and past studies) contains most of the organic-humic materials. Typically the upper portion is composed of loose leaves; the lower portion is partly decomposed organic matter. Below the O horizon is the A horizon, which is composed mainly of mineral matter, but can contain some organics (Figure 1.6). The E horizon is a zone of finer particles and soluble inorganic soil components from the upper portions of the profile. The E horizon lies below the A horizon and is referred to as a zone of eluviation and leaching. The B horizon (below the E horizon), commonly referred to as the zone of accumulation, contains clay particles that are transported from overlying zones. The C horizon (below the B horizon) contains fragments of altered parent material, which lies directly below this horizon (Tarbuck and Lutgens, 2008).

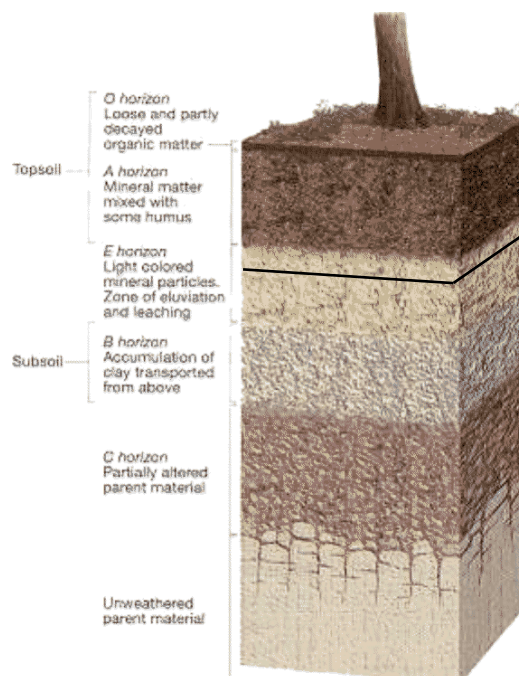


Figure 1.6. Typical soil horizon profile. Black line is approximate depth of current study (Modified from Tarbuck and Lutgens, 2008).

1.5. PREVIOUS STUDIES OF THE AREA

The current study is the fifth conducted in the area over a 40 year time span. The first was by Bolter et al., in 1974. Another study in 1975 by Butherus, Bolter's student, takes into consideration results from Bolter's previous study and incorporated more data. Bornstein completed another study of the area in 1989. The last study completed in the area was Rucker (2000).

The Bolter et al. (1974) study was focused mainly on soil sample analysis and leaf litter for trace metal contamination. Soil was only analyzed at one inch depth in the areas of the current study, while other areas around the smelter were studied to greater depths. In the Bolter study, it was found that a large amount of metals resided in the leaf litter, especially the decomposed leaf litter and in the first inch of soil. The soil had reduced

amounts of metals in comparison to the overlying leaf litter. Elevated levels for lead above regional background levels (20 ppm) continued in the NNW direction of the smelter for around 12 to 15 miles (Bolter et al., 1974).

Butherus (1975) incorporated and furthered the Bolter et al. (1974) study. These samples were collected in the late fall and winter of 1972-73, and followed eight trend lines that extend outwards from the smelter and at 45° angles to one another. Soil cores were taken 0.25 mile, 0.5 mile, and every mile position thereafter along each ray. Butherus' lead values are the same as those in the Bolter et al. study. Some of the soil cores he analyzed followed a N45W traverse from what was then termed the AMAX Smelter (Butherus Octant Ray samples). Data from cores along this traverse will be used for comparison to the current study, as it gives concentrations for all trace metals.

Around 15 years after Butherus, Bornstein (1989) collected soil samples in October and December 1988 to greater depths than the previous study, providing more extensive analyses. In addition, Bornstein also looked at pH, clay mineralogy, and soil hydrologic conditions. He concluded that there was no increase in the concentration of metals within the soils relative to the previous studies, and attributed this to the soils being saturated with metals in the early years of smelting. He did not address the fate of excess lead in the system. Additionally, he suggests low soil permeability allowed the soluble metals and complexes to be washed away by precipitation. Acidic pH values near the smelter (3.5 to 4) were accredited to greater amounts of sulfur being released and deposited onto the soil.

In 2000, Rucker presented data on four soil core samples that were collected in 1998. Rucker conducted the same analyses as Bornstein, but added Scanning Electron

Microscopy-Energy Dispersive Spectroscopy (SEM-EDS) to help determine metal associations within the soil. He concluded that metal concentrations were similar to the previously conducted studies. He attributed smectite clays to sorbing contaminants. SEM-EDS data showed metals in association with iron and manganese oxides as well as residual galena (PbS) grains that were only partially dissolved. Rucker found the soil pH became overall more acidic with depth. He noted the pH values in the Oh were higher than those found by Bornstein (1989). However, Rucker used the pH values Bornstein reported that compared forested and pasture pH variations instead of pH depth profiles.

Witt et al. (2014) studied dust produced from unsurfaced roads in the Missouri Viburnum trend mining district. Similar to the current study, the samples were digested using the sequential extraction procedure, and analyzed using the SEM-EDS. They found the exchangeable-plus-carbonate extract contained a large portion of the lead concentration. This was in comparison to dust from unsurfaced roads outside the district, where the lead concentration was mainly in the immobile oxidizable and non-silicate bound residual phases. SEM-EDS analysis suggested the mobile lead was associated with the lead carbonate, cerussite. An earlier study by Witt et al. (2013) found that dust from a road located approximately 0.1 to 0.2 of a mile north of core 4 in the same northwest direction from the smelter contained the highest concentrations of lead, zinc, copper, and cadmium.

2. EXPERIMENTAL PROCEDURES

2.1. SAMPLE LOCATION AND CORING

Sample locations were at approximately the same distances from the BRRD on a N40W transect line that Rucker (2000) used for his studies. Distances from the smelter to core 2 and core 4 were approximately 0.72 km and 1.55 km, respectively (from Rucker's thesis). Cores were collected, sampled, crushed and sieved by a Missouri S&T student under the supervision of David Wronkiewicz in June 2010. Procedures were as follows.

Leaf litter was collected from the sampling sites and stored in plastic bags. A handheld Shelby Tube sampler was used to collect the core. This piece of equipment utilizes an inner core barrel and an outer core barrel attached to a core driving hammer to drive the Shelby tubes to depth. This depth was variable between sample locations and depends on when the resistance becomes too much for the hammer to go any further. At this point, the driving hammer was removed and a T-shaped tool was used to remove the outer core barrel from the ground. The inner steel core barrel was removed by pushing it at the core bit end. The inner core barrel was then capped, labeled accordingly, and stored in the upright position while in the field.

Back in the lab, the cores were carefully transferred from the barrels into a pre-cleaned PVC pipe using a pre-cleaned stainless steel extrusion plunger. The core was then removed from the PVC onto plastic wrap, where the length and other observations were noted. Starting at the bottom of the core, a one inch section was cut off using a clean knife. Once this section was removed from the core, the outer surface was carefully removed to avoid any down-core contamination produced by soil smearing during

collection. The inch thick core circle was cut in half, and each was placed into a labeled core box to dry.

Crushing, sieving, and splitting were performed the same way as that listed in Rucker (2000). The crushed soil that passed through a #80 sieve (less than 180 microns) was collected and hand crushed using an agate mortar and pestle. Using stainless steel sieves #10, #20, and #80, the samples were mechanically shaken and checked for clumps of soil. If any were present, the sample was re-crushed. Any sample that passed the #80 sieve was split using an aluminum V-splitting trough to obtain two near-equal fractions. The splits were placed in clean glass vials labeled with the collector's initials, the core number, the inch interval, and the letter a or b for the split. Butherus (1975) and Bornstein (1989) also analyzed the soil that passed through the #80 mesh.

2.2. SEQUENTIAL EXTRACTION

Sequential extraction analyses were executed on sample splits from cores 2 and 4. This process was adopted from the Community Bureau of Reference (BCR, now Standards, Measurements and Testing Programme; Rauret et al., 2001). The modified procedure by Witt et al. (2014) was used to determine trace metal association with soil in this study. The BCR procedure originally called for three-step procedure, with an aqua regia of the residual. Witt et al. (2014) combined these to form a four-step procedure, with slight modification of the aqua regia segment. Refer to Appendix C for the reagents used in this procedure.

In this procedure, progressively stronger acids are used to remove trace metals from different components within in the soil. Extract A reflects trace metals released

from carbonates or water exchangeable fractions. Extract B shows the amount of trace metals released from iron or manganese oxides. Extract C contains the trace metals released from organic substances or sulfides. The final extract, Extract D, shows the remaining trace metals in the residual that was attached to any remaining non-silicates in the soil. Some minerals like quartz require stronger acids to dissolve them, or minerals like zircon are resistant to weathering and alteration. These latter fractions likely represent the natural silicate-rock background fraction and are not extracted during the procedure.

The procedure used for the current study was as follows:

1. One gram of sample was added to a 50 mL centrifuge tube (polypropylene copolymer, Environmental Express) which was pre-cleaned with 5 percent HNO₃ (high purity nitric acid) for at least 16 hours in a 90°C oven. After the addition of 40 mL of 0.11 mol/L acetic acid (glacial, trace metal grade), or Reagent A, the test tube was capped and shaken for at least 16 hours at room temperature.
2. After shaking, the extract was then separated from the residue by centrifuging at 3000 g for 20 minutes. The extract was decanted into a 50 mL digestion vessel (homopolymer polypropylene, Environmental Express) and filtered using a 0.45 µm plunger filter (FilterMate PTFE Certified Filter). All digestion vessels were capped and stored at 4°C until analysis. This first step resulted in Extract A.
3. The remaining residue in the centrifuge tube was washed by adding 20 mL of high purity deionized water (MST Milli-Q system) to the centrifuge tube. After manually shaking the residue (approximately 15 minutes), the tube was

centrifuged using the same settings listed above. After centrifuging, the supernatant was discarded.

4. After washing, the residue was then ready for the addition of 40 mL of Reagent B, 0.5 mol/L hydroxylammonium hydrochloride (ACS Reagent Grade, crystalline). The centrifuge tube was then capped and shaken for at least 16 hours at room temperature.
5. Similar to the step in Extract A, after shaking, the test tube was centrifuged and the extract decanted to a clean digestion tube and filtered with a 0.45 μm plunger filter (FilterMate PTFE Certified Filter). This extract (Extract B) was stored at 4°C until analysis. The remaining residue was washed, centrifuged, and the supernatant discarded (keeping the residue) similar to the procedure used at the end of Extract A.
6. Taking the washed residue remaining after Extract B, 10 mL of 8.8 mol/L hydrogen peroxide (ACS Certified) was added to the residue in small increments while the samples were digested using a 90°C hot block. Occasional manual shaking was provided over an hour after peroxide addition. A reflux cap was used to contain evaporation of the mixture to about 3 mL.
7. After the previous step, 10 mL more of 8.8 mol/L hydrogen peroxide was added and covered with a reflux cap and digested for an hour at 90°C in the hot block. After an hour, the cap was removed and the sample was allowed to dry to near dryness.
8. When the sample was nearly dry, 50 mL of 1.0 mol/L ammonium acetate (Certified ACS, crystalline) was added and manually shaken to ensure the entire

residue interacted with the reagent. After all the residue was in suspension, the sample was capped and shaken for at least 16 hours at room temperature.

9. Similar to the previous extracts, after shaking, the test tube was centrifuged, the extract decanted to a clean digestion tube, filtered with a 0.45 μm plunger filter (FilterMate PTFE Certified Filter), and stored at 4°C until analysis. This provided Extract C. The remaining residue was washed, centrifuged, and the supernatant discarded (the residue was saved) similar to the procedure used at the end of Extract A.
10. The final step of the extraction process included adding 6 mL of high purity deionized water (MST Milli-Q system), 3 parts HCl, and 1 part HNO₃ (trace metal grade) to each sample centrifuge test tube. After suspending the sample by manually shaking each test tube, the tubes were left to digest 1 hour in a 90°C hot block with a reflux cap.
11. After the reaction period, the reflux cap was removed to allow the mixture to evaporate to near dryness.
12. After step 11 was completed, 25 mL of 1 mol/L HNO₃ was added, and the sample manually shaken. The sample was then centrifuged, the extract decanted into a clean digestion tube, filtered with a 0.45 μm plunger filter (FilterMate PTFE Certified Filter) and stored at 4°C until analysis. This was the final extract (Extract D).
13. The samples were analyzed on the Perkin-Elmer Optima 2000 DV Inductively Coupled Plasma - Optical Emission Spectrometry (ICP-OES).

For quality control, BCR-701 standard reference material was processed through the procedure and analyzed. Additionally, a digestion blank of each reagent was run to check for contamination.

2.3. TOTAL DIGESTION

Samples were processed according to the United States Environmental Protection Agency's "Standard Operating Procedure for the Digestion of Aqueous and Solid Samples," Method 200.2 (USEPA, 2003). This procedure should release metals from most soil components with the exception of those components resistant to acid treatment which may require a stronger acid to digest completely. One-inch sample intervals from each core were digested according to the following procedure:

1. Approximately 0.5 grams of each sample was weighed out and placed into a 5% HNO₃ (high purity) cleaned screw top 50 mL centrifuge tube (polypropylene, Corning). For samples that did not contain enough material, 0.25 grams was used, and subsequent processing procedures altered accordingly. For each run, a digestion blank was analyzed for possible contamination. A BCR-701 sample was run to check process recovery. A digested 5 ppm spike, spiked with a known standards solution prior to digestion, was run to check the digestive procedure. Duplicate and triplicate samples were run to test for consistency in the measured values.
2. 2 mL of 1+1 HNO₃ and 5 mL of 1+4 HCl acid (1 HCl [Optima Grade] + 4 ASTM Type 1 water) was added to each of the digestion tubes. A swirling stirring

procedure was used to ensure all sediments interacted with the acids before being placed in the hot block.

3. The hot block was set to 115°C and allowed to warm to obtain digestion temperatures of 91°C to 93°C. Care was exercised to keep the acid from boiling.
4. The digestion vessels with acid and sample were placed into the hot block and covered with a plastic watch glass which was pre-cleaned with 3% HNO₃ acid (trace metal grade; MST Environmental Research Center). They were then allowed to digest for 65 minutes within the hot block.
5. After 65 minutes, the hot block was turned off and the samples were allowed to cool to approximately 40°C (about 4 hours).
6. After the samples were cooled, they were removed from the hot block. The watch glasses were held by clean tweezers and were rinsed into the digestion vessels using ASTM Type 1 water. The samples were brought to a 50 mL volume using the markings on the digestion vessel. The screw top lids were placed on the vessels and the samples were hand shaken. Watch glasses were discarded.
7. After a 24 hour settling period, the liquid was filtered using a 20 mL syringe and 0.45 µm Nalgene syringe filter into a 30 mL Nalgene bottle and 18 mL test tube, both of which were cleaned using 5% HNO₃ acid (high purity).
8. The samples were stored at room temperature until analysis on the Perkin-Elmer Optima 2000 DV ICP-OES.

2.4. X-RAY DIFFRACTION (XRD)

The XRD analysis was a continuous, fast scan with a Cu-K_{α1} radiation source with a wavelength of 1.540598. A 2-theta scan range of 1.99° to 59.99959° was used. XRD slides were prepared using a sample split of approximately 0.5 grams of pulverized soil from each sample. These sections were created by combining two, one-inch increments to produce a one gram total for XRD slide preparation (e.g., 0.5 g of BZ4-2a and 0.5 BZ4-3a). Due to the small amount of sample available, two-inch sections were analyzed at two-inch intervals down the depths of the cores.

These combined soil samples were mixed into approximately 40 to 50 mL of deionized water (DIW) and stirred. Five minutes was allotted for settling, before mixing the water and soil again. This time, after 15 seconds, the material was decanted into another beaker. This removed any sand-size or larger particles that settled rapidly through the solution. At this point, a few drops of Calgon were added to the decanted fraction to prevent the clay materials from flocculating. After remaining in suspension for ten minutes, the clay-sized particles were removed from the upper few millimeters of the solution in the beaker and placed onto a glass slide using a pipette.

Due to time constraints between preparation and analysis, slides were oven dried at a low temperature (90°C) for around 30 to 60 minutes (until dry) which is not part of the typical procedure. The low temperature should not affect the clay structures. Typically, kaolinite begins to dehydrate around 400 to 525°C (Deer et al., 1966). This is not considered a significant factor in the current study as many of the XRD peaks in the location where kaolinite occur are narrow, suggesting a well-ordered structure. In

addition, this peak shows very little decrepitation with heating (250, 300 and 375°C; Appendix E).

Three separate runs were conducted using the PANalytical X'Pert Pro Multi-Purpose X-ray Diffractometer (PANalytical, Netherlands) in the Missouri S&T Materials Research Center. The first was an untreated run. The second was an ethylene glycol treated run. The untreated slides were placed in an enclosed chamber over ethylene glycol for 24 hours before being run again. This determined if there was smectite in the sample because the clay would absorb the glycol, and thus produce a shift of peaks in comparison to the untreated run. The third was the heat-treated run. The slides were heated for 30 minutes at 375°C in an oven. This latter run helps differentiate between clays whose peaks may show significant overlap. Chlorite, smectite, and vermiculite have similar 2-theta peaks with the potential to overlap at 6.2°. Differentiation between the three is by heat and ethylene glycol treatments. Kaolinite and chlorite share a similar 2-theta peak location at around 12.4°. Kaolinite is only verified if a secondary peak at 24.9° is present. After the initial three runs, two separate additional heat runs (250°C and 300°C for an hour each) were conducted on two samples to determine the decrepitation point at the 6.0 to 6.2° 2-theta peaks. The relative proportion of each clay mineral type was quantified using the equations found in Appendix E.

2.5. SCANNING ELECTRON MICROSCOPY - ENERGY DISPERSIVE SPECTROSCOPY (SEM-EDS)

High density particles were selected for SEM-EDS analysis, as those particles were likely to contain contaminant metals. Therefore, to eliminate lighter minerals, a Napolytungstate solution was used to separate the minerals by a heavy liquid separation

process. The Na-polytungstate comes in powder form, but can be dissolved in water to produce a density of about 2.85 g/mL. This solution was tested against standards of quartz (2.65 g/cm^3), dolomite (2.85 g/cm^3), and calcite (2.72 g/cm^3) to produce a solution of the desired density. High specific gravity minerals like galena, cerussite, and iron oxyhydroxides are expected to sink in the solution, while lower specific gravity minerals like clays and quartz will be segregated as the float fraction.

After mixing the Na-polytungstate to the correct density, 0.25 grams of soil sample (determined to be high in lead concentration by the ICP-OES results) was added to a glass vial that was half-filled with the Na-polytungstate solution. The vials were then placed in an ultrasonic vibrator for 30 minutes. The samples were removed from the ultrasonic vibrator and allowed to cool to room temperature and settle for approximately 24 hours.

After the settling period, most of the lighter minerals were removed from the top surface with a pipette, without disturbing the particles sitting on the bottom. This was done to reduce the chance of accidentally collecting particles from the top surface when removing the heavy particles for analysis from the bottom. Pipette tips were changed and inserted all the way down to the bottom of the vial to pick up the heavier particles. These were then transferred to a new clean vial, where deionized water (DIW) was added to remove any residual Na-polytungstate off the particles. When rinsing was complete, the particles were vacuum filtered using a $0.45 \mu\text{m}$ cellulose filter.

An aluminum stub was prepared with a carbon sticky paper and a section of the filter paper with particles from the sample was adhered to the carbon paper. An air gun was used to remove any loose dust particles before coating with gold and palladium in

the Denton coater. This coating was applied for 90 seconds to reduce any chances of overcoating, which can hinder EDS data and prevent surface features from being visible. With this amount of time, particles will become slightly charged but not overcharged in the SEM. The sputter set point was at 8 mA.

To recycle any remaining Na-polytungstate, the liquid was first filtered through a Kimwipe in a glass funnel to remove larger soil particles. That liquid was then filtered through Whatman 54 Filter Paper to remove any remaining finer sized particles. The Na-polytungstate was then tested using the mineral density standards specified above. If the liquid still floated the minerals, the Na-polytungstate was then ready to be re-used. If standards did not float, the Na-polytungstate was heated in order to evaporate water, then cooled and re-tested.

Samples were analyzed using the Hitachi S-4700 scanning electron microscope (SEM), with a 15 kV accelerating voltage using secondary electron mode. This lower accelerating voltage prevents the particle being analyzed from becoming charged, and also allows for better imaging of the particle surface, where metals are likely to be present. The secondary electron lower detector was utilized because it allows metals to illuminate brighter and thus differentiates them from background particles. The EDS system was then used to semi-quantitatively determine the element composition on a specific area of focus.

2.6. SOIL pH

In order to conserve the limited amount of soil samples, pH tests were run with combined inch intervals. Five soil pH samples were run for each soil core along with one

deionized water (DIW) blank. One-half gram of soil from each inch was weighed into a clean plastic vial (i.e. 0.5 g from Core 4, 0 to 1 inch and 0.5 g from Core 4, 1 to 2 inches) to produce 1 gram total of soil. To this, one mL of DIW was added to the soil and stirred occasionally. The first soil-DIW mixture pH reading was taken 30 minutes after initial mixing and the remaining readings taken during 24 hour intervals the following days. An Orion 920A pH meter with a Fisher Scientific soil pH probe (13-620-289), calibrated using 4.00 and 7.00 pH standards, was used for all readings. The probe was checked using the standards both before and after running all the soil samples. The before and after standard checks were averaged, and produced a standard deviation of 0.01 and 0.02 for pHs of 4 and 7, respectively. The accuracy was measured from the average of the quality controls for the eight days and measured 3.99 and 6.97, for pHs of 4 and 7, respectively.

The pH was measured once daily, until values remained steady over a span of three days. The average of those three days was used as the final pH value for the soil.

2.7. ICP-OES PROCEDURE AND QUALITY CONTROL

All sequential extractions and total digestion solutions were analyzed using the Perkin-Elmer Optima 2000 DV Inductively Coupled Plasma - Optical Emission Spectrometry (ICP-OES) in the Missouri S&T Environmental Research Center. The method was set to analyze the samples for lead, zinc, nickel, copper, cadmium, cobalt, antimony, arsenic, phosphorus, iron, and manganese.

The ICP-OES was calibrated using 0.1, 1, 10, and 100 ppm of freshly mixed standard solution. After calibration and quality control checks, the samples were

analyzed. After each sample, the tubing was washed for 45 seconds with 1% HNO₃ (trace metal grade) before moving on to the next sample. After every 10 samples, quality control checks were run for the one and 10 ppm standards. The lower and upper limit of failure was set to 0.8 and 1.2 ppm for the one ppm standard and 9.0 and 11.0 ppm for the ten ppm standard with the exception of phosphorus (8.0 and 12.0 ppm limits). A review of all quality control values is in Appendix B.

2.7.1. Sequential Extraction Quality Control. For sequential extractions, precision of the ICP-OES instrument was measured by the standard deviation of quality control values. The standard deviation was usually below 0.1 for quality control standards of 0.1 and one ppm, but was around 0.25 to 2.90 for ten ppm quality controls in sequential extractions.

Maximum error percentage was calculated to determine accuracy. This calculation takes into consideration the largest deviated value from the known standard value to determine the largest potential accuracy percentage error. Typically, most of these maximum error values for the 0.1, one, and ten ppm quality controls were at or below $\pm 10\%$.

Elements not meeting the $\pm 10\%$ maximum error values in core 2 sequential extractions were: cadmium, antimony, arsenic, and phosphorus in the 0.1 ppm quality control; cadmium, antimony, and arsenic in the one ppm quality control; zinc and cadmium in the ten ppm quality control.

In core 4 sequential extractions, cadmium, antimony, and arsenic all had maximum errors higher than 10% at $\pm 30\%$, $\pm 20\%$, and $\pm 60\%$, respectively. All of the one ppm quality controls for core 4 sequential extractions were above the $\pm 10\%$ with the

highest deviations in zinc ($\pm 16\%$), cadmium ($\pm 26\%$), antimony ($\pm 17\%$), and arsenic ($\pm 24\%$). The 10 ppm quality controls were slightly better with 4 of the elements analyzed at or below $\pm 10\%$ with the exception of zinc ($\pm 14\%$), iron ($\pm 11\%$), nickel ($\pm 11\%$), cadmium ($\pm 42.2\%$), antimony ($\pm 12\%$), and arsenic ($\pm 11\%$).

It should be noted that in quality control checks of reagent blanks, Reagent C Blank returned results indicating a minor contamination in zinc (0.52 ppm). This contamination only affected the zinc concentrations in the Reagent C extract; therefore, analyses with greater concentrations of zinc would be acceptable, while those with concentrations below one ppm should be of concern. Additionally, some crystallization occurred on the outside ridge lid portions of some of the Extract C vessels. Care was taken to not allow these crystals to fall into the solution being analyzed.

BCR-701 reference material consists of known values of five metals (zinc, nickel, copper, cadmium, and lead). This material was processed to validate the recovery of the sequential extraction procedure. The percentage change (expected vs. actual reading) of each element is variable from extract to extract (Appendix B). In addition, some spike analyses were conducted. Spike recovery for sequential extracts was not very accurate. Due to the limited amount of sample for analysis, spike samples had to be diluted. Given the instrumental detection limit (0.1 ppm), spike values may be off due to being diluted and thus below the accurate detection limit. Those elements which had greater concentrations (above 1 ppm) generally had the better accuracy in the spikes.

2.7.2. Total Digestions Quality Control. Similar quality control checks were run for total digestion analysis. Standard deviations were once again used to calculate the precision of the instrument.

Core 2 total digestions had standard deviations of the elements below 0.1 for one ppm quality control, and 0.25 for 10 ppm quality control. Quality control results for core 2 total digestions showed large maximum error percentages (>10%) in arsenic (0.1 and 1.0 ppm), antimony (1.0 ppm), iron (1.0 ppm) and phosphorus (0.1 and 1.0 ppm). BCR reference material was fairly accurate (<10% change) with the exception of zinc, which had a -33.5 percent change from the expected value.

Core 4 total digestions had standard deviations of elements below 0.15 for one ppm quality control and 1.75 for 10 ppm quality control. Core 4 total digestions had large maximum error percentages (>10%) for cadmium (1.0 and 10 ppm), arsenic (0.1 and 1.0 ppm), lead (0.1 and 1.0 ppm), zinc (1.0 and 10 ppm), iron (0.1 ppm), nickel (10 ppm), antimony (0.1 and 1.0 ppm), and phosphorus (0.1 ppm). Reference material percent change was greater (about -10 percent to -30 percent) than those values from core 2 reference material analysis.

A digested spike sample was very close to expected values, suggesting that there was no issue of recovery of contaminants through the digestion process. Duplicate analyses were below ± 10 percent change. Full quality control data can be seen in Appendix B.

2.7.3. Manganese Quality Control. The element manganese was analyzed in all the samples at a later date. None of the reagents showed signs of contamination. Quality control results for this run were varied from the previous 10-element analysis. The 0.1 ppm quality control repeatedly registered as a negative value in the ICP-OES. The 0.1 ppm solution was prepared from the one ppm quality control solution. In order to verify that the error was indeed the machine and not the standards solution, new solution was

mixed and reanalyzed. The machine still failed to register a 0.1 ppm reading. However, the one ppm standard had a ± 14 percent maximum error percentage, while the 10 ppm had a ± 16 percent maximum error percentage. Therefore, in the datasets in Appendices C and D, concentrations in red indicate values that have been calculated from instrument values between 0.1 and one ppm, and have the potential to reflect error of the ICP-OES.

All concentrations for the current study have been corrected for soil weight, and thus are reported as determined soil concentrations (ppm [mg/kg]).

3. RESULTS

3.1. TOTAL DIGESTION CONCENTRATIONS

Total digestions differ in respect to sequential extractions as it used a combination of strong acids (hydrochloric and nitric) to remove the majority of the metals from the soil in one step instead of in several steps. Theoretically, in this respect, total digestion concentrations should equal the sum of all four sequential extract concentrations for a one-inch interval (i.e. Oh total digestion lead concentration = Oh lead concentrations for Extracts A+B+C+D).

The results from comparing these two methods vary, but appear to be consistent for the most part between cores 2 and 4. While concentrations do not match perfectly, the trends with increasing depth are very similar. Lead, the metal of main concern in this study, has concentration levels almost the same in both methods, with some minor variations. In core 2, total digestion concentration (4743 ppm) of lead in the Oh (0 inches) was 89 percent of total lead concentration of all the extracts in sequential extraction (5303 ppm). In core 4, sequential extraction total lead (4260 ppm) in the Oh (0 inches) was 99 percent of the total lead in total digestion (4303 ppm). Total digestion concentrations (Appendix D) are discussed for each core and are compared to background concentration levels for the regional soil (Table 3.1). Total digestions were run on each inch interval.

Table 3.1. Background concentration levels for regional soils (Tidball, 1984).

	As	Cd	Co	Cu	Fe	Ni	P	Pb	Sb	Zn	Mn
Concentration (ppm)	8.7	<1.0	10	13	2.11%	14	0.059%	20	N/A	49	740

3.1.1. Core 2 Results. Core 2 results are plotted in Figure 3.1. Lead from total digestions showed a similar trend, with the exception of higher concentrations, to the sequential extractions. Lead concentrations decreased substantially over the first three inches of depth (Oh – 4743 ppm to 2 to 3 inches – 212 ppm), before a slight jump in concentration at 3 to 4 inches depth (673 ppm). Below 4 to 5 inches of depth, the concentrations remained below 41.0 ppm, but revealed an inconsistent trend.

Zinc had its highest concentration in the Oh (184 ppm) before decreasing to below regional soil background values at 0 to 1 inches. For the remaining depth of the soil core, concentrations remained fairly constant, with the exception at 3 to 4 inches where a slight spike occurs.

Nickel was detectable in the Oh (13.0 ppm), before falling below detection limit (<10 ppm) from 0 to 1 to 8 to 9 inches. At 9 to 10 inches, nickel became measureable again, and displayed an overall increasing trend with increasing depth to the bottom of the soil core.

Copper was concentrated in the Oh (103 ppm), and decreased with depth. After spiking slightly at 3 to 4 inches (19.5 ppm), the levels fell below the detection limit (<10 ppm) from 4 to 5 inches until 6 to 7 inches. At 9 to 10 inches, the concentration was detectable again and showed increasing concentrations with increasing depth until the bottom of the soil core, following a trend similar to nickel for this portion of the core.

Antimony was only detected at 1 to 2 inches (13.2 ppm). Arsenic was concentrated in detectable amounts in the first two inches of this core. Cobalt and cadmium were below instrument detection levels for the entire depth profile (<10 ppm).

Major elements analyzed were phosphorus, iron, and manganese. Phosphorus was present throughout the entire core depth profile, with the highest concentration in the Oh (186 ppm). The concentration remained fairly steady with increasing depth. Iron concentrations showed a definite increase with increasing depth, with a concentration in the Oh of 5939 ppm to a high at 14 to 15 inches of 61,951 ppm. Manganese was present throughout the core, with the highest concentrations at depth (12 to 15 inches) in the soil core (255 ppm at 14 to 15 inches).

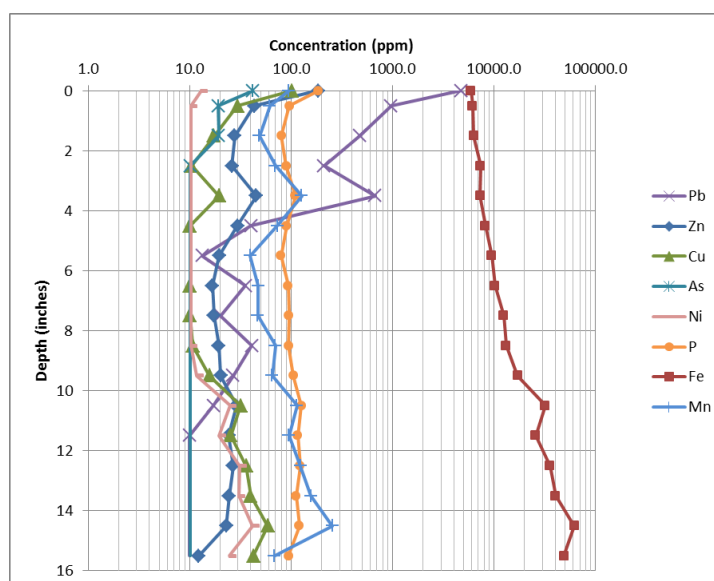


Figure 3.1. Concentration trends for core 2 total digestion experiments. Cobalt and cadmium were below analytical detection limit (10 ppm). Antimony was only above detection limit at 1 to 2 inches (13.2 ppm). Plotted using the average depth value and with Oh at 0 inches.

3.1.2. Core 4 Results. Core 4 results are plotted in Figure 3.2. Lead, unlike in core 2, had concentrations in the thousands of ppm for both the Oh (4303 ppm) and 0 to 1 inch (3235 ppm) depths. Levels began to show significantly decreasing concentrations

with increasing depth after 1 to 2 inches (577 ppm). From 4 to 5 inches, concentrations fluctuated between increasing and decreasing, before falling below the detection limit (<10 ppm) at 10 to 11 inches.

Zinc also had high concentration levels in the Oh (239 ppm) and 0 to 1 inches (145 ppm) before falling near the regional soil background levels at 1 to 2 inches. Concentrations remained near constant for the rest of the depth of the core with the exception of a decreasing concentration tail from around 12 to 15 inches.

Nickel was only detectable in the Oh (16.2 ppm), 0 to 1 inches (11.3 ppm), and 10 to 11 inches (13.4 ppm) in depth.

Copper was present in the first two inches of depth, with highest concentrations in the Oh (93.3 ppm) and 0 to 1 inch interval (62.7 ppm). Below 1 to 2 inches, the concentrations were below detection limit (<10 ppm). Copper reappeared with constant concentrations from 7 to 8 inches to 11 to 12 inches in depth.

Cadmium and antimony were only detectable in the Oh. Arsenic was detected in the first 4 inches of depth. Cobalt was below instrument detection levels for the entire depth of the core (<10 ppm for entire depth of the core with exception of <20 ppm in the Oh horizon).

Phosphorus was present throughout the soil core profile, and had a slight decrease in concentrations with increasing depth. Iron concentrations did not provide a definite trend as they did in core 2, but still displayed overall increasing concentration with increasing depth (Oh – 7159 ppm, 14 to 15 inches – 14,055 ppm). Manganese concentrations in the core were opposite of those in core 2. Concentrations decreased overall with increasing depth, with the highest concentrations in the shallow depths of the

soil core. The greatest concentration was in the 0 to 1 inch depth (457 ppm). Complete datasets for the total digestions can be found in Appendix D.

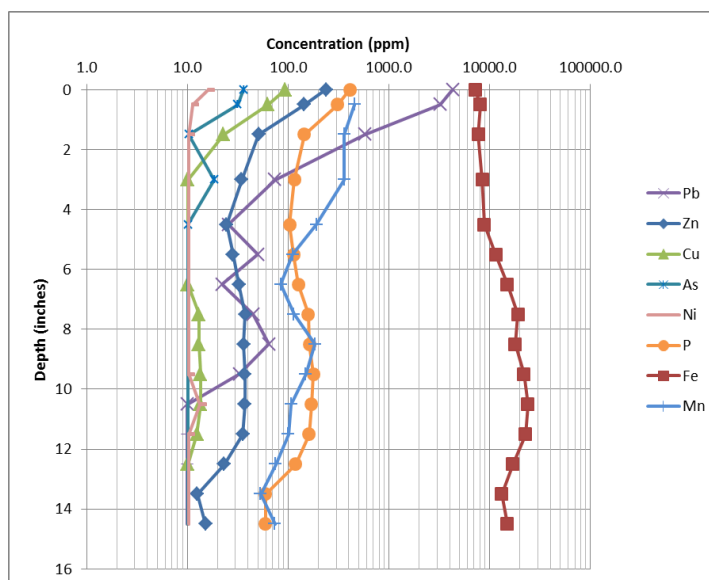


Figure 3.2. Concentration trends for core 4 total digestion experiments. Cobalt was below analytical detection limit (20 ppm in Oh; 10 ppm 0 to 15 inches). Cadmium and antimony were only above detection limit in the Oh horizon (11.5 and 16.1 ppm, respectively). Plotted using the average depth value and with Oh at 0 inches.

3.2. SEQUENTIAL EXTRACTION RESULTS

Sequential extraction procedures were executed on both cores 2 and 4 for each inch of soil below the top Oh layer to seven inches and then for every other inch interval (8 to 9 inches, 10 to 11 inches, 12 to 13 inches, etc.). Extract A used acetic acid to remove any metals from carbonates or exchangeable sites (surfaces and interlayers of clays). Extract B used hydroxylammonium hydrochloride to reduce and dissolve iron or manganese oxides (which includes oxide, hydroxide, and oxyhydroxide phases), and release any trace metals associated with these phases. Extract C used hydrogen peroxide

and ammonium acetate to release metals from organics or sulfides in the soil. Extract D used hydrochloric and nitric acid to release metals attached with any remaining soil components except for acid insoluble silicates (e.g., zircon).

3.2.1. Core 2, Extract A Results. In Extract A (Figure 3.3), lead decreased with increasing depth (Oh: 2218 ppm; 14 to 15 inches: <4 ppm), with the exception of at 3 to 4 inches where it deviated from the trend with a slight increase (382 ppm). Lead fell below background levels for regional soils at 4 to 5 inches.

Zinc was present in low concentrations throughout the entire core depth (<12.5 ppm). Copper, arsenic, and phosphorus all had their highest concentration in the Oh before dropping below background values for regional soils, and eventually below detection limit (<4.0 ppm) at 4 to 5 inches. Cobalt, nickel, cadmium, and antimony were all below the detection limit of the ICP-OES machine at <16.0 ppm in the Oh and <4.0 ppm for the remaining depth of the core. Iron varied in concentration with increasing depth, but ranged from 4.8 ppm to 21.2 ppm. Manganese varied in concentrations, but fell below analytical detection limit at 5 to 15 inches.

3.2.2. Core 2, Extract B Results. In Extract B (Figure 3.4), lead once again had its greatest concentration in the Oh layer (2756 ppm) and followed an overall trend of decreasing concentration with increasing depth. Deviations from the trend occurred at 3 to 4 inches (268 ppm) and 6 to 7 inches (18.7 ppm). However, after 6 to 7 inches, concentrations began to decrease again.

Zinc was only detectable in the Oh layer (13.8 ppm), and this value is below regional soil background values. Copper, arsenic, and phosphorus had their greatest concentrations in the Oh layer, and had overall decreasing concentrations with increasing

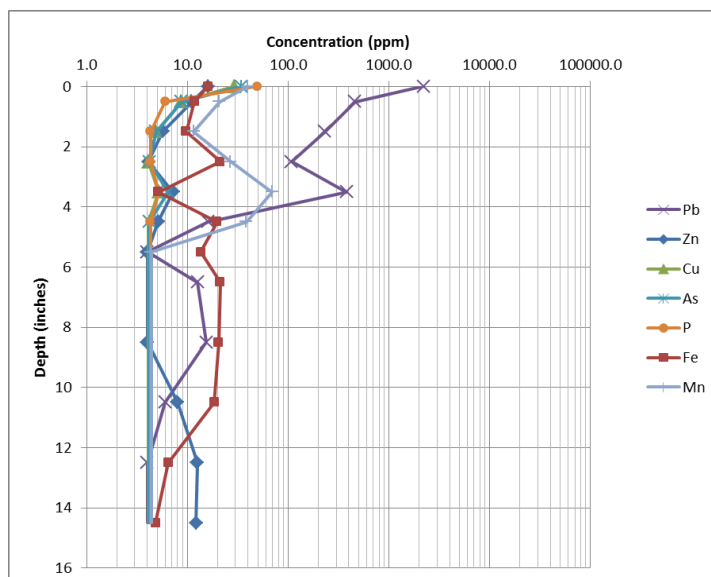


Figure 3.3. Extract A concentrations (in ppm) for core 2. This graph shows trends for elements released from carbonates and exchangeable ions in the soil. Cobalt, nickel, cadmium, and antimony were all below the analytical detection limit of 4.0 ppm. Plotted using the average depth value and with Oh at 0 inches.

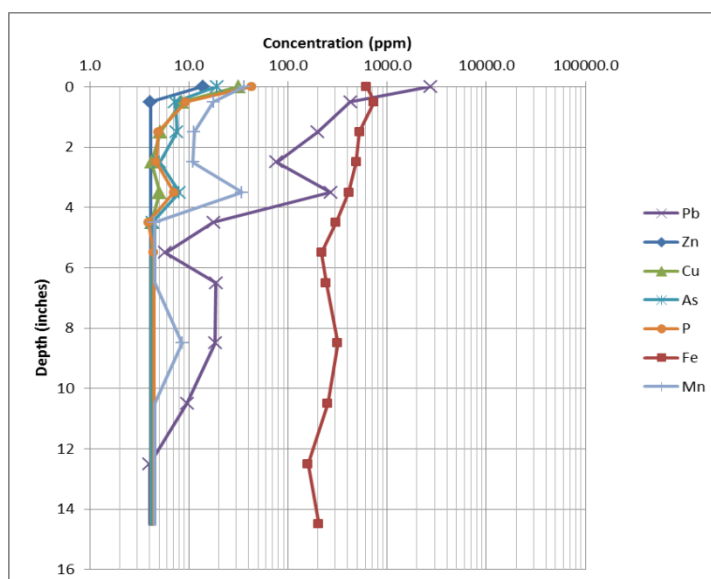


Figure 3.4. Extract B concentrations (in ppm) for core 2. This graph shows trends for elements released from iron or manganese oxides in the soil. Cobalt, nickel, cadmium, and antimony all below the analytical detection limit (4 ppm). Plotted using the average depth value and with Oh at 0 inches.

depth. These all fell below the ICP-OES detection limit (<4.0 ppm) at around 4 to 5 and 5 to 6 inches. Cobalt, nickel, cadmium, and antimony were once again below the ICP-OES detection limit (<4.0 ppm). Iron concentrations were much greater in the top section of this core (618 ppm) and displayed an overall decreasing trend with increasing depth. Manganese concentrations decreased over the first few inches of depth, with a slight increase at 3 to 4 inches (34.4 ppm), before falling below the analytical detection limit for all but one of the remaining intervals in the soil core.

3.2.3. Core 2, Extract C Results. In Extract C (Figure 3.5) lead had its greatest concentration in the Oh horizon (247 ppm), with overall decreasing concentrations with increasing depth; exceptions were at 3 to 4 (44.4 ppm) and 8 to 9 inches (7.7 ppm).

Zinc was detected at all intervals and had fairly constant concentrations with increasing depth (52.4 ppm to around 25.3 ppm at depth). Copper concentration was greatest in the Oh horizon (22.0 ppm), before dropping below detection limit (<5.0 ppm) at 1 to 2 inches. Phosphorus had its greatest concentrations in the Oh horizon (49.7 ppm) before following an overall decreasing concentration with increasing depth trend, with an exception at 3 to 4 inches (28.3 ppm). Cobalt, nickel, cadmium, antimony, and arsenic were all below detection limit (<5.0 ppm) in this extract. Iron concentrations had an overall trend of increasing concentration with increasing depth. Manganese was below analytical detection limits (<5.0 ppm) for the entire depth of the core.

3.2.4. Core 2, Extract D Results. In Extract D (Figure 3.6), lead had its lowest starting concentrations in this extract (82.3 ppm). It fell below detection limit (<5.0 ppm) at 4 to 5 inches.

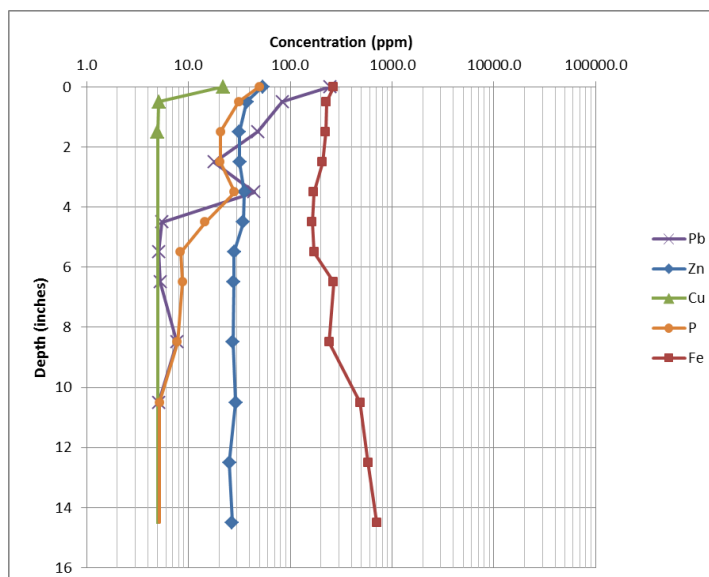


Figure 3.5. Extract C concentrations (in ppm) for core 2. This graph shows trends for elements released from organics or sulfides in the soil. Cobalt, nickel, cadmium, antimony, and arsenic were all below the analytical detection limit (5 ppm). Plotted using the average depth value and with Oh at 0 inches.

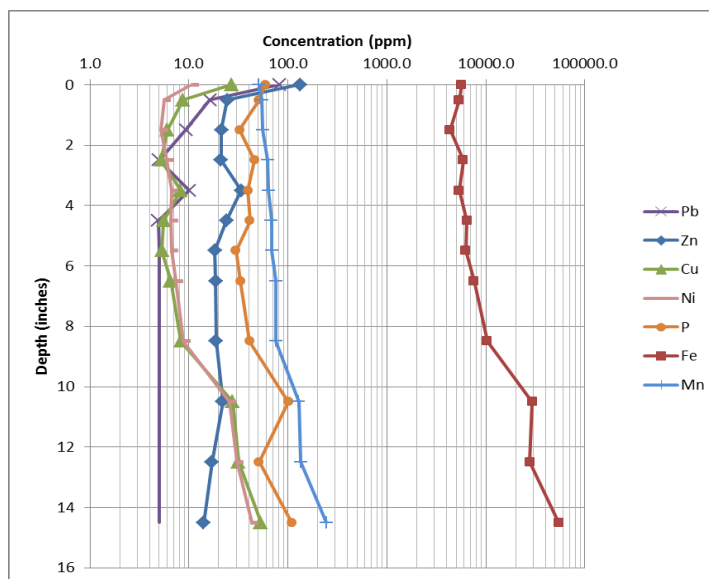


Figure 3.6. Extract D concentrations (in ppm) for core 2. This graph shows trends for elements released from any remaining non-silicates within the residual soil. Cobalt was only above detection limit in the Oh horizon (6.2 ppm). Cadmium, antimony, and arsenic were all below the analytical detection limit (5 ppm). Plotted using the average depth value and with Oh at 0 inches.

Zinc was in detectable concentrations throughout the soil core, with the highest concentration in the Oh (133 ppm) before remaining fairly constant in concentrations with increasing depth (around 14.0 to 33.9 ppm). Cobalt was only detectable in the Oh (6.2 ppm); that value was below regional soil background. Nickel and copper were both present throughout the soil core profile. Both see their highest values at 14 to 15 inches in depth (Ni: 43.0 ppm, Cu: 53.1 ppm). These two metals behaved in a similar manner with increasing depth and both showed a significant concentration increase at 10 to 11 inches that continued until 14 to 15 inches in depth. Phosphorus was present throughout the soil core, showing an overall increase in concentration with increasing depth. Cadmium, antimony, and arsenic were all below analytical detection levels (<5.0 ppm). Iron posted the highest concentration levels in this extract, and showed an overall increasing concentration with increasing depth (5684 ppm in Oh to 54,601 ppm at 14 to 15 inches). Manganese showed an overall increase in concentrations with increasing depth (Oh horizon: 51.1 ppm to 244 ppm in 14 to 15 inches).

Comparing all the extracts against each other for core 2, Extracts A and B contain the greatest percentages of total lead from all the extracts. Extract B holds the greatest percentage of lead in the Oh (52.0 percent) and 4 to 5 (45.3 percent) to 10 to 11 (61.5 percent) inches, while Extract A has the greatest percentages from 0 to 1 (46.5 percent) to 3 to 4 (54.2 percent) inches. Zinc concentrations are most prominent in Extract C, with the exception of the Oh layer where 66.4 percent of the zinc is found in Extract D. Copper is almost equal across all extracts for the Oh level to 1 to 2 inches, but with increasing depth, all of the copper was found in Extract D. Arsenic was found mainly in Extracts A and B. Phosphorus was equally split between all the extracts for the Oh layer,

but Extract D held the most of the total phosphorus from all the extracts. Iron was dominantly recovered in Extract D, with percentages ranging from 84.6 percent to 98.4 percent of total iron. All datasets for the sequential extracts and percentage breakdowns can be found in Appendix C.

3.2.5. Core 4, Extract A Results. In Extract A (Figure 3.7) for core 4, the highest concentrations of lead were found in the first two inches of depth, with the highest concentration at 0 to 1 inches (389 ppm). At 2 to 4 inches, the concentrations of lead fell below the regional soil background levels.

Zinc concentrations started below regional soil background levels and saw a further decrease in concentration with depth. Copper was only detected at 1 to 2 inches depth (4.4 ppm), while arsenic was only present at 0 to 1 inches depth (4.3 ppm); both values were below regional soil background values (not displayed on Figure 3.7). Cadmium was present in the first inch of depth of the core (4.4 ppm in the Oh and 4.7 at 0 to 1 inch). Phosphorus was detectable only in the first two inches of depth. Cobalt, nickel, and antimony were all below instrument detection levels (<4.0 ppm). Iron concentrations were low and remained fairly constant with increasing depth, with the exception from 4 to 5 inches to 8 to 9 inches, where concentrations were below instrument detection limits (<4.0 ppm). Manganese overall decreased in concentration with increasing depth, with an exception at 8 to 9 inches. The greatest concentrations for this element were in the Oh horizon with a reading of 497 ppm.

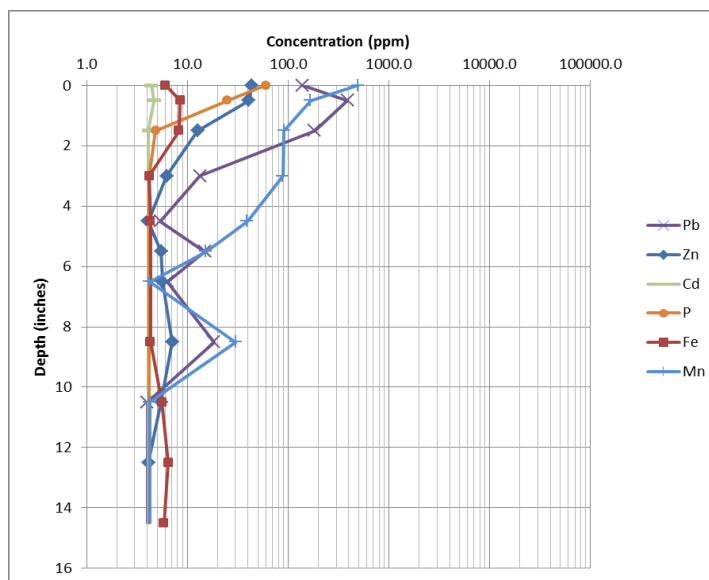


Figure 3.7. Extract A concentrations (in ppm) for core 4. This graph shows trends for elements released from carbonates or exchangeable ions within the soil. Cobalt, nickel, and antimony were below the analytical detection limit (4 ppm). Copper is only above detection limits at 1 to 2 inches (4.4 ppm), and arsenic only at 0 to 1 inch depth (4.3 ppm). Plotted using the average depth value and with Oh at 0 inches.

3.2.6. Core 4, Extract B Results. In Extract B (Figure 3.8), high lead concentrations were found in the first two inches (Oh – 3452 ppm, 0 to 1 inch – 2476 ppm, 1 to 2 inches – 362 ppm). The trend with increasing depth was similar to Extract A, with concentration level spikes at 5 to 6 and 8 to 9 inches.

Zinc was only detected in the first four inches of depth, with the only concentration above regional background values occurring in the Oh soil layer. Cobalt, nickel, and cadmium were only detected in the Oh layer. Copper was present in the first two inches of depth, with a peak at 0 to 1 inches. Arsenic was present in the top two inches with the Oh and 0 to 1 inches being above background levels (Oh – 14.8 ppm, 0 to 1 inch – 13.3 ppm). Phosphorus was only detectable in the first four inches of depth. Antimony was below the detection limit for the entire depth of the core (<4.0 ppm for

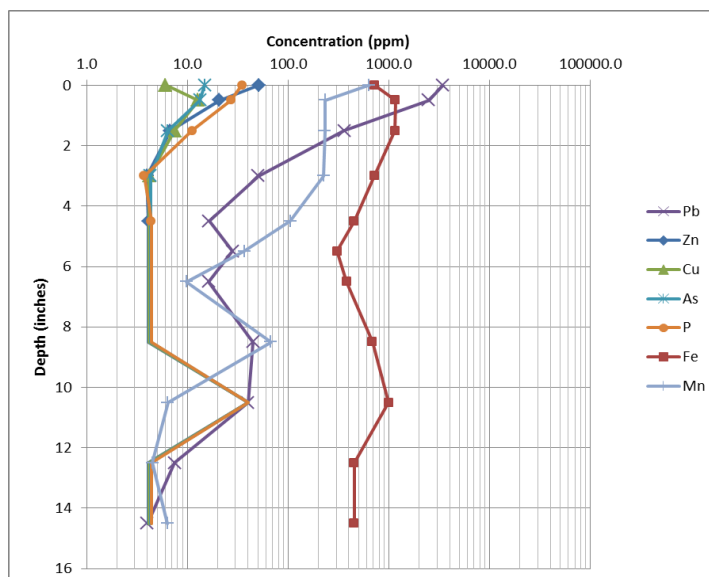


Figure 3.8. Extract B concentrations (in ppm) for core 4. This graph shows trends for elements released from iron or manganese oxides within the soil. Antimony was below the analytical detection limit (4 ppm), while several elements were below detection limit (40 ppm) at 10 to 11 inches. Cobalt, nickel, and cadmium were only above detection limit in the Oh horizon, with values of 4.3, 5.8, and 5.5 ppm, respectively. Plotted using the average depth value and with Oh at 0 inches.

entire core with exception of <40.0 ppm at 10 to 11 inches). Iron displayed varying concentrations with increasing depth in the core, with two of the highest concentrations at 0 to 1 and 1 to 2 inches (0 to 1 inch – 1156 ppm, 1 to 2 inches – 1155 ppm). Manganese showed an overall decrease with increasing depth with an exception at 8 to 9 inches.

3.2.7. Core 4, Extract C Results. In Extract C (Figure 3.9), the highest concentration of lead was found in the Oh horizon (569 ppm) and 0 to 1 inch range (224 ppm), and had a decrease in concentration with increasing depth, with small spikes at 5 to 6 and 8 to 9 inches.

Zinc was present throughout the core depth with concentrations decreasing over the first two inches before remaining constant. Copper was detected in the Oh horizon (63.1 ppm) and first inch (18.3 ppm) of depth, while arsenic was only detected in the Oh

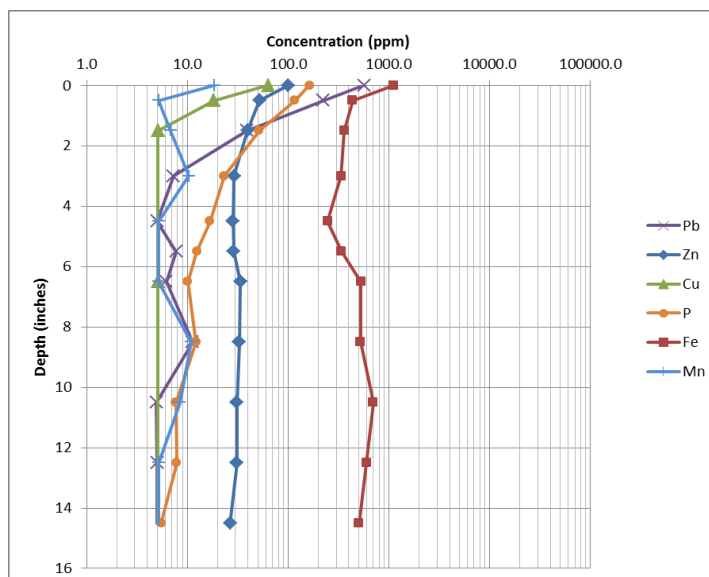


Figure 3.9. Extract C concentrations (in ppm) for core 4. This graph shows trends for elements released from organics or sulfides within the soil. Cobalt, nickel, cadmium, and antimony were below the analytical detection limit (5 ppm). Arsenic was only above detection limit in the Oh horizon (7.9 ppm). Plotted using the average depth value and with Oh at 0 inches.

layer (7.9 ppm). Phosphorus was present throughout the entire core depth, with concentrations decreasing the first two inches before steadying in the rest of the core. Cobalt, nickel, cadmium, and antimony were all below instrument detection levels (<5.0 ppm). Iron concentrations showed a decrease in the upper portion of the core, until around 4 to 5 inches before it started an increasing trend to the bottom of the soil core. Manganese concentrations were variable for this extract, but remained below 18.7 ppm.

3.2.8. Core 4, Extract D Results. Extract D (Figure 3.10) revealed lead only being detected in the first inch of depth of the soil core (Oh – 102 ppm, 0 to 1 inch – 34.7 ppm).

Concentrations for zinc showed a decrease with increasing depth, with the highest reading in the Oh (80.5 ppm). Nickel and copper were measureable throughout the entire

core depth. Copper decreased in concentration with increasing depth, while nickel had a slight increase with increasing depth. Phosphorus was also present throughout the core, with a variable concentration, but showing an overall decreasing trend. Cobalt, cadmium, antimony, and arsenic all came in below the detection limit of the ICP-OES instrument (<5.0 ppm). Iron had its highest concentrations out of all the extracts and showed an overall increase in concentration with increasing depth through the first 12 inches of core before decreasing at 12 to 13 and 14 to 15 inches, after the highest concentration at 10 to 11 inches (19,933 ppm). Manganese showed an overall increase in concentration with increasing depth.

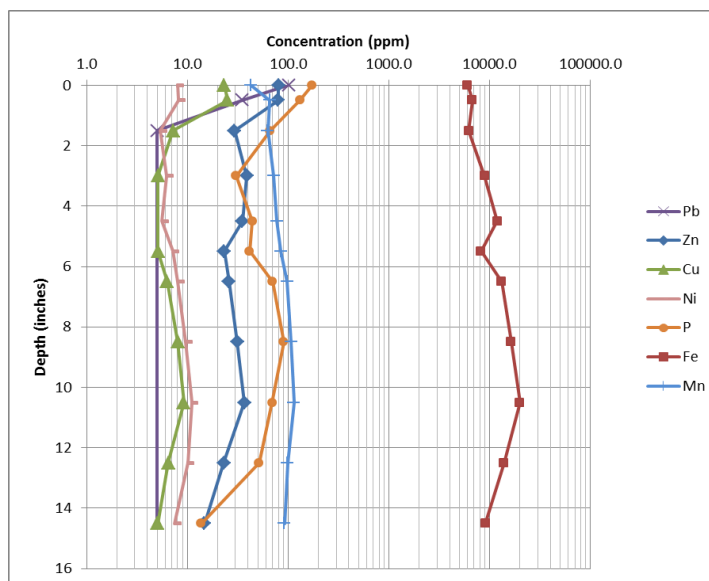


Figure 3.10. Extract D concentrations (in ppm) for core 4. This graph shows trends for elements released from any remaining non-silicates within the soil. Cobalt, cadmium, antimony, and arsenic were all below the analytical detection limit (5 ppm). Plotted using the average depth value and with Oh at 0 inches.

Comparing all the extracts to each other, 81 percent of the total lead from all extracts in the Oh horizon resides in Extract B. Extract B also holds the majority of the lead for the remaining depth of the core. The majority of the zinc resides in Extracts C and D. Copper is found heavily in association with Extract C in the Oh, before the remaining amount of copper is found mostly in Extract D. Arsenic is found mostly in Extract B. Extract D accounts for most of the phosphorus concentrations, with similar percentages of the element found in Extract C. Iron sees most of its concentrations in Extract D. All datasets for core 4 sequential extractions and percentage breakdowns can be found in Appendix C.

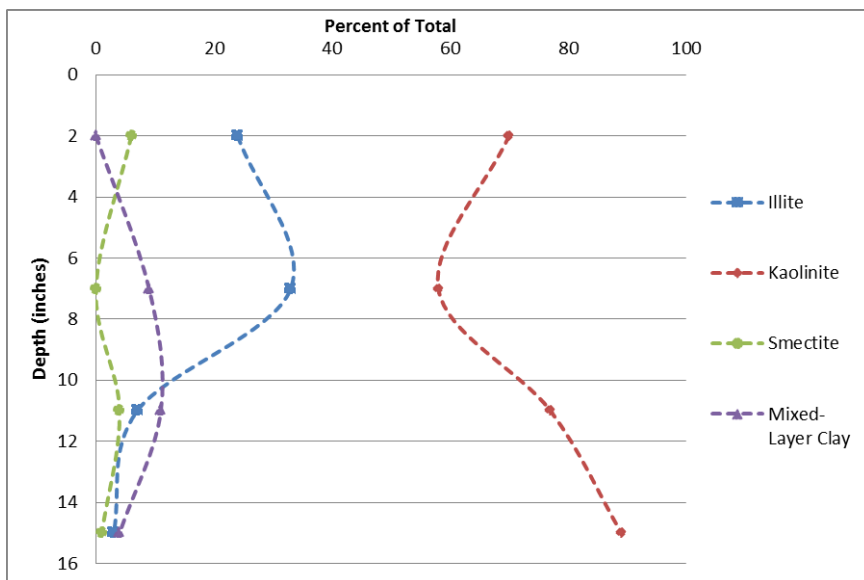
3.3. SOIL MINERALOGY

In X-Ray Diffraction (XRD), clays are identified by specific 2-theta peak positions. Kaolinite is identified by its 2-theta peaks at 12.4° and 24.9°, while illite by its 8.8° and 17.9° peaks. Mixed-layered clays are variable in their 2-theta peak locations, dependent upon the clay composition. Proportions of the two or more clay amounts and the stacking order also affect the 2-theta location. This situation is somewhat comparable to the potential smectite peak that can exist in between the two smectite end-member peaks due to mixing of the two.

The variability in the modal abundance of clays as a function of depth is reported in Table 3.2 and shown in Figures 3.11 and 3.12. XRD results indicate that the majority of the clay-sized particles in the two soil cores were kaolinite (46 to 89 percent). Illite was the second most common (3 to 49 percent) while montmorillonite (smectite) represented the least amount of clay (0 to 6 percent). Significant amounts of mixed layer

Table 3.2. Clay distribution in soil cores in percent.

Core 2 Percentage of Total Clay				
Inches	Illite	Kaolinite	Smectite	Mixed-Layer Clay
1-3	24	70	6	0
6-8	33	58	0	9
10-12	7	77	4	11
14-16	3	89	1	4
Core 4 Percentage of Total Clay				
Inches	Illite	Kaolinite	Smectite	Mixed-Layer Clay
0-2	16	47	4	33
5-7	49	48	3	0
9-11	25	46	1	28
13-15	18	71	5	7

**Figure 3.11.** Percentages of isolated clay-sized fraction particles in core 2. Collected by gravity separation. Kaolinite comprises most of the clays in the core. Plotted using the average depth values.

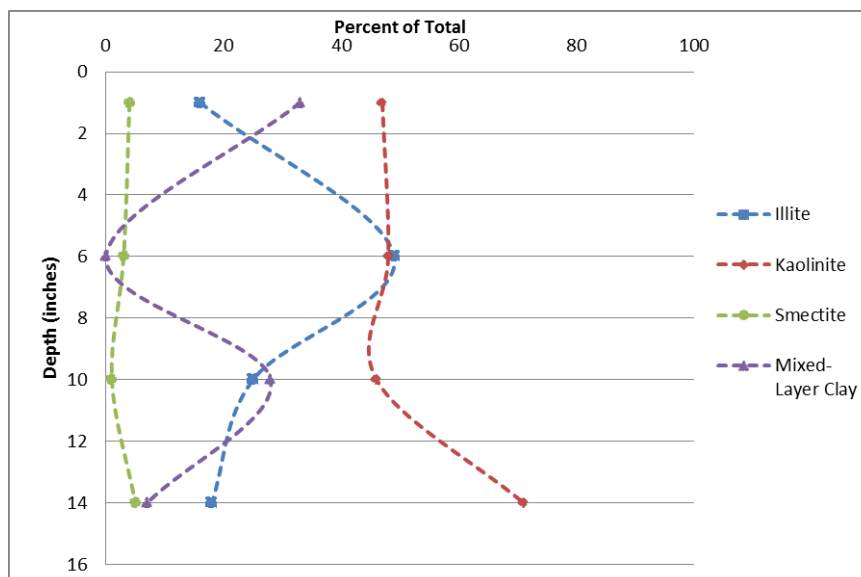


Figure 3.12. Percentages of isolated clay-size fraction particles in core 4. Collected by gravity separation. Kaolinite comprises most of the clays in the core. Plotted using the average depth values.

clays were also noted, but in extremely variable concentrations (0 to 33 percent). Large peaks for quartz were present, but were not included in the quantification procedures to determine the relative proportion of clay minerals in the clay-sized fraction of the soils.

In core 2, kaolinite and illite concentrations were inverse with increasing depth (Figure 3.11). Kaolinite increased with depth while illite decreased, with the exception at 6 to 8 inches where kaolinite decreased slightly and illite increased. Smectite concentration was variable with increasing depth, while mixed-layer clays showed an increase with depth until 10 to 12 inches before decreasing in concentration.

In core 4, kaolinite remained fairly constant with increasing depth before increasing significantly at 13 to 15 inches (Figure 3.12). Illite showed a large jump in concentration at 5-7 inches (49 percent), which was virtually indistinguishable from the kaolinite concentrations (48 percent), before illite then tapered off with increasing depth.

Smectite showed a slight increase with depth, while mixed-layer clays had extremely variable concentrations with increasing depth.

Quantifying the proportion of smectite in these soils proved difficult. In the quantification procedures, only the smectite peak at 5.2° 2-theta in the glycol run is used. There was never a significant peak at this location. In all samples, a peak existed between 6.175° - 6.35° 2-theta in the untreated run, which correlated with peaks between the Ca-montmorillonite (5.7° 2-theta) and Na-montmorillonite (7.1° 2-theta). In the glycol run, however, this peak never shifted, except for one sample when the shift was relatively minor. A shift is expected with smectite clays. After heating, this peak no longer existed, and in some samples, the illite peak intensity increased slightly. These varying smectite peaks were not included within the quantifications; however, if they were substituted for the 5.2° 2-theta peak in calculations, concentration percentages of smectite in both cores increased (with a 7 to 20 percent range in core 2 and 7 to 17 percent range in core 4). Consequently, changes in the percentage concentrations of kaolinite, illite, and mixed-layer clays would also occur with this calculation. Therefore, given the complexity of the situation, values are only reported utilizing the original calculation procedure in Appendix E. All XRD data can also be found in Appendix E.

3.4. SEM-EDS RESULTS/MINERAL SPECIES

Soil fractions from a one inch interval from each soil core with the highest lead concentrations (Core 2, 0h; Core 4, 0 to 1 inch) were processed and analyzed using SEM-EDS analysis. In both cores, the textures of the particles varied. There were no

definitive crystal forms observed to support the EDS results for a particular mineral phase.

The background carbon dot and filter paper, which, when an empty section of filter paper was analyzed, had a substantial amount of carbon (57.0 atomic (molar) percent), nitrogen (11.9 atomic (molar) percent), and oxygen (30.1 atomic (molar) percent) and minor amounts of silicon (0.8 atomic (molar) percent) and gold (0.2 atomic (molar) percent). Tungsten (W) peaks can be disregarded as the use of Na-polytungstate in sample processing can remain as a coating on the particles. EDS spectra have been corrected to remove tungsten (W) from quantifications. Gold (Au) and palladium (Pd) peaks can also be disregarded due to coating of the particles to prevent charging in the microscope. Tungsten (W) and silicon (Si) share similar peak locations (~1.7-1.8 keV), and thus may affect correct identification. Oxygen is not detected accurately in EDS data, and should be used sparingly when trying to determine compositions.

Between the two soil cores, particles containing appreciable lead concentrations displayed textures that were somewhat botryoidal or flaky (Figures 3.13 to 3.15). Figure 3.13 shows an image from core 2 of a particle with lead that had a botryoidal habit. EDS analysis indicated 9.2, 25.1, and 57.8 atomic (molar) percent of lead, carbon, and oxygen, respectively. Figure 3.14 is also from core 2; this particle displayed a more flaky texture. Regardless, the EDS data for this particle was similar to that in Figure 3.13. Figure 3.15 is another image of two particles from core 2. It had a botryoidal texture that is composed of much smaller masses than in Figure 3.13. Both particles had similar EDS data (7.3 atomic (molar) percent Pb, 42.9 atomic (molar) percent C, and 48.1 atomic (molar)

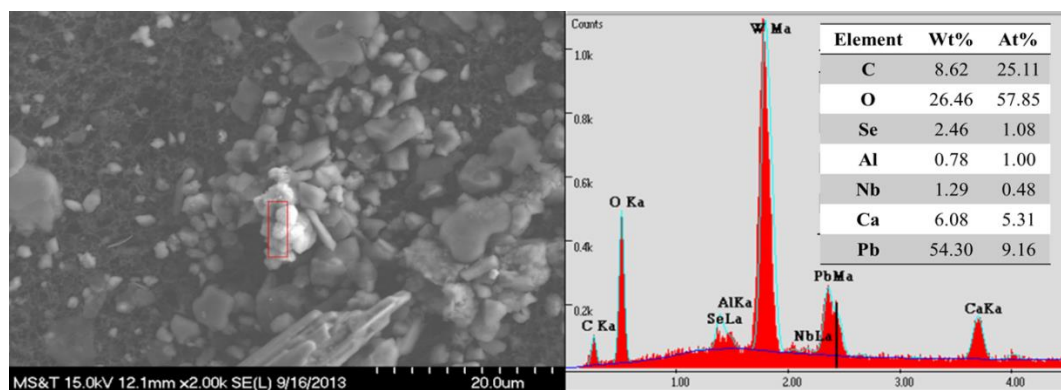


Figure 3.13. SEM image of a botryoidal-textured particle containing lead in core 2. The EDS data of the area highlighted in red is presented at right. Tungsten is a residual contaminant from the gravity separation process used to isolate the grains from the soil.

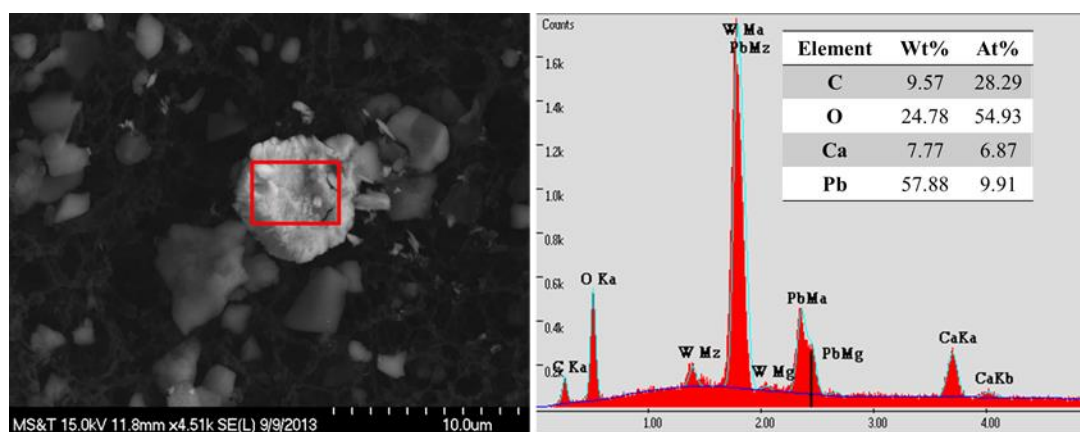


Figure 3.14. SEM image and EDS data of a flaky-textured particle containing lead in core 2.

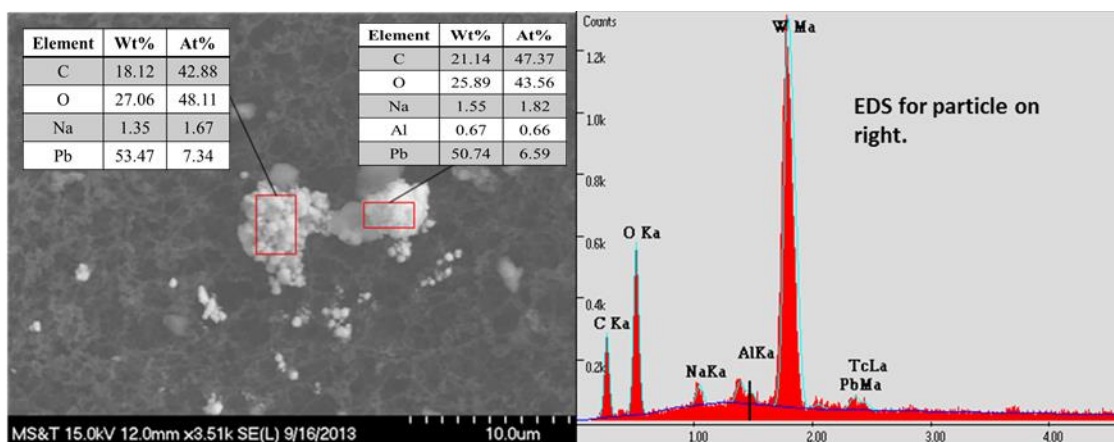


Figure 3.15. SEM image of two particles with lead in core 4. The textures are more granular, but the EDS spectra between the two particles are similar, suggesting they are the same mineral.

percent O) to one another, but the values were slightly less than EDS data values obtained from earlier particles.

One particle containing lead in core 4 varied texturally from the others, as it appeared to be smoother (Figure 3.16). Analytically, the atomic molar percentages for this particle are very close to the atomic weight percentages of the other particles containing lead analyzed in core 2 (10.3 atomic (molar) percent Pb, 28.9 atomic (molar) percent C, and 54.5 atomic (molar) percent O).

While EDS data is semi-quantitative, the values recorded appear to best fit the cerussite composition of PbCO_3 . However, there is some discrepancy as the lead peak and sulfur peak in EDS spectra are very close. Typically, sulfur peaks appear as a “shoulder” to the lead peak, therefore making the lead peak much broader (Figure 3.17). This makes quantification difficult when trying to differentiate between the two elements. Lead peaks in many of the EDS spectra were broad, which could mean the presence of some sulfur in the particle. Given the other elements present and the potential presence of sulfur, particles could reflect galena that has weathered to cerussite, or the presence of galena or anglesite.

When a sample of cerussite from Lake County, Colorado (mounted on copper) was analyzed in the microscope, values of lead, carbon, and oxygen came out almost equal (Figure 3.18). Technically, this would be fairly accurate, since a large crystal was analyzed and very little influence from the background would occur. The oxygen values were most likely off due to its inability to be measured accurately using the EDS system. Analysis of smaller particles in the soil samples allow for more interaction with the background which can reflect inaccurate values.

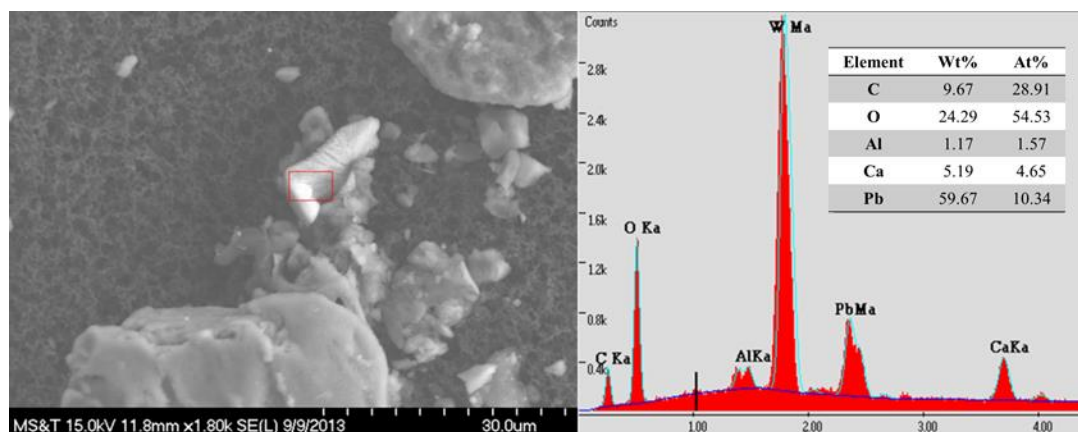


Figure 3.16. SEM image of a smooth particle with lead in core 4. This particle displays a smoother surface, but still has EDS data that is similar to the previously analyzed particles.

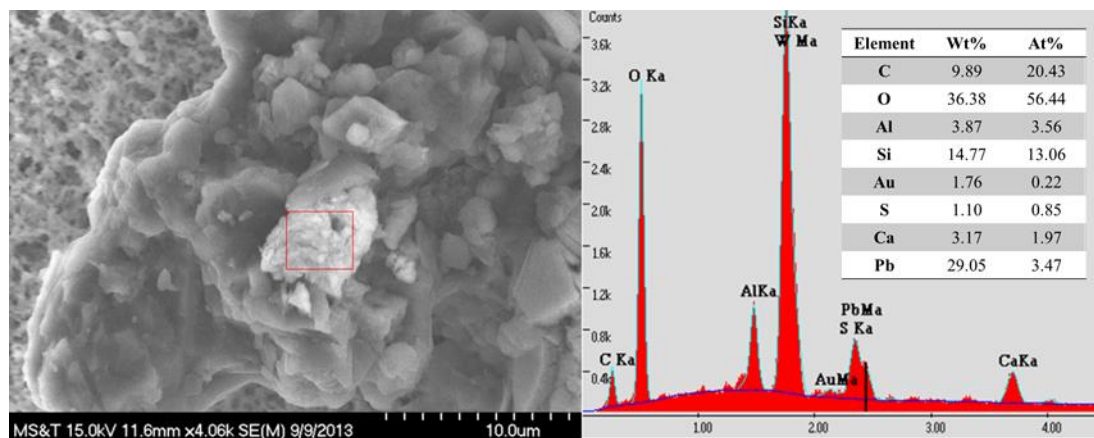


Figure 3.17. SEM image and EDS spectra of a flaky particle containing lead in core 4. This particle has similar elemental composition to previously analyzed particles. Notice sulfur peak shoulder adjacent to the lead peak.

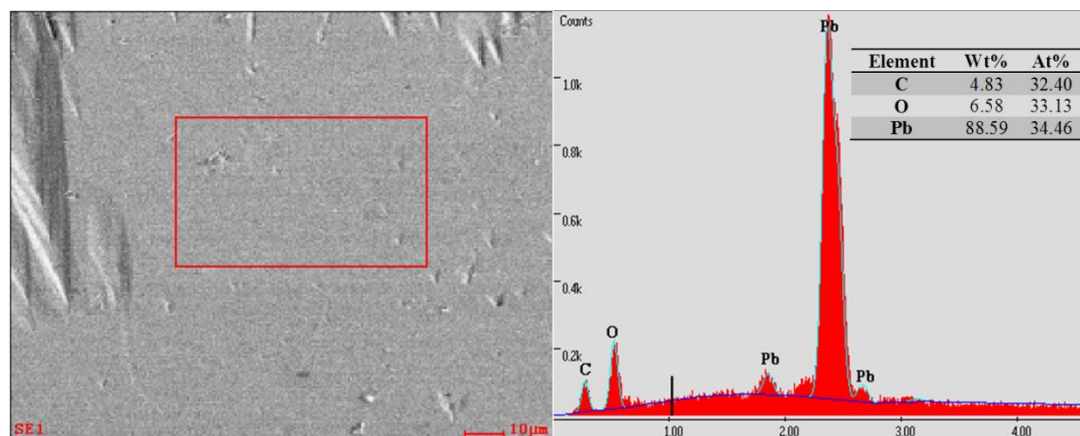


Figure 3.18. EDS spectra for a cerussite (PbCO_3) mineral standard in the Hitachi S-4700 Microscope. The atomic percent determinations for Pb vs. C occurred at approximately the expected 1:1 ratio, however, the EDS detection for C vs. O was below the anticipated value.

Other elements in the contaminated particles were silicon, aluminum, potassium, calcium, and sodium. Most of these elements are common soil constituents, but do not reflect the results of the sequential extracts, where lead was associated Extract B and where metals were released from manganese or iron oxides. One particle containing lead in core 2 reflected possible association with iron-oxide (Figure 3.19). The particle to which the lead-bearing particle is attached had 49.7 atomic (molar) percent oxygen and 20.3 atomic (molar) percent of iron. Finalizing a list of associated minerals is difficult given the variability in oxygen and carbon readings, but it is likely that aluminum/potassium could be associated with clays, with potassium reflecting illite.

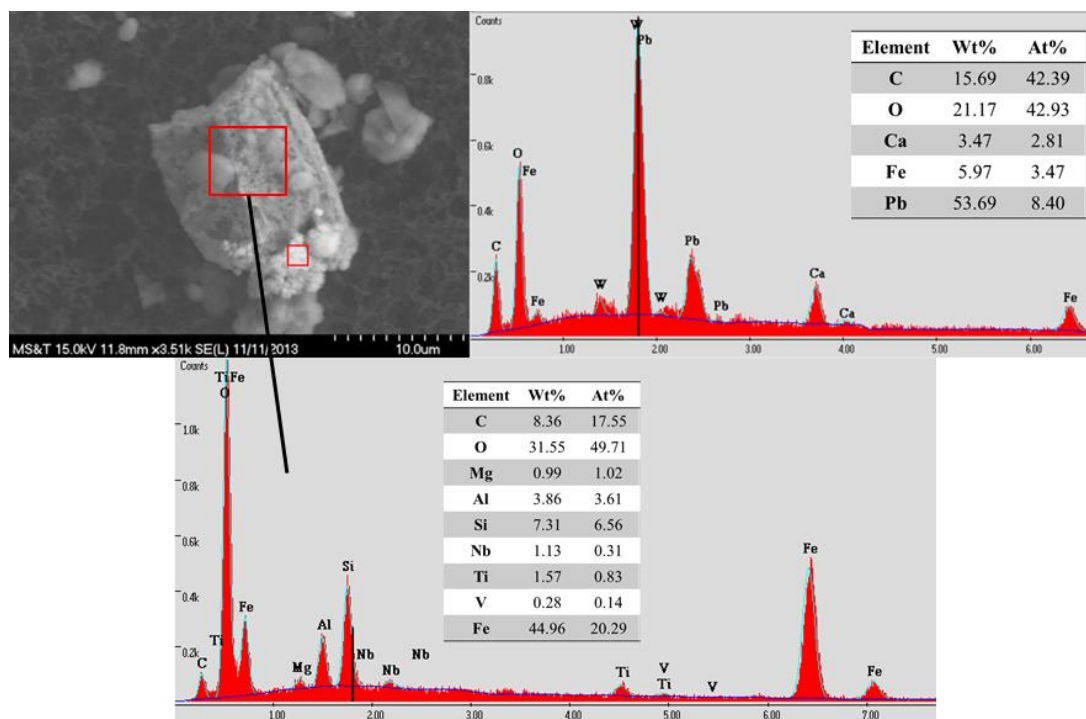


Figure 3.19. SEM-EDS results of a particle containing lead in core 2. The larger soil particle is possibly an iron-oxide (EDS spectra on bottom).

3.5. SOIL pH

Both core 2 and core 4 followed similar pH trends in regards to increasing depth (Figure 3.20). Core 2 was slightly acidic in the Oh to 1 inch depth with a pH of 5.20. This value became more acidic with increasing depth. At 11 to 13 inches, the pH bottomed out at 3.80 before slightly rebounding to 3.89 at 14 to 16 inches.

Core 4 had a pH that was less acidic at 0 to 2 inches at 5.95. The soil continued to become more acidic with increasing depth. The most acidic reading of 3.83 was at 10 to 12 inches depth, and rebounded slightly back to 3.89 at 13 to 15 inches in depth.

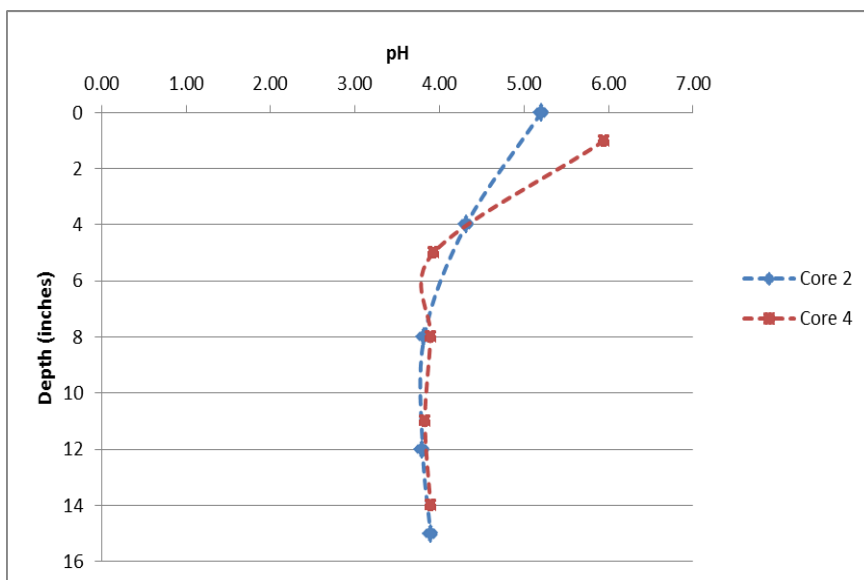


Figure 3.20. Soil pH profiles for core 2 and core 4. Each profile displays a decreasing pH with increasing depth. Plotted using average depth values.

4. DISCUSSION

4.1. TOTAL DIGESTIONS

Total digestion results suggested metal concentrations decrease with increasing distance from the smelter and are primarily within the first few inches of soil.

Concentration levels of lead from Oh horizon in core 2 (4737 ppm) were slightly greater than those in core 4 (4303 ppm), which would be expected due to its location closer to the smelter than core 4 (0.72 km vs. 1.55 km). However, core 2 lead concentrations dropped below 1000 ppm between 0 to 1 inches in depth, whereas core 4 had lead concentrations still above 3000 ppm at 0 to 1 inches of depth (Figures 3.1 and 3.2).

Varying lead concentrations could be due to variability in soil constituents that allow the lead greater downward mobility in core 4. At 0 to 2 inches depth in core 4, mixed-layered clays composed 33 percent of the soil and could be a factor in reducing lead mobility by adsorption. It is also probable that variations in the soil mineralogy forms a more adsorptive layer in core 2 at 3 to 4 inches that increases concentrations of lead, zinc, copper, and phosphorus (Figure 3.1). However, the majority of the clay-sized fraction was kaolinite at the 1 to 3 inch depth in core 2, which should not affect lead immobilization and thus increase concentrations. The effect of clays on trace metals will be discussed later in the discussion.

In core 2, zinc, copper, lead, and arsenic showed an initial decrease in concentration within the first three inches of depth. It appeared that copper, zinc, iron, and nickel have similar increasing trends at depth (9 to 16 inches), suggesting that factors that affect their mobility through the soil profile are the same (Figure 3.1).

Correlation coefficients comparing linear behavior of iron versus each respective contaminant element produced R^2 values of 0.06, 0.77, and 0.98 for zinc, nickel, and copper, respectively from 9 to 16 inches of depth (Figure 4.1). This suggests that the iron is a strong factor in concentration of copper and nickel, but has minimal influence on zinc distributions. The same elements in core 2 were compared to manganese and resulted in R^2 values of 0.11, 0.79, and 0.65 for zinc, nickel, and copper, respectively at 9 to 16 inches.

Core 4 correlations were difficult to determine due to lower overall metal concentrations and several intervals that were below the ICP-OES detection limit (<10 ppm) for nickel and copper. However, zinc versus iron correlation resulted in a R^2 value 0.97 for 9 to 15 inches of depth. Copper versus iron correlation for 7 to 12 inches of depth resulted in a R^2 value of 0.04 (Figure 4.2). These are opposite of those found in core 2, and suggest that while zinc might be absorbed or adsorbed by iron oxides or smectite, copper is likely being affected by other factors. Lead versus manganese correlations for core 4 total digestions resulted in a R^2 value of 0.13 for 4 to 11 inches depth. This is unexpected considering lead was associated with the iron or manganese oxides extract in sequential extractions.

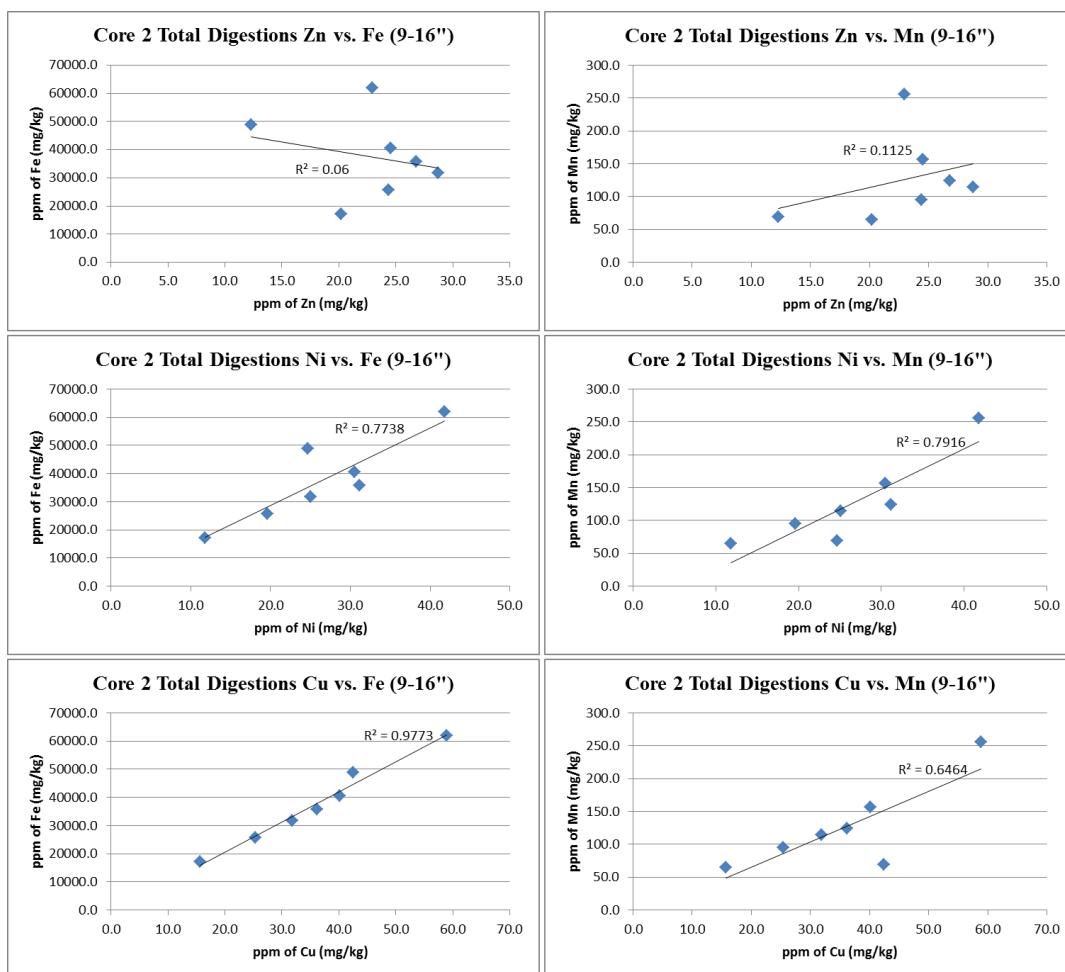


Figure 4.1. Correlation coefficients for zinc, nickel, and copper in core 2 total digestions. All are plotted against iron (left column) and manganese (right column).

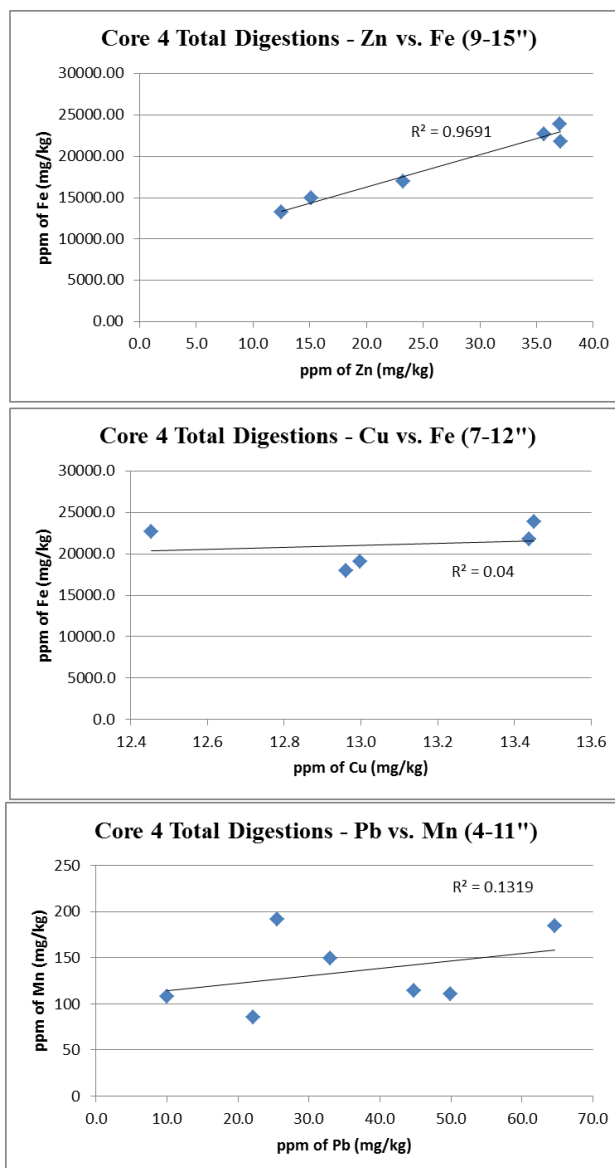


Figure 4.2. Correlation coefficients for zinc, copper, and lead for core 4 total digestions. Zinc and copper plotted against iron, while lead is plotted against manganese.

4.2. SEQUENTIAL EXTRACTION

Sequential extractions, while providing support to the total digestion results, mainly help determine what metals are associated with each soil constituent and how easily they are released. Lead concentrations for both cores were highest in the upper

portions of the core in Extract B (Figures 3.4 and 3.8). This suggests that lead is in association with iron or manganese oxides (Appendix C).

Hettiarachchi and Pierzynski (2004) report preferential adsorption of lead by manganese oxides compared to other oxides. These adsorption processes are almost irreversible, limiting the metal's bioavailability. McKenzie (1980) found that lead adsorbs to manganese oxides 40 times more effectively than it did to iron oxides. Wong and Li (2004) study of urban soils in Hong Kong stated that around 60 percent of their total lead was associated with iron and manganese oxide fractions. They also noted that the two most mobile fractions in soils are the exchangeable and carbonate fractions, which would correlate with Extract A in the current study.

In the current study, core 2 lead was associated mainly with the iron or manganese extract (49 percent) and carbonates or exchangeable sites (44 percent; Figure 4.3). In core 4, the majority of the lead was associated with the iron or manganese oxide extract (78 percent; Figure 4.4). These results correlate with those reported in Wong and Li (2004). Iron is found to be greatest in Extract D in the current study. This extract is associated with iron that is not readily removed from the soil.

Similar to total digestions, correlations were calculated for iron versus zinc, nickel, and copper in Extract D. In core 2, R^2 values for iron versus zinc, nickel, and copper were 0.40, 0.93, and 0.98, respectively for 8 to 15 inches in depth (Figure 4.5). The R^2 values for manganese versus zinc, nickel, and copper were 0.52, 0.89, and 0.96, respectively, for 8 to 15 inches in depth. In core 4, R^2 values with iron were 0.79, 0.86, and 0.97 for zinc, nickel, and copper, respectively, for 5 to 15 inches (Figure 4.6). The R^2 for the same elements compared to manganese was 0.67, 0.82, and 0.94 for zinc, nickel,

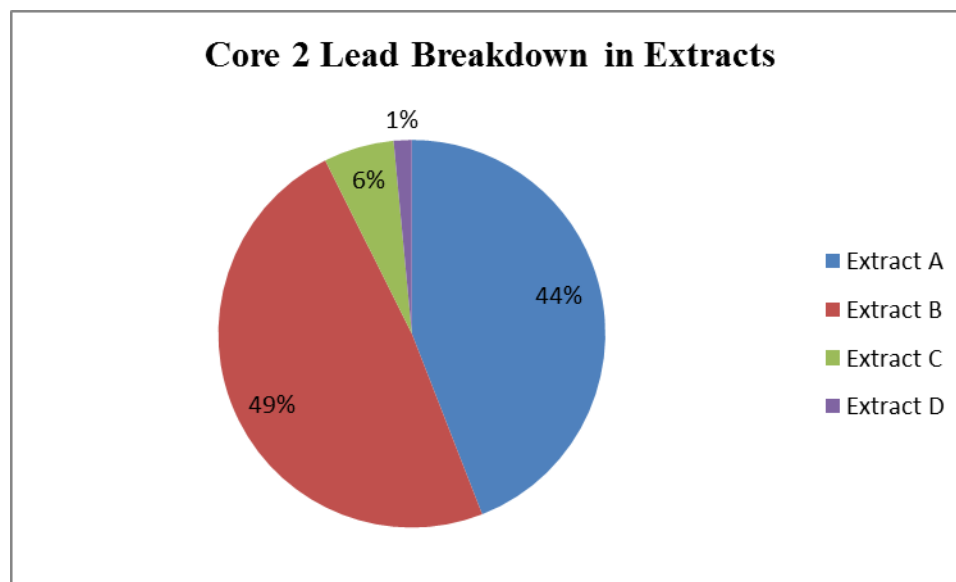


Figure 4.3. Percentage of lead contained in each extract for core 2 sequential extractions. These percentages are based on all measurable lead concentrations in each extract.

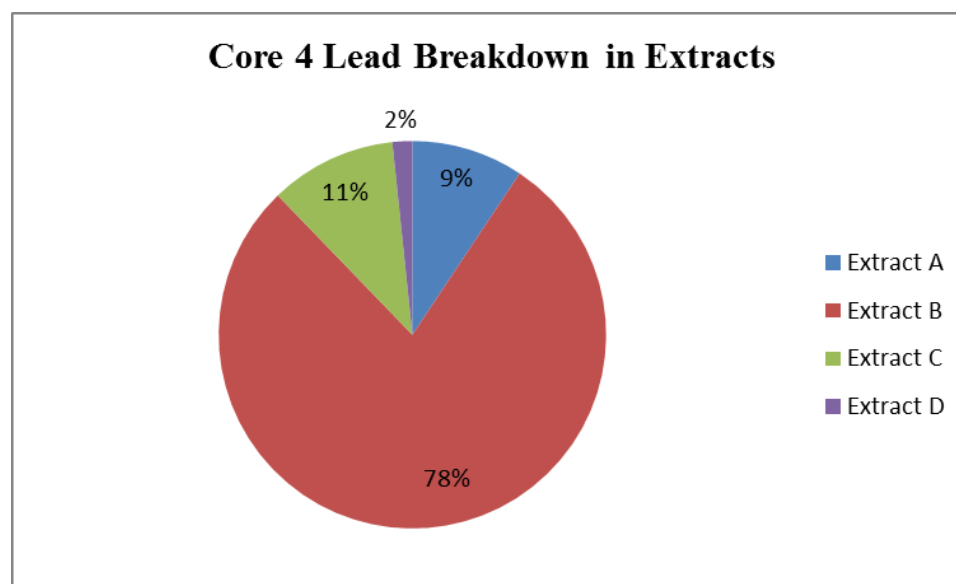


Figure 4.4. Percentage of lead contained in each extract for core 4 sequential extractions. These percentages are based on all measurable lead concentrations in each extract.

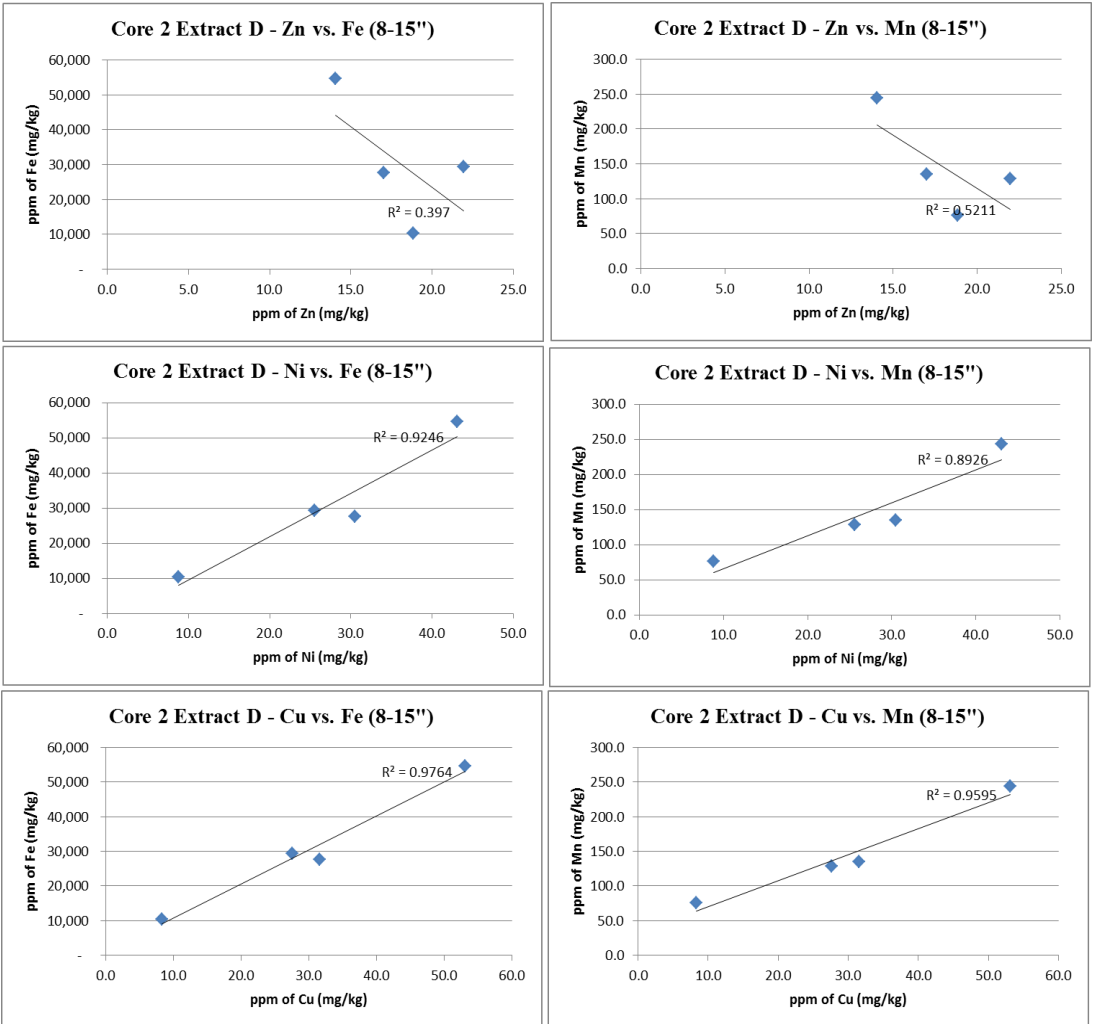


Figure 4.5. Correlation coefficients for zinc, nickel, and copper in core 2, Extract D. All are plotted against iron (left column) and manganese (right column).

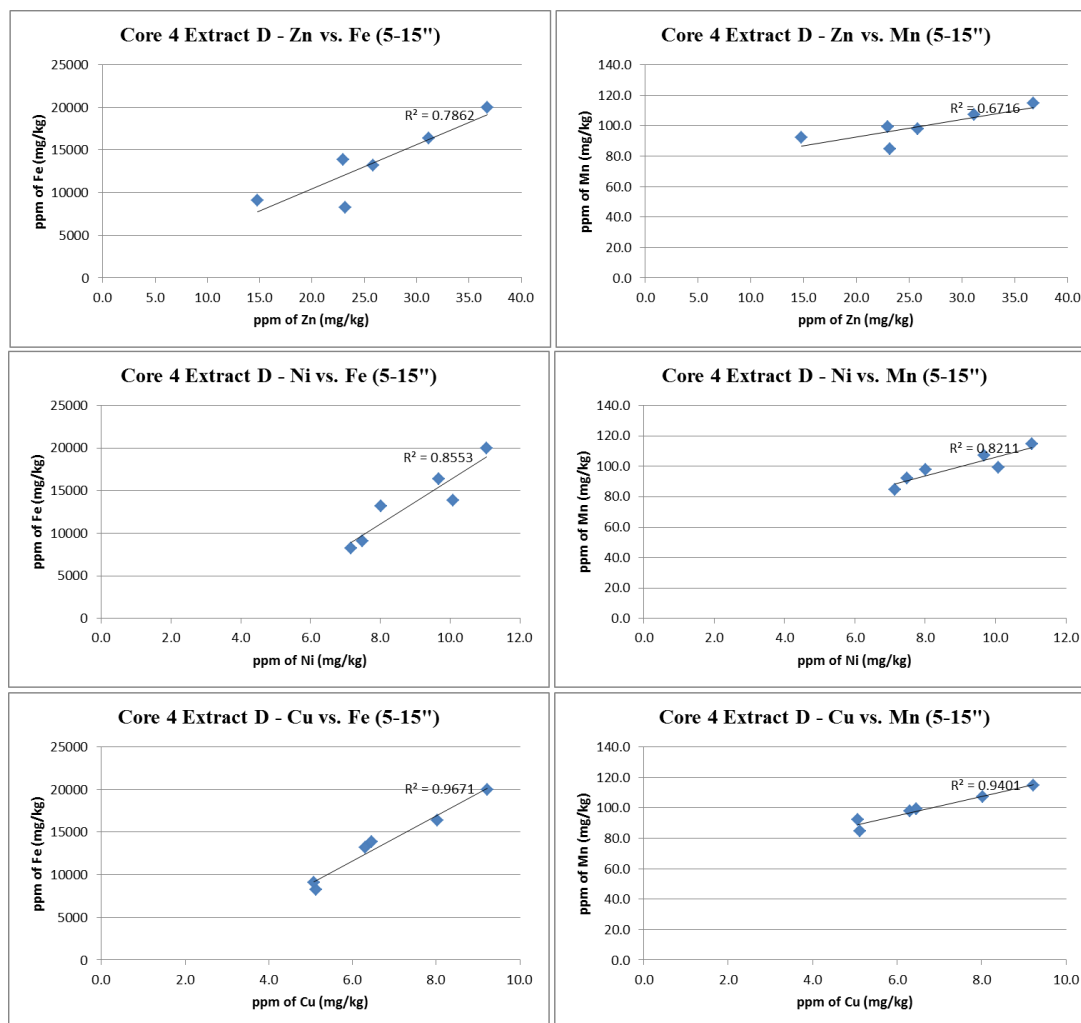


Figure 4.6. Correlation coefficients for zinc, nickel, and copper in core 4, Extract D. All are plotted against iron (left column) and manganese (right column).

and copper, respectively, for 5 to 15 inches. The correlation coefficients for iron and manganese versus these elements are very similar, suggesting both iron and manganese are likely factors in their adsorption or lack thereof. This also suggests that the iron and manganese correlating with these metals are not oxides, as they do not show this trend in the Extract B.

Considering lead concentrations are highest in Extract B, which releases lead from iron or manganese oxides, one would expect the trends for iron, manganese, and

lead to be similar. This is not the case. This is validated when the R^2 value for lead versus manganese in core 2, Extract B was 0.45 for the depth from the Oh horizon to 4 inches.

All of the metals (zinc, copper, nickel) that showed an increase in concentration at depth appeared to have greater downward mobility than lead, which is contained mainly in the upper three inches of depth of soil. Factors that affect trace metal mobility will be discussed later. Lead, the main metal of concern, did not appear to be above background levels (in ppm) below 10 to 11 inches of depth in both soil cores.

4.3. SEM-EDS

SEM-EDS analysis was used to determine what mineral species of lead and what minerals are associating with lead in the soil. SEM-EDS analysis in the current study did not strongly support lead-bearing particles being associated with iron or manganese oxides as found with the sequential extraction results. It is possible that those particular associations were not found and analyzed by the microscope.

SEM-EDS data reflected the presence of a lead carbonate, cerussite, which could be a product of weathered galena. Galena can alter to anglesite, cerussite, or pyromorphite when in the presence of an oxidized environment (Hettiarachchi and Pierzynski, 2004). X-ray diffraction of particles from leaves gathered in a study of the BRRD area by Jackson and Watson (1977) indicated the presence of lead oxide (PbO) and lead sulfate (PbSO₄). Galena (PbS), the mineral smelted at the Buick Smelter at the time of their study and before conversion to a recycling smelter, was minimally present.

Ruby et al. (1994) noticed in photomicrographs of galena particles from a port facility that several lead mineral associations were present around galena crystals. They

inferred that the galena, which was the primary phase, altered to anglesite or cerussite and eventually to lead phosphate. A similar alteration process may be occurring in the soils near the BRRD.

Ruby et al. (1994) noted the relative K_{sp} values of lead compounds under equilibrium earth-surface conditions. The values from Ruby et al. were used because they provided K_{sp} for all lead mineral species. Using these values, the solubility of lead for the various mineral states can be calculated. Lead sulfide was not calculated, because it will not precipitate in an oxidizing environment. For lead oxide, lead solubility is calculated to be 2.8×10^{-6} m. Lead sulfate has a calculated lead solubility of 1.41×10^{-4} m, while lead carbonate has a lead solubility of 3.97×10^{-7} m. Finally, lead phosphate has a calculated lead solubility of 4.15×10^{-9} m. Outside variables of the soil, like pH, will affect these lead solubility values.

Lead phosphate is the most stable form of lead in soil and is less soluble than other forms (Nedwed and Clifford, 1997; Ruby et al., 1994). While no phosphorus suggestive of phosphate formation was found associated with the lead during SEM-EDS analysis, there is still a significant amount (59.0 to 410 ppm) of phosphorus in the results from the total digestion analyses. If phosphates were controlling mobility, there should be a correlation between lead and phosphorus, which there is not (Figures 3.1 and 3.2). This may indicate that the lead occurs in concentrations in excess of what the phosphate can complex with or the phosphate is bound to other soil components and was unavailable to bind with lead.

Previous studies SEM-EDS analyses of lead-bearing particles in the area did not indicate the presence of lead phosphate mineral species, but rather the slightly less

soluble minerals of anglesite and cerussite. Rucker (2000) found particles that were cubic in nature, but the EDS spectra did not support the presence of galena. He suggested an oxidized coating (probably anglesite) on a galena crystal. In Witt et al. (2013), a cubic crystal was also found using SEM-EDS, with weathering of anglesite and cerussite. In 2014, Witt et al. found dipyramidal cerussite crystals using SEM-EDS. These findings correlate to the presence of cerussite, or potentially anglesite in the current study.

4.4. FACTORS POTENTIALLY AFFECTING LEAD MOBILITY

Since soils are heterogeneous and complex chemically and physically, it is difficult to attribute metal concentration changes to one specific thing. Overall, clay content, soil pH, and weather conditions can all affect the distribution of metals in a soil profile.

4.4.1. Clay Mineralogy. Clay mineralogy can be a factor in the reduction of lead mobility. While smectite does not compose a majority of the soil, there is a slight increase in its quantity deeper in the soil core (Figures 3.11 and 3.12). Smectite is a 2:1 phyllosilicate, with two tetrahedral layers sandwiched between an octahedral layer. This structure repeats in a stacking behavior, with an interlayer site located between each 2:1 phyllosilicate sheet. This interlayer is capable of exchanging cations present in the local environment in an effort to balance the charge of the clay, and could remove contaminants from within the soil (Deer et al., 1966).

Typically, smectite has a 5.2° 2-theta peak in the glycol run and shows a shift when compared to the untreated runs. However, there is the issue of the unidentified peak that occurred around between 6.175° - 6.35° 2-theta and showed no shrink/swell properties

(Appendix E). In addition, some samples showed a presence of mixed clays. This peak might correspond to a mixed-layer clay that contains illite and smectite. It is difficult to predict the stacking sequence and the ratio of smectite to illite if this is the case. With little shifting in the glycol run, illite could compose a majority of the structure. Plus, in some instances after the heated XRD runs, the illite peak at 8.8° 2-theta increased slightly, which is indicative when smectite dehydrates.

The quantification procedures do not account for smectite identification if it is contained in a mixed-layer clay, and therefore it is possible that more smectite exists within the soil than was calculated. Lead and other trace metals are susceptible to adsorption to the interlayer of these clays, which could then prohibit them from migration downwards to the water table. Alternatively, depending on chemical composition, layers may be more strongly linked together, which could reduce the sorptive capability for metals. Rucker (2000) attributed non-swelling behavior seen in his XRD study to metal adsorption in the interlayer of smectites.

Iron concentrations were greater at depth in the soils could be a result of iron oxides or the iron-rich smectite, nontronite. These provide potential sorptive materials for removing nickel, zinc, and copper from the soil and thus increasing concentrations in the deeper soil profiles. Considering the largest concentrations of iron were in Extract D instead of B (which is the association with iron oxide extract), it is possible that most of the iron at this depth is due to the presence of the clay mineral nontronite, rather than iron oxy-hydroxides.

Kaolinite and illite make up the majority of the clays in the two soil cores, similar to what Rucker determined in his study. Due to their structures and low cation exchange

capability (McBride, 1994), these clays are less likely to be a significant factor in metal adsorption. While concentrations of smectite are low in his study, Rucker (2000) believed they might control a small portion of the metal adsorption, and resulted in an increase in concentrations of some metals at depth. In the current study, nickel and copper were the two metals that showed increased concentrations at depth.

Witt et al. (2014) stated that lead has a smaller ionic potential, which can hamper its adsorption rate onto clays. Ionic potential is determined by dividing the ion's charge by its radius. Lead has a potential of 1.14, while nickel and copper have potentials of 1.61 and 1.56, respectively. The fact that nickel and copper concentrations both increase at depth and that both have nearly the same ionic potential could be a factor for their potential adsorption on clays.

4.4.2. Soil Grain Size. Additionally, the size of soil grains or particles have the potential to affect metal adsorption. Bradl (2004) stated that coarse-grained soils are less likely to adsorb heavy metals in comparison to finer-grained soils. This is attributed to the finer-grained fraction having larger surface areas of clays, oxides, and compounds, which is prime for adsorption. Witt et al. (2014) found that the $<1\mu\text{m}$ particle fraction had larger concentrations than the $>1\mu\text{m}$ particle fraction. It was also noted that Al-Si clay particles existed in the $<1\mu\text{m}$, which could be weak adsorption sites for lead metal. It is impossible to say if soil particle size is a factor in the current study since it was not studied, but it would be useful to include in future studies.

4.4.3. pH. Overall, pH plays the most important role in lead stability and sorption within the soils, as it can affect lead speciation and charges on the soils surface groups (Martínez-Villegas et al., 2004).

The current study had a general decreasing pH (more acidic) trend with increasing depth for both cores (Figure 3.18). Rucker's (2000) study also presented a general decrease in pH with increasing depth; however the values were not steady and fluctuated heavily between intervals. Bornstein's (1989) sampling points are offset from the current study, but he noted that the pH decreased slightly with depth, and increased overall with increasing distance from the smelter stack. He also noted that acidity of the soil was much higher near the smelter due to sulfide minerals weathering and producing sulfuric acid.

A higher pH or increasing soil pH can increase the sorption of lead (Martínez-Villegas et al., 2004). In the current study, the majority of the lead resided in the first few inches of soil where the pH is highest, where it would be stable/insoluble. Thus, it is possible that pH is the major controlling factor in the mobility of trace metals in the upper portion of the soil cores.

4.4.4. Potential Weather Conditions. The weather conditions (precipitation, temperatures) during the sampling years are not noted. This information would be a valuable addition to future studies of this area.

Nedwed and Clifford (1997) cited two main mechanisms for controlling lead mobility at lead battery recycling sites, or more specifically, mobility in the soils around the battery-breaking area. These are the removal of lead-bearing soils during heavy rains and the transport of lead-containing dust through the air. While this study did not analyze soils in direct contact with battery processing, similar processes could occur in soils contaminated by air emissions.

In the current study, if a lack of rainfall and more drought conditions persisted, it may have affected the lead concentrations. Average rainfall values for St. Louis for the time period of 2000 to 2009 was 40.92 inches per year, with the highest rainfalls of 57.96 inches and 50.92 inches in 2008 and 2009, respectively. This average is greater than the 38.06 inches of rain average for the years 1988 to 1997, right before Rucker's (2000) study. Likewise, the average temperature for 2000 to 2009 was 57.3°F, while for 1988 to 1997 it was 56.8°F (National Weather Service, 2014). All of these values are very close to the averages listed by the U.S.D.A. None of these values suggest a possible drought; however, the increased levels of rainfall in the two years prior to sampling in 2010 could have influenced the removal of lead.

The standard solubility constant (K_{sp} : 7.40×10^{-14}) for cerussite was used to determine the solubility of lead in cerussite (2.7×10^{-7} M). Using the solubility of lead in cerussite, the highest lead concentration observed in total digestions (4743 ppm), and the average rainfall (40.92 in/yr), the amount of lead that can be removed from soil can be calculated. This assumes that the lead phase present in the soil is cerussite and the density of soil is around 2.0 g/cm^3 . It was calculated that 4.58×10^{-5} moles of lead/ cm^3 exist within a theoretical block of soil (1 cm^3). With the average rainfall for the area and the solubility of lead in cerussite, it was calculated that 2.78×10^{-8} moles of lead/year can be removed from the soil. This value is less than the amount of lead calculated in a block of soil, which means it will take a much longer time to remove all of the 4743 ppm (around 1647.5 years). This means that rainfall is not a large factor in the removal of lead from soil, but it is possible it still plays a role in the removal of some lead.

4.5. COMPARISON TO PREVIOUS STUDIES

Comparison between the previous studies and the current study is limited in some cases, due to differences in study structures. Butherus (1975), Bornstein (1989) and Rucker (2000) only analyzed to one, six, and seven inch depths, respectively. Butherus studied soils to greater depths in other areas around the smelter, but found that most contamination was in the Oh horizon and first inch of soil. The current study analyzed to depths of 16 inches in core 2 and 15 inches in core 4; some greater concentrations are seen in the greater depths of the cores. To the depths available, trends in core 2 appear to best match Rucker's study.

Variations in the metal concentrations could be influenced by changes within the smelting facility. The facility switched to a recycling smelter in 1988, thus Butherus' (1975) and Bornstein's (1989) data would reflect effects of only primary lead ore smelting. Rucker's (2000) study was the first conducted after a significant amount of time since the conversion of the smelter to lead recycling.

4.5.1. Lead Concentrations. Compared to previous studies, trace metal concentrations have varied over time. Butherus' (1975) soil data for Oh horizon near core 2 shows lead to be much lower than Rucker (2000) and Bornstein's (1989) values, but close to the current measured value (4743 ppm). Core 4 lead concentrations in the Oh from the previous studies are all similar with the exception of Rucker's study, which is more than 3 times as much as the current study (Figures 4.7 and 4.8). The reason for Rucker's greater lead value is unknown.

Bornstein (1989) described a "maximum loading" theory which Rucker (2000) references as the reason for minimal variation in lead concentrations between the two

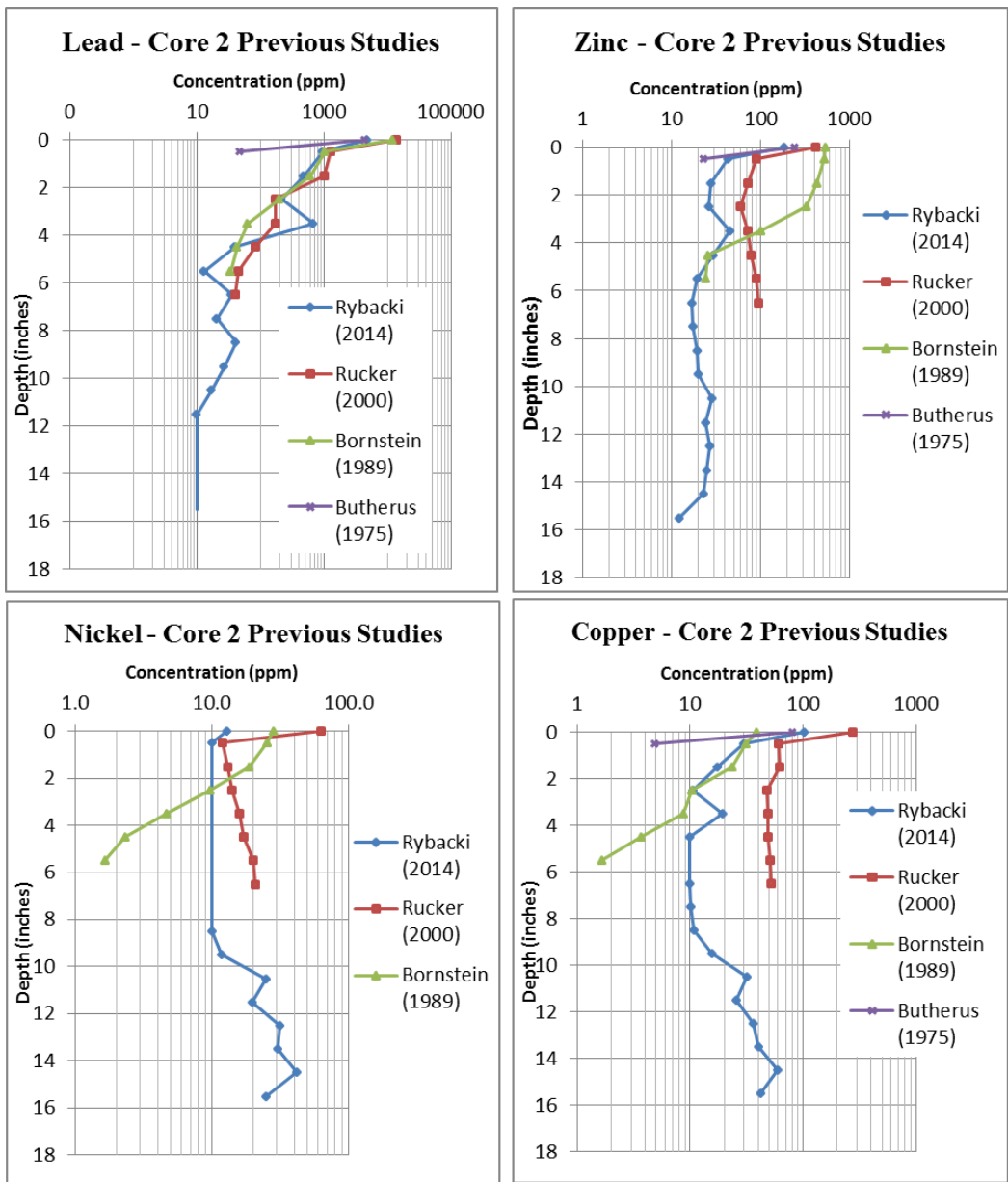


Figure 4.7. Metal concentration trends for core 2 compared to cores from similar locations in previous studies. Points plotted at average depths, with Oh at 0 inches. Review data values in Appendix A for detection limits.

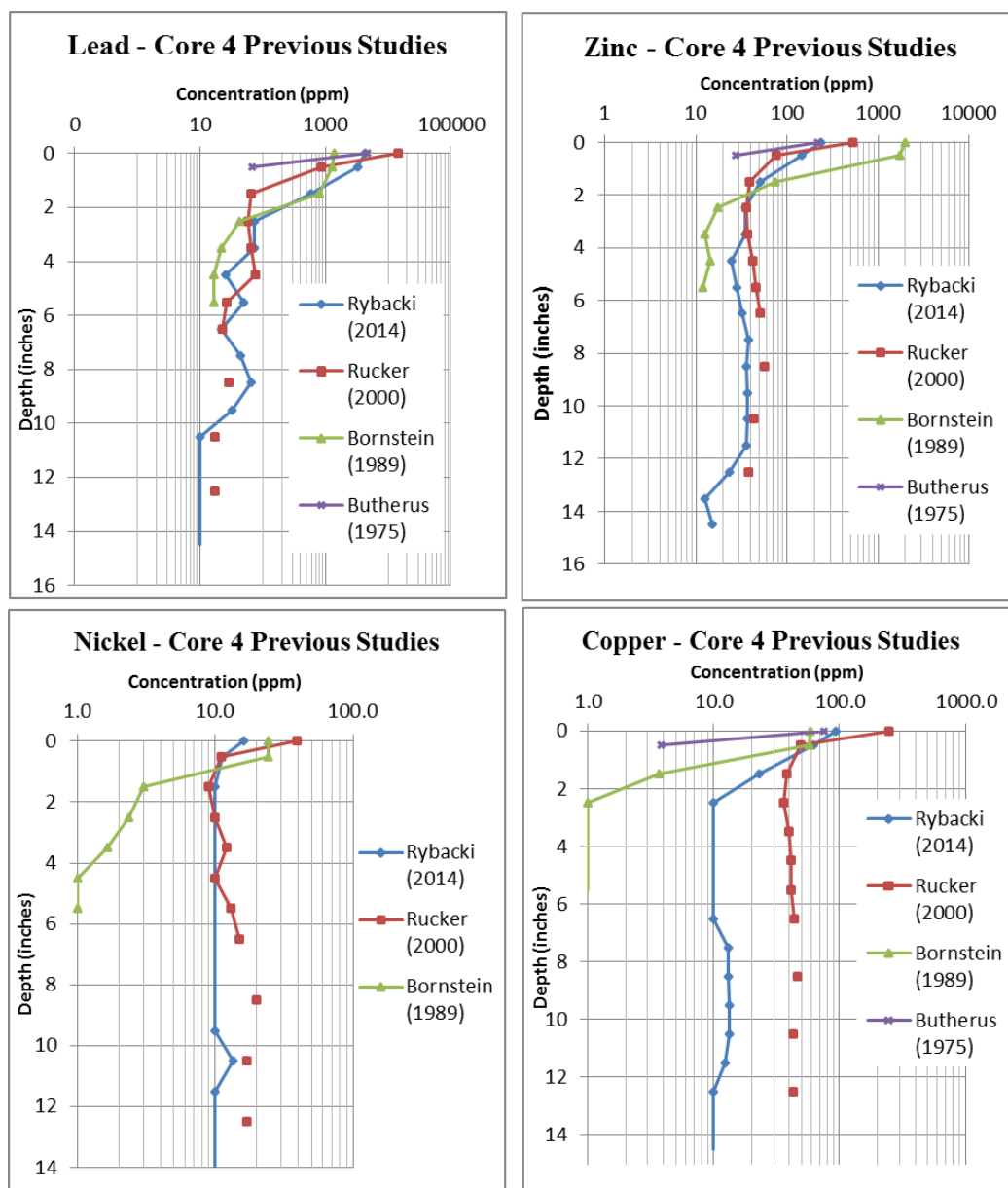


Figure 4.8. Metal concentration trends for core 4 compared to cores from similar locations in previous studies. Points plotted at average depths, with Oh at 0 inches. Review data values in Appendix A for detection limits.

studies. Bornstein believed the soil reached maximum loading within the first years of smelting. Rucker suggested that if this is the case, any other metals added could be solubilized and washed away. While maximum loading can occur when all sorptive sites

in the soil are occupied, this does not mean particulate lead concentrations within the soil cannot increase.

4.5.2. Other Metal Comparisons. In core 2, zinc concentrations from the current study are generally lower than the Rucker (2000) and Bornstein (1989) studies throughout the soil core. Bornstein's zinc concentration trend appeared to stay fairly constant in the first 2 inches of depth, when most of the other studies showed a decrease in concentration. In core 4, zinc concentrations in the Oh were highest in Bornstein's study (1970 ppm) compared to the other studies (216 to 531 ppm). Overall, all the trends decrease with increasing depth.

In core 2, copper concentrations from the current study and Rucker's (2000) study were greater at depth than the previous two studies. In the current study, values steadied out at 10 ppm at around 7 to 9 inches of depth, and then increased to 58.9 ppm around 14 to 15 inches depth. Without the greater depths in the other studies, it is impossible to compare, but all the previous studies showed a decline in the first 2 inches of depth. In core 4, all of the previous studies appeared to decrease significantly in concentrations over the first two inches of depth, similar to the current study.

In core 2, nickel concentrations in the Oh were highest in Rucker's (2000) study (62.7 ppm). The current study, Rucker's study, and Bornstein's (1989) study all showed decreasing concentration with increasing depth. However, Rucker's study showed a slight increase in concentration at the bottom of his soil core. In core 4, Rucker provided the best overall trend, which decreased with increasing depth and then slightly increased in concentration at 8 to 9 inches depth. Bornstein's concentrations decreased significantly over the first three inches of depth (25 ppm to 2 ppm).

Cadmium, cobalt, and antimony in the current study were sporadically present or below detection limits. Cadmium was detected in all previous studies. Butherus (1975) and Bornstein (1989) had their highest cadmium concentrations in the Oh horizon and then decreasing concentrations with increasing depth. Rucker (2000) found his highest cadmium concentrations in the Oh horizon, a decrease in concentration with increasing depth, and a slight increase in concentration at the bottom of the soil core.

Cobalt in Rucker's (2000) study was highest in the Oh horizon for both cores (Core 2: 18 ppm; Core 4: 15 ppm) and decreased with increasing depth. Bornstein (1989) had a similar trend to Rucker's but at higher concentrations in both cores (Oh Core 2: 58.33 ppm; Oh Core 4: 23 ppm). Antimony was only analyzed for in Rucker's study, and was only present in the Oh horizon of core 2 (1.46 ppm).

Lead-based batteries contain antimony, arsenic, cadmium, copper, selenium and tin as additives, and thus are present in significantly lower concentrations than lead (Nedwed and Clifford, 1997). In comparison to primary smelting times, the Buick orebody was chiefly lead, zinc, and copper sulfides (Rogers and Davis, 1977).

4.5.3. Sequential Extraction Comparison. The sequential extraction procedure was not applied to the soils collected in any of the previous studies near the Buick smelter. However, comparisons can be made between Rucker's (2000) SEM-EDS data and sequential extraction results from this study.

Rucker (2000), utilizing SEM-EDS, found particles of lead in association with iron and manganese hydroxides, which would correspond with Extract B in the current study. Rucker also mentioned complexes with organic compounds, which, in the current study, would likely be associated with Extract C. Stevenson and Welch (1979) mentioned

that concentrated organic matter can complex with lead to become a soluble chelate complex. They go on further to mention that downward movement of lead in soil profiles is due to decaying organics. While Extract C was not associated with a large amount of the metals, except for zinc in both cores and copper in core 4, organic concentrations are likely greatest in the upper portion of the soil profile (the Oh and 0 to one inch intervals), as indicated by a darker, black color present in these soil horizons. This could explain the large concentrations of metals retained in the first few inches of soil depth.

4.6. COMPARISON TO OTHER SMELTER STUDIES

Several studies conducted on soils around other smelters produced similar results to those of the current study. Soils near zinc smelters in Pennsylvania, studied by Buchauer (1973), noted concentrations of zinc, cadmium, copper, and lead that decreased significantly with increasing depth. In fact, 85 to 95 percent of the total zinc resided in the top 15 cm of the soil core. Soil pH also decreased around smelters that released sulfur (Buchauer, 1973).

Increased metal concentrations in soil, grasses, and aerosol tests were found in a study near a smelter in Idaho. The soils closest to the smelter showed the greatest concentrations, which were similar to concentrations in tailing pile samples (Ragaini et al., 1977).

Prapaipong et al. (2008) studied soil and trees surrounding a primary lead smelter in Glover, Missouri (located ~28 miles [45 km] southeast from the Buick smelter) which was in operation from 1963 to 2003. The authors found that lead concentrations decreased substantially with increasing distance from the smelter. In tree cores, the

highest concentrations were not found until samples dated 1975-1990. While within 1.5 km of the smelter, concentration levels were lower below 30 cm in depth. Their study of lead in tree cores yielded results where concentrations were below 0.5 mg/kg for samples earlier than 1970, while from 1975 to 1990 there was a significant increase. After 1990, the concentrations only increased, with maximum concentrations varying from 1 to 10 mg/kg.

With tree cores showing larger amounts of lead present, Prapaipong and coworkers suggested the contamination is likely to have come through the roots of the tree. If this theory is correct, and roots are tapped into the groundwater, tree cores have the potential to point to groundwater lead contamination. However, they cited the source of lead within the tree rings most likely to come from the vadose zone and not groundwater.

Since analyses in the current and past studies of the Buick smelter did not go to great soil depths, it is beyond our knowledge to know if lead is concentrated at a greater depth than the current study spans. Trees would be a valuable way to determine if trace metal concentrations are increasing at depth, or how far trace metals have migrated.

5. CONCLUSIONS

In this study, current metal concentrations and their distribution in the soils around the Buick Resource Recycling Division smelter were determined. This data was compared to previous studies to determine any changes in metal concentrations over time. Additionally, analyses on soil mineralogy and soil pH provided information on soil properties that may affect metals within the soil.

This study used sequential extraction methodology, which had not been used in previous studies of the area, to determine trace metal associations and concentrations within the soil. Similar to previous studies, total digestions were conducted to determine trace metal concentrations. X-Ray Diffraction (XRD) was used to determine clay mineralogy and Scanning Electron Microscopy-Energy Dispersive Spectroscopy (SEM-EDS) was used to determine mineral species and trace metal associations.

Several differences exist when comparing metal concentrations from the current study to previous studies conducted in the area. Lead concentrations were lower in the current study. Lead was still significantly retained in the upper portions of the soil profile. Other trace metals, like cadmium, cobalt, and antimony were variably distributed throughout both cores. Concentrations in the Oh horizon decreased as distance from the smelter increased. Concentrations of some metals decreased sharply with increasing depth in the soil cores.

Sequential extraction results indicated that the majority of lead is associated with iron or manganese oxides, carbonates, and exchangeable ions. Other metals like zinc, nickel, and copper were more often associated with organics, sulfides, and any non-

silicates remaining in the soil. Lead concentrations from total digestions and sequential extractions were in agreement.

Clays were primarily kaolinite. However, smectite, with the ability to sorb metals, was present in small amounts. Another clay, potentially a smectite/illite combination, did not show expansive properties and could also be a factor limiting metal movement in the soil profile. Some quantitative issues existed in clay mineral analysis. SEM results indicated lead potentially in association with clays.

SEM-EDS also suggested the presence of the mineral cerussite. However, there were some issues in EDS spectra peaks that prevented a definitive answer as to what lead mineral was present. A pH decrease with increasing depth in the soil cores does not promote stability of lead and other trace metals through the soil column.

APPENDIX A.

PREVIOUS STUDIES DATASETS

Table A-1. Lead concentrations (in ppm) from previous studies conducted at or near core 2 site (0.72 km).

Depth (in.)	<i>Rybacki (2014)</i>	<i>Rucker (2000)</i>	<i>Bornstein (1989)</i>	<i>Butherus (1975)</i>
Oh	4743	13,600	12,166.66	4400
0-1	971	1250	1019.66	49
1-2	473	1010	596.66	
2-3	212	170	195.55	
3-4	673	170	62.22	
4-5	40.3	83	43.66	
5-6	13.3	44	33.66	
6-7	35.4	40		
7-8	20.3			
8-9	40.9			
9-10	26.8			
10-11	17.2			
11-12	<10			
12-13	<10			
13-14	<10			
14-15	<10			
15-16	<10			

Table A-2. Nickel concentrations (in ppm) from previous studies conducted at or near core 2 site (0.72 km).

Depth (in.)	<i>Rybacki (2014)</i>	<i>Rucker (2000)</i>	<i>Bornstein (1989)</i>	<i>Butherus (1975)</i>
Oh	13.0	62.7	28	
0-1	<10	12	25.33	
1-2	<10	13	18.66	
2-3	<10	14	9.66	
3-4	<10	16	4.66	
4-5	<10	17	2.33	
5-6	<10	20	1.66	
6-7	<10	21		
7-8	<10			
8-9	<10			
9-10	11.8			
10-11	25.0			
11-12	19.6			
12-13	31.2			
13-14	30.5			
14-15	41.8			
15-16	24.7			

Table A-3. Copper concentrations (in ppm) from previous studies conducted at or near core 2 site (0.72 km).

Depth (in.)	<i>Rybacki (2014)</i>	<i>Rucker (2000)</i>	<i>Bornstein (1989)</i>	<i>Butherus (1975)</i>
Oh	103	277	38.5	80.0
0-1	29.6	61	31.33	4.8
1-2	17.4	62	23.33	
2-3	10.5	48	10.33	
3-4	19.5	49	8.66	
4-5	<10	49	3.66	
5-6	<10	51	1.66	
6-7	<10	52		
7-8	10.1			
8-9	10.8			
9-10	15.7			
10-11	31.8			
11-12	25.4			
12-13	36.2			
13-14	40.1			
14-15	58.9			
15-16	42.5			

Table A-4. Zinc concentrations (in ppm) from previous studies conducted at or near core 2 site (0.72 km).

Depth (in.)	<i>Rybacki (2014)</i>	<i>Rucker (2000)</i>	<i>Bornstein (1989)</i>	<i>Butherus (1975)</i>
Oh	184	411	526.66	240
0-1	43.2	90.3	523	23.0
1-2	27.7	71.3	430	
2-3	26.0	60	326.66	
3-4	45.2	73	100.33	
4-5	29.7	79	25.66	
5-6	19.6	90	24.33	
6-7	16.8	94		
7-8	17.4			
8-9	19.4			
9-10	20.2			
10-11	28.7			
11-12	24.4			
12-13	26.8			
13-14	24.5			
14-15	22.9			
15-16	12.3			

Table A-5. Lead concentrations (in ppm) from previous studies conducted at or near core 4 site (1.55 km). *The 3 and 4 inch intervals were combined

Depth (in.)	<i>Rybacki (2014)</i>	<i>Rucker (2000)</i>	<i>Bornstein (1989)</i>	<i>Butherus (1975)</i>
Oh	4303	14,300	1367	4600
0-1	3235	866	1268	69.0
1-2	577	65	786.66	
2-3	74.0	59	43.33	
3-4	*3/4 inch	65	21.66	
4-5	25.5	77	16.33	
5-6	49.9	27	16.66	
6-7	22.1	23		
7-8	44.8	--		
8-9	64.6	29		
9-10	32.9	--		
10-11	<10	17		
11-12	<10	--		
12-13	<10	17		
13-14	<10			
14-15	<10			

Table A-6. Nickel concentrations (in ppm) from previous studies conducted at or near core 4 site (1.55 km).

Depth (in.)	<i>Rybacki (2014)</i>	<i>Rucker (2000)</i>	<i>Bornstein (1989)</i>	<i>Butherus (1975)</i>
Oh	16.2	39	24	
0-1	11.3	11	24.33	
1-2	<10	9	3	
2-3	<10	9.9	2.33	
3-4	*3/4 inch	12	1.66	
4-5	<10	10	<1	
5-6	<10	13	<1	
6-7	<10	15		
7-8	<10	--		
8-9	<10	20		
9-10	<10	--		
10-11	13.4	17		
11-12	<10	--		
12-13	<10	17		
13-14	<10			
14-15	<10			

Table A-7. Copper concentrations (in ppm) from previous studies conducted at or near core 4 site (1.55 km).

Depth (in.)	<i>Rybacki (2014)</i>	<i>Rucker (2000)</i>	<i>Bornstein (1989)</i>	<i>Butherus (1975)</i>
Oh	93.3	247	59	75.0
0-1	62.7	49	57.66	3.8
1-2	22.8	38	3.66	
2-3	<10	36	1	
3-4	*3/4 inch	40	<1	
4-5	<10	41	<1	
5-6	<10	41	<1	
6-7	<10	44		
7-8	13.0	--		
8-9	13.0	46		
9-10	13.4	--		
10-11	13.5	43		
11-12	12.5	--		
12-13	<10	43		
13-14	<10			
14-15	<10			

Table A-8. Zinc concentrations (in ppm) from previous studies conducted at or near core 4 site (1.55 km).

Depth (in.)	<i>Rybacki (2014)</i>	<i>Rucker (2000)</i>	<i>Bornstein (1989)</i>	<i>Butherus (1975)</i>
Oh	239	531	1970	216
0-1	145	76.2	1738.9	27.0
1-2	51.1	39	73.3	
2-3	34.6	36	17.33	
3-4	*3/4 inch	37	12.66	
4-5	24.4	42	14.33	
5-6	28.4	46	12	
6-7	32.6	51		
7-8	37.6	--		
8-9	36.2	57		
9-10	37.1	--		
10-11	37.1	43		
11-12	35.7	--		
12-13	23.3	38		
13-14	12.5			
14-15	15.2			

APPENDIX B.
QUALITY CONTROL DATA

Table B-1. 0.1 ppm ICP-OES Quality Control core 2 sequential extractions. Bold indicates value used to calculate maximum error percentage.

	Zn	Fe	Co	Ni	Cu	Cd	Sb	Pb	As	P
Trial 1	0.09	0.10	0.09	0.10	0.10	0.10	0.01	0.10	0.18	0.11
Trial 2	0.09	0.10	0.10	0.10	0.10	0.10	0.12	0.11	0.14	0.13
Trial 3	0.09	0.10	0.10	0.10	0.10	0.10	0.11	0.11	0.16	0.12
Trial 4	0.10	0.11	0.10	0.11	0.11	0.16	0.12	0.11	0.10	0.10
Average	0.09	0.10	0.10	0.10	0.10	0.12	0.09	0.11	0.15	0.12
Standard Deviation	0.01	0.01	0.01	0.01	0.01	0.03	0.05	0.01	0.03	0.01
Maximum Error %	± 10 %	± 10%	± 10%	± 10%	± 10%	± 60%	± 20%	± 10%	± 80%	± 30%

Table B-2. One ppm ICP-OES Quality Control checks core 2 sequential extractions. Bold indicates value used to calculate maximum error percentage.

	Zn	Fe	Co	Ni	Cu	Cd	Sb	Pb	As	P	Notes
Trial 1	1.03	0.99	1.02	1.03	1.04	1.02	1.07	1.05	1.21	1.03	
Trial 2	1.03	1.01	1.04	1.05	1.07	1.05	1.10	1.06	1.22	1.05	
Trial 3	1.01	0.98	1.01	1.02	1.04	1.03	1.07	1.03	1.17	1.03	
Trial 4	1.04	1.01	1.04	1.06	1.07	1.05	1.11	1.07	1.22	1.08	
Trial 5	1.05	1.01	1.04	1.06	1.06	1.04	1.09	1.06	1.22	1.08	
Trial 6	1.05	1.02	1.05	1.07	1.06	1.05	1.11	1.07	1.21	1.07	
Trial 7	1.06	1.02	1.05	1.07	1.06	1.05	1.09	1.06	1.23	1.08	
Trial 8	1.04	1.01	1.04	1.06	1.05	1.03	1.09	1.06	1.19	1.05	
Trial 9	1.06	1.04	1.04	1.05	1.06	1.14	1.12	1.08	1.20	1.03	
Trial 10	1.04	1.02	1.04	1.05	1.06	1.11	1.09	1.06	1.13	1.04	
Trial 11	1.06	1.06	1.07	1.08	1.07	1.67	1.12	1.08	1.16	1.04	
Trial 12	1.05	1.04	1.05	1.07	1.06	1.64	1.10	1.07	1.16	1.02	
Trial 13	0.93	0.94	0.96	0.97	0.99	1.51	1.00	0.97	1.02	0.94	
Trial 14	0.94	0.94	0.96	0.96	0.98	1.51	1.01	0.97	1.10	0.93	
Trial 15	0.97	0.99	1.00	1.01	1.03	1.56	1.05	1.01	1.09	0.98	
Trial 16	0.99	1.00	1.01	1.02	1.02	1.57	1.05	*	*	*	*Ran out of standard solution
Average	1.02	1.01	1.03	1.04	1.05	1.25	1.08	1.05	1.17	1.03	
Standard Deviation	0.04	0.03	0.03	0.04	0.03	0.26	0.04	0.04	0.06	0.05	
Maximum Error %	± 7%	± 6%	± 7%	± 8%	± 7%	± 67%	± 12%	± 8%	± 23%	± 8%	

Table B-3. Ten ppm ICP-OES Quality Control checks core 2 sequential extractions. Bold indicates value used to calculate maximum error percentage.

	Zn	Fe	Co	Ni	Cu	Cd	Sb	Pb	As	P
Trial 1	10.10	9.63	9.96	9.99	10.20	10.20	10.10	10.00	10.30	9.99
Trial 2	10.60	10.10	10.40	10.50	10.50	10.40	10.40	10.40	10.70	10.40
Trial 3	10.70	10.00	10.50	10.50	10.40	10.50	10.30	10.40	10.40	10.20
Trial 4	11.20	10.60	10.70	11.00	10.70	10.60	10.70	10.80	10.80	10.70
Trial 5	11.00	10.50	10.60	10.70	10.60	10.40	10.60	10.70	10.70	10.50
Trial 6	10.50	10.40	10.40	10.50	10.60	16.40	10.40	10.50	10.40	10.20
Trial 7	10.60	10.30	10.50	10.60	10.60	16.20	10.50	10.40	10.50	10.10
Trial 8	9.49	9.55	9.51	9.68	9.90	15.10	9.61	9.56	9.58	9.14
Trial 9	9.97	9.99	10.10	10.20	10.30	15.80	10.20	10.10	9.93	9.77
Average	10.46	10.12	10.30	10.41	10.42	12.84	10.31	10.32	10.37	10.11
Standard Deviation	0.53	0.37	0.38	0.39	0.25	2.90	0.32	0.38	0.39	0.46
Maximum Error %	± 12%	± 6%	± 7%	± 10%	± 7%	± 64%	± 7%	± 8%	± 8%	± 8.6%

Table B-4. 0.1 ppm ICP-OES Quality Control checks core 4 sequential extractions. Bold indicates value used to calculate maximum error percentage.

	Zn	Fe	Co	Ni	Cu	Cd	Sb	Pb	As	P
Trial 1	0.10	0.10	0.10	0.10	0.10	0.10	0.12	0.10	0.10	0.10
Trial 2	0.11	0.11	0.11	0.11	0.11	0.11	0.12	0.11	0.11	0.11
Trial 3	0.10	0.10	0.09	0.10	0.10	0.07	0.11	0.10	0.16	0.11
Average	0.10	0.10	0.10	0.10	0.10	0.09	0.12	0.10	0.12	0.11
Standard Deviation	0.01	0.01	0.01	0.01	0.01	0.02	0.01	0.01	0.03	0.01
Maximum Error %	± 10%	± 10 %	± 10%	± 10%	± 10%	± 30%	± 20%	± 10%	± 60%	± 10%

Table B-5. One ppm ICP-OES Quality Control checks core 4 sequential extractions. Bold indicates value used to calculate maximum error percentage.

	Zn	Fe	Co	Ni	Cu	Cd	Sb	Pb	As	P	Notes
Trial 1	1.07	1.06	1.06	1.06	1.06	0.80	1.12	1.08	1.15	1.06	
Trial 2	1.06	1.05	1.06	1.07	1.06	1.09	1.13	1.08	1.13	1.05	
Trial 3	1.06	1.05	1.06	1.06	1.06	1.09	1.12	1.09	1.11	1.06	
Trial 4	1.05	1.05	1.05	1.06	1.05	1.08	1.12	1.08	1.15	1.05	
Trial 5	1.03	1.03	1.03	1.04	1.04	1.05	1.10	1.05	1.09	1.03	
Trial 6	1.07	1.07	1.06	1.08	1.06	1.08	1.11	1.08	1.18	1.07	
Trial 7	1.13	1.12	1.11	1.13	1.11	1.13	1.17	1.13	1.21	1.11	
Trial 8	1.12	1.11	1.12	1.11	1.11	1.11	1.15	1.11	1.21	1.09	
Trial 9	1.04	1.02	1.02	1.04	1.06	1.07	1.07	1.07	1.24	1.12	
Trial 10	1.16	1.06	1.07	1.09	1.02	1.03	1.08	1.12	1.24	1.10	
Trial 11	1.04	1.01	1.00	1.02	1.03	1.01	1.08	1.04	1.15	1.01	
Trial 12	1.07	1.05	1.04	1.07	1.06	1.05	1.11	1.07	1.20	1.02	
Trial 13	1.11	1.08	1.08	1.10	1.08	1.07	1.14	1.10	1.18	1.08	
Trial 14	1.01	0.99	0.99	1.01	1.01	0.99	1.07	1.02	1.10	0.99	
Trial 15	1.04	1.03	1.02	1.05	1.04	0.74	1.10	1.05	1.03	*	*Ran out of Standard Solution
Average	1.07	1.05	1.05	1.07	1.06	1.03	1.11	1.08	1.16	1.06	
Standard Deviation	0.04	0.03	0.04	0.03	0.03	0.11	0.03	0.03	0.06	0.04	
Maximum Error %	± 16%	± 12%	± 12%	± 13%	± 11%	± 26%	± 17%	± 13%	± 24%	± 12%	

Table B-6. Ten ppm ICP-OES Quality Control checks core 4 sequential extractions. Bold indicates value used to calculate maximum error percentage.

	Zn	Fe	Co	Ni	Cu	Cd	Sb	Pb	As	P
Trial 1	10.60	10.70	10.50	10.50	10.40	10.60	10.60	10.40	10.40	10.30
Trial 2	10.60	10.30	10.30	10.40	10.30	10.50	10.40	10.30	10.30	10.10
Trial 3	10.80	10.60	10.60	10.70	10.40	10.60	10.70	10.60	10.70	10.40
Trial 4	11.20	10.90	10.90	11.10	10.70	11.10	11.10	11.00	11.10	10.80
Trial 5	11.30	11.10	11.00	11.00	10.90	11.00	11.20	11.00	11.00	10.80
Trial 6	11.00	10.70	10.60	10.80	10.70	10.50	10.60	10.60	10.80	10.40
Trial 7	11.40	10.80	10.80	11.00	10.70	10.50	10.80	10.80	11.00	10.60
Trial 8	11.30	10.90	10.80	10.90	10.70	10.70	10.80	10.80	10.90	10.50
Trial 9	10.40	10.10	10.00	10.20	9.95	9.86	10.20	9.97	10.10	9.78
Trial 10	10.60	10.30	10.20	10.50	10.20	5.78	10.30	10.10	10.20	9.83
Trial 11	11.20	10.90	10.60	10.90	10.70	10.50	10.70	10.30	10.40	10.10
Average	10.95	10.66	10.57	10.73	10.51	10.15	10.67	10.53	10.63	10.33
Standard Deviation	0.36	0.31	0.31	0.29	0.28	1.48	0.31	0.35	0.36	0.35
Maximum Error %	± 14%	± 11%	± 10%	± 11%	± 9%	± 42.2%	± 12%	± 10%	± 11%	± 8%

Table B-7. ICP-OES analysis of reagent blanks for sequential extractions (in ppm).

	Zn	Fe	Co	Ni	Cu	Cd	Sb	Pb	As	P
Reagent A	0.00	0.00	0.00	0.00	0.00	0.00	0.02	0.00	-0.03	0.01
Reagent B	0.04	0.04	0.00	0.00	0.00	0.00	0.03	0.00	-0.01	0.01
Reagent C	0.52	0.01	0.00	0.00	0.00	0.00	0.02	0.01	-0.08	0.02
Reagent D	0.00	0.00	0.00	0.00	0.00	0.00	0.01	0.00	-0.02	0.00

Table B-8. Community Bureau of Reference (BCR) reference material sequential extraction results. The letter behind the BCR indicates the extract.

	BCR-A Expected	BCR-A	% Change		BCR-C Expected	BCR-C	% Change
Zn	205 ± 6	223	8.8	Zn	45.7 ± 4	<5.0	-
Ni	15.4 ± 0.9	16.2	5.2	Ni	15.3 ± 0.9	17.5	14.4
Cu	49.3 ± 1.7	51.7	4.9	Cu	55.2 ± 4	76.5	38.6
Cd	7.34 ± 0.35	6	-18.3	Cd	0.27 ± 0.06	<5.0	-
Pb	3.18 ± 0.21	3.2	0.6	Pb	9.3 ± 2	11.1	19.4

	BCR-B Expected	BCR-B	% Change		BCR-D Expected	BCR-D	% Change
Zn	126 ± 3	106	-15.9	Zn	95 ± 13	55.8	-41.3
Ni	26.6 ± 1.3	31.2	17.3	Ni	41.4 ± 4	36.1	-12.8
Cu	124 ± 3	109	-12.1	Cu	38.5 ± 11.2	41.0	6.5
Cd	3.77 ± 0.28	<4.0	-	Cd	0.13 ± 0.08	<10.0	-
Pb	126 ± 3	116	-7.9	Pb	11.0 ± 5.2	<10.0	-

Table B-9. 0.1 ppm ICP-OES Quality Control checks core 2 total digestions.

	Zn	Fe	Co	Ni	Cu	Cd	Sb	Pb	As	P
Trial 1	0.09	0.11	0.10	0.10	0.10	0.11	0.09	0.11	0.12	0.13
Maximum Error %	± 10%	± 10 %	± 0%	± 0%	± 0%	± 10%	± 10%	± 10%	± 20%	± 30%

Table B-10. One ppm ICP-OES Quality Control checks core 2 total digestions. Bold indicates value used to calculate maximum error percentage.

	Zn	Fe	Co	Ni	Cu	Cd	Sb	Pb	As	P
Trial 1	1.06	1.04	1.03	1.05	1.05	1.04	1.21	1.06	1.34	1.09
Trial 2	1.01	1.02	1.04	1.05	1.07	1.05	1.17	1.07	1.38	1.09
Trial 3	0.99	1.00	1.00	1.03	0.99	1.00	1.11	1.05	1.31	1.07
Trial 4	1.01	0.99	1.01	1.03	1.00	1.02	1.14	1.05	1.32	1.07
Trial 5	1.04	1.20	1.06	1.08	1.07	1.05	1.16	1.09	1.33	1.11
Trial 6	1.03	1.06	1.03	1.07	1.06	1.04	1.18	1.07	1.32	1.09
Trial 7	1.00	1.06	1.03	1.05	1.04	1.01	1.09	1.05	1.39	1.06
Trial 8	0.97	1.01	1.01	1.04	1.04	1.01	1.12	1.03	1.33	1.06
Average	1.01	1.05	1.03	1.05	1.04	1.03	1.15	1.06	1.34	1.08
Standard Deviation	0.03	0.07	0.02	0.02	0.03	0.02	0.04	0.02	0.03	0.02
Maximum Error %	± 6%	± 20%	± 6%	± 8%	± 7%	± 5%	± 21%	± 9%	± 39%	± 11%

Table B-11. Ten ppm ICP-OES Quality Control checks core 2 total digestions. Bold indicates value used to calculate maximum error percentage.

	Zn	Fe	Co	Ni	Cu	Cd	Sb	Pb	As	P
Trial 1	10.30	10.20	10.20	10.40	10.40	10.10	10.30	10.10	10.50	10.20
Trial 2	10.20	10.30	10.60	10.60	10.60	10.20	10.60	10.30	10.80	10.60
Trial 3	9.99	10.10	10.20	10.30	10.50	10.20	10.40	10.00	10.30	10.30
Average	10.16	10.20	10.33	10.43	10.50	10.17	10.43	10.13	10.53	10.37
Standard Deviation	0.16	0.10	0.23	0.15	0.10	0.06	0.15	0.15	0.25	0.21
Maximum Error %	± 3%	± 3%	± 6%	± 6%	± 6%	± 2%	± 6%	± 3%	± 8%	± 6%

Table B-12. ICP-OES analysis (in ppm) of blanks for core 2 total digestions.

	Zn	Fe	Co	Ni	Cu	Cd	Sb	Pb	As	P
BLANK	0.02	0.00	0.00	0.00	0.01	0.01	0.11	0.03	-0.01	0.00

Table B-13. Community Bureau of Reference (BCR) reference material for total digestions core 2 (in ppm).

	Expected	Result	% Change
Zn	454 ± 19	302	-33.5
Ni	103 ± 4	99.6	-3.3
Cu	275 ± 13	291	5.8
Cd	11.7 ± 1	<40.0	-
Pb	143 ± 6	154	7.7

Table B-14. Duplicate Quality Control on core 2, 1-2 inches (in ppm).

	Result	Duplicate	% Change
Zn	27.7	26.8	-3.3
Fe	6319	6522	3.2
Co	<10.0	<10.0	-
Ni	<10.0	<10.0	-
Cu	17.4	17.9	2.9
Cd	<10.0	<10.0	-
Sb	13.2	<10.0	-
Pb	473	454	-4.0
As	19.4	20.6	6.2
P	80.3	79.9	-0.5

Table B-15. 0.1 ppm ICP-OES Quality Control checks core 4 total digestions.

	Zn	Fe	Co	Ni	Cu	Cd	Sb	Pb	As	P
Trial 1	0.11	0.12	0.11	0.11	0.11	0.11	0.12	0.12	0.18	0.12
Maximum Error %	± 10%	± 20%	± 10%	± 10%	± 10 %	± 10%	± 20%	± 20%	± 80%	± 20%

Table B-16. One ppm ICP-OES Quality Control checks core 4 total digestions. Bold indicates value used to calculate maximum error percentage.

	Zn	Fe	Co	Ni	Cu	Cd	Sb	Pb	As	P
Trial 1	1.03	1.02	1.02	1.04	1.07	0.93	1.11	1.05	1.27	1.03
Trial 2	1.08	1.07	1.06	1.09	1.09	1.08	1.13	1.10	1.27	1.06
Trial 3	1.09	1.05	1.06	1.09	1.09	1.07	1.14	1.09	1.29	1.07
Trial 4	1.11	1.08	1.08	1.10	1.07	0.92	1.10	1.10	1.26	1.09
Trial 5	1.11	1.07	1.06	1.10	1.07	0.71	1.14	1.09	1.27	1.06
Trial 6	1.11	1.09	1.06	1.10	1.08	1.06	1.14	1.11	1.29	1.09
Trial 7	1.12	1.07	1.07	1.10	1.07	1.07	1.13	1.10	1.24	1.09
Average	1.09	1.06	1.06	1.09	1.08	0.98	1.13	1.09	1.27	1.07
Standard Deviation	0.03	0.02	0.02	0.02	0.01	0.14	0.02	0.02	0.02	0.02
Maximum Error %	± 12%	± 9%	± 8%	± 10%	± 9%	± 29%	± 14%	± 11%	± 29%	± 9%

Table B-17. Ten ppm ICP-OES Quality Control checks core 4 total digestions. Bold indicates value used to calculate maximum error percentage.

	Zn	Fe	Co	Ni	Cu	Cd	Sb	Pb	As	P
Trial 1	11.00	10.60	10.70	10.90	10.70	10.90	10.70	10.60	10.80	10.60
Trial 2	11.00	10.70	10.70	10.90	10.70	10.80	10.80	10.70	11.00	10.70
Trial 3	11.30	10.70	10.70	11.00	10.70	10.90	10.80	10.70	11.00	10.70
Trial 4	11.20	10.70	10.70	10.80	10.60	6.54	10.70	10.70	11.00	10.70
Trial 5	11.40	10.90	10.70	11.10	10.60	10.90	10.80	10.80	11.00	10.90
Trial 6	11.40	10.70	10.70	11.10	10.60	10.50	10.80	10.80	10.90	10.80
Average	11.22	10.72	10.70	10.97	10.65	10.09	10.77	10.72	10.95	10.73
Standard Deviation	0.18	0.10	0.00	0.12	0.05	1.75	0.05	0.08	0.08	0.10
Maximum Error %	± 14%	± 9%	± 7%	± 11%	± 7%	± 34.6%	± 8%	± 8%	± 10%	± 9%

Table B-18. ICP-OES analysis (in ppm) of blanks for core 4 total digestions.

	Zn	Fe	Co	Ni	Cu	Cd	Sb	Pb	As	P
BLANK	0.03	0.01	0.00	0.00	0.00	0.00	0.02	0.01	0.03	0.01

Table B-19. Community Bureau of Reference (BCR) reference material for total digestions core 4 (in ppm).

	Expected	Result	% Change
Zn	454 ± 19	317	-30.2
Ni	103 ± 4	86.2	-16.3
Cu	275 ± 13	239	-13.1
Cd	11.7 ± 1	<40.0	-
Pb	143 ± 6	129	-9.8

Table B-20. Duplicate Quality Control on Core 4, 5-6 inches (in ppm). Duplicate run only used 0.25 g of material instead of 0.5 g.

	Result	Duplicate	% Change
Zn	28.4	26.0	-8.5
Fe	11,482	10,558	-8.1
Co	<10.0	<10.0	-
Ni	<10.0	<10.0	-
Cu	<10.0	<10.0	-
Cd	<10.0	<10.0	-
Sb	<10.0	<10.0	-
Pb	49.9	46	-7.8
As	<10.0	<10.0	-
P	113	102	-9.7

SPIKES

Table B-21. One ppm spike of core 4, 6-7 inches Extract C, sequential extraction solution. The sample was spiked with standard solution after digestions, but before analysis. Spike corrected is the concentration after accounting for dilution and spike amount. Sample expected is concentrations obtained from original ICP-OES analysis.

	Zn	Fe	Co	Ni	Cu	Cd	Sb	Pb	As	P
1:10 Spike (1 ppm)	0.24	1.19	0.13	0.11	0.10	0.09	0.13	0.10	0.12	0.10
Spike Corrected	1.37	10.90	0.28	0.12	-0.04	-0.11	0.29	0.04	0.15	-0.02
Sample Expected	0.70	10.90	0.02	0.03	0.05	0.00	0.01	0.13	-0.11	0.21

Table B-22. One ppm spike of core 2, 3-4 inches, total digestion solution. The sample was spiked with standard solution after digestions, but before analysis. Spike corrected is the concentration after accounting for dilution and spike amount. Sample expected is concentrations obtained from original ICP-OES analysis.

	Zn	Fe	Co	Ni	Cu	Cd	Sb	Pb	As	P
1:2 Spike (1 ppm)	1.0	39.5	0.9	1.1	1.2	1.1	1.2	4.2	1.5	1.7
Spike Corrected	1	78	0.8	1.2	1.4	1.2	1.4	7.4	2	2.4
Sample Expected	0.5	73.1	0.0	0.1	0.2	0.0	0.0	6.7	0.1	1.1

Table B-23. Five ppm spike of core 4, 5-6 inches, total digestion solution. The sample was spiked prior to digestions with standard solution. Spike corrected is the concentration after subtracting spike amount. Sample expected is concentrations obtained from original ICP-OES analysis.

	Zn	Fe	Co	Ni	Cu	Cd	Sb	Pb	As	P
Spike (5 ppm)	5.9	115	5.3	5.4	5.3	5.5	2.9	5.9	5.6	6.6
Spike Corrected	0.9	110	0.3	0.4	0.3	0.5	-2.1	0.9	0.6	1.6
Sample Expected	0.3	115	0.0	0.1	0.1	0.0	0.0	0.5	-0.1	1.1

Table B-24. ICP-OES Quality Control for manganese analysis. Maximum error percentage calculated off bolded value.

	0.1 ppm	1 ppm	10 ppm
Trial 1	-0.06	0.88	10.50
Trial 2	-0.06	0.91	10.90
Trial 3	-0.06	0.88	10.80
Trial 4	-0.07	0.88	10.60
Trial 5	-0.06	0.88	10.80
Trial 6	-0.06	0.91	10.60
Trial 7	-0.06	0.90	10.70
Trial 8		0.94	11.00
Trial 9		0.95	11.10
Trial 10		0.89	10.50
Trial 11		0.91	10.90
Trial 12		0.86	10.80
Trial 13		0.94	11.60
Trial 14		0.95	11.30
Trial 15		0.96	10.90
Average		0.91	10.87
Standard Deviation		0.03	0.30
Maximum Error %		± 14%	± 16%

Table B-25. ICP-OES analysis of reagents for manganese (in ppm).

Reagent A	-0.17
Reagent B	-0.17
Reagent C	-0.17
Reagent D	-0.17
Total Digestions	-0.17

APPENDIX C.

SEQUENTIAL EXTRACTION DATASETS

Reagents used for each extract. Refer to Witt et al. (2014) on how to prepare reagents.

Reagent A: 0.11 mol/L acetic acid

Reagent B: 0.5 mol/L hydroxylammonium hydrochloride (made using 2 mol/L HNO₃)

Reagent C: 8.8 mol/L hydrogen peroxide (1.0 mol/L ammonium acetate added after evaporation)

Reagent D: 3 HCl:1 HNO₃ (1 mol/L HNO₃ added after evaporation)

Table C-3. Soil weight and dilution corrected dataset for Core 2, Sequential Extract C (in ppm).

Depth (in.)	Zn	Fe	Co	Ni	Cu	Cd	Sb	Pb	As	P	Mn
Oh	53.4	266	<5.0	<5.0	22.0	<5.0	<5.0	247	<5.0	49.7	<5.0
0-1	37.4	227	<5.0	<5.0	5.1	<5.0	<5.0	84.0	<5.0	31.2	<5.0
1-2	31.6	224	<5.0	<5.0	<5.0	<5.0	<5.0	47.9	<5.0	20.7	<5.0
2-3	31.9	208	<5.0	<5.0	<5.0	<5.0	<5.0	17.9	<5.0	20.5	<5.0
3-4	35.6	170	<5.0	<5.0	<5.0	<5.0	<5.0	44.4	<5.0	28.3	<5.0
4-5	34.5	164	<5.0	<5.0	<5.0	<5.0	<5.0	5.5	<5.0	14.7	<5.0
5-6	28.2	171	<5.0	<5.0	<5.0	<5.0	<5.0	<5.0	<5.0	8.4	<5.0
6-7	27.8	267	<5.0	<5.0	<5.0	<5.0	<5.0	5.3	<5.0	8.7	<5.0
8-9	27.4	241	<5.0	<5.0	<5.0	<5.0	<5.0	7.7	<5.0	7.8	<5.0
10-11	29.1	484	<5.0	<5.0	<5.0	<5.0	<5.0	<5.0	<5.0	<5.0	<5.0
12-13	25.3	583	<5.0	<5.0	<5.0	<5.0	<5.0	<5.0	<5.0	<5.0	<5.0
14-15	26.8	705	<5.0	<5.0	<5.0	<5.0	<5.0	<5.0	<5.0	<5.0	<5.0

Table C-4. Soil weight and dilution corrected dataset for Core 2, Sequential Extract D (in ppm).

Depth (in.)	Zn	Fe	Co	Ni	Cu	Cd	Sb	Pb	As	P	Mn
Oh	133	5684	6.2	10.6	27.0	<5.0	<5.0	82.3	<5.0	58.8	51.1
0-1	24.4	5351	<5.0	5.6	8.7	<5.0	<5.0	16.3	<5.0	51.0	54.5
1-2	21.2	4356	<5.0	5.2	6.1	<5.0	<5.0	9.3	<5.0	32.7	55.5
2-3	21.1	5890	<5.0	6.0	5.2	<5.0	<5.0	<5.0	<5.0	46.0	62.4
3-4	33.9	5356	<5.0	6.7	8.2	<5.0	<5.0	10.1	<5.0	39.5	63.6
4-5	23.8	6422	<5.0	6.6	5.5	<5.0	<5.0	<5.0	<5.0	41.4	68.1
5-6	18.2	6245	<5.0	6.6	5.4	<5.0	<5.0	<5.0	<5.0	29.7	68.9
6-7	18.6	7605	<5.0	7.4	6.5	<5.0	<5.0	<5.0	<5.0	33.2	76.1
8-9	18.8	10,313	<5.0	8.8	8.3	<5.0	<5.0	<5.0	<5.0	41.1	76.0
10-11	21.9	29,283	<5.0	25.6	27.6	<5.0	<5.0	<5.0	<5.0	101	128
12-13	17.0	27,667	<5.0	30.5	31.6	<5.0	<5.0	<5.0	<5.0	50.8	135
14-15	14.0	54,601	<5.0	43.0	53.1	<5.0	<5.0	<5.0	<5.0	109	244

Table C-7. Soil weight and dilution corrected dataset for Core 4, Sequential Extract C (in ppm). Red values indicate values that can reflect error due to manganese quality control results.

Depth (in.)	Zn	Fe	Co	Ni	Cu	Cd	Sb	Pb	As	P	Mn
Oh	100	1123	<5.0	<5.0	63.1	<5.0	<5.0	569	7.9	163	18.7
0-1	51.8	436	<5.0	<5.0	18.3	<5.0	<5.0	224	<5.0	116	<5.0
1-2	39.5	361	<5.0	<5.0	<5.0	<5.0	<5.0	39.0	<5.0	51.6	6.8
2-4	29.1	334	<5.0	<5.0	<5.0	<5.0	<5.0	7.3	<5.0	23.3	10.4
4-5	28.4	248	<5.0	<5.0	<5.0	<5.0	<5.0	<5.0	<5.0	16.7	<5.0
5-6	28.7	338	<5.0	<5.0	<5.0	<5.0	<5.0	7.7	<5.0	12.4	<5.0
6-7	33.7	529	<5.0	<5.0	<5.0	<5.0	<5.0	6.2	<5.0	10.0	<5.0
8-9	32.7	523	<5.0	<5.0	<5.0	<5.0	<5.0	11.3	<5.0	12.2	10.9
10-11	31.0	699	<5.0	<5.0	<5.0	<5.0	<5.0	4.9	<5.0	7.7	8.4
12-13	31.0	601	<5.0	<5.0	<5.0	<5.0	<5.0	<5.0	<5.0	7.8	<5.0
14-15	26.6	503	<5.0	<5.0	<5.0	<5.0	<5.0	<5.0	<5.0	5.5	<5.0

Table C-8. Soil weight and dilution corrected dataset for Core 4, Sequential Extract D (in ppm).

Depth (in.)	Zn	Fe	Co	Ni	Cu	Cd	Sb	Pb	As	P	Mn
Oh	80.5	6025	<5.0	8.0	23.1	<5.0	<5.0	102	<5.0	173	42.4
0-1	79.7	6728	<5.0	8.2	24.9	<5.0	<5.0	34.7	<5.0	131	66.0
1-2	29.4	6202	<5.0	5.4	7.2	<5.0	<5.0	<5.0	<5.0	66.5	62.8
2-4	38.8	8934	<5.0	6.2	<5.0	<5.0	<5.0	<5.0	<5.0	30.3	72.1
4-5	35.1	11,944	<5.0	5.6	<5.0	<5.0	<5.0	<5.0	<5.0	44.1	77.6
5-6	23.2	8233	<5.0	7.1	5.1	<5.0	<5.0	<5.0	<5.0	41.6	84.5
6-7	25.8	13,200	<5.0	8.0	6.3	<5.0	<5.0	<5.0	<5.0	69.9	97.5
8-9	31.2	16,391	<5.0	9.7	8.0	<5.0	<5.0	<5.0	<5.0	90.7	107
10-11	36.8	19,933	<5.0	11.0	9.2	<5.0	<5.0	<5.0	<5.0	69.5	115
12-13	23.0	13,848	<5.0	10.1	6.5	<5.0	<5.0	<5.0	<5.0	51.6	99.0
14-15	14.8	9072	<5.0	7.5	5.1	<5.0	<5.0	<5.0	<5.0	13.7	92.0

Table C-9. Breakdown of lead distribution between extracts in core 2.

Depth (inches)	Total SE Pb (ppm)	Extract A Pb (ppm)	% of Total in Extract A	Extract B Pb (ppm)	% of Total in Extract B	Extract C Pb (ppm)	% of Total in Extract C	Extract D Pb (ppm)	% of Total in Extract D
Oh	5303	2218	41.8	2756	52.0	247	4.7	82.3	1.6
0-1	988	460	46.5	428	43.3	84.0	8.5	16.3	1.6
1-2	488	231	47.3	200	41.0	47.9	9.8	9.3	1.9
2-3	204	109	53.5	76.7	37.7	17.9	8.8	<5.0	--
3-4	705	382	54.2	268	38.0	44.4	6.3	10.1	1.4
4-5	39.2	16.0	40.8	17.7	45.2	5.5	14.0	<5.0	--
5-6	5.8	<0.1	--	5.8	100.0	<5.0	--	<5.0	--
6-7	36.6	12.6	34.4	18.7	51.1	5.3	14.5	<5.0	--
8-9	41.4	15.4	37.2	18.3	44.2	7.7	18.6	<5.0	--
10-11	15.6	6.0	38.5	9.6	61.5	<5.0	--	<5.0	--
12-13	--	<4.0	--	<4.0	--	<5.0	--	<5.0	--
14-15	--	<4.0	--	<4.0	--	<5.0	--	<5.0	--

Table C-10. Breakdown of zinc distribution between extracts in core 2.

Depth (inches)	Total SE Zn (ppm)	Extract A Zn (ppm)	% of Total in Extract A	Extract B Zn (ppm)	% of Total in Extract B	Extract C Zn (ppm)	% of Total in Extract C	Extract D Zn (ppm)	% of Total in Extract D
Oh	200.2	<16.0	--	13.8	6.9	53.4	26.7	133	66.4
0-1	72.9	11.1	15.2	<4.0	--	37.4	51.3	24.4	33.5
1-2	58.5	5.7	9.7	<4.0	--	31.6	54.0	21.2	36.2
2-3	57.1	4.1	7.2	<4.0	--	31.9	55.9	21.1	37.0
3-4	76.7	7.2	9.4	<4.0	--	35.6	46.4	33.9	44.2
4-5	63.4	5.1	8.0	<4.0	--	34.5	54.4	23.8	37.5
5-6	46.4	<4.0	--	<4.0	--	28.2	60.8	18.2	39.2
6-7	46.4	<4.0	--	<4.0	--	27.8	59.9	18.6	40.1
8-9	46.2	<4.0	--	<4.0	--	27.4	59.3	18.8	40.7
10-11	59.0	8.0	13.6	<4.0	--	29.1	49.3	21.9	37.1
12-13	54.8	12.5	22.8	<4.0	--	25.3	46.2	17.0	31.0
14-15	53.0	12.2	23.0	<4.0	--	26.8	50.6	14.0	26.4

Table C-11. Breakdown of copper distribution between extracts in core 2.

Depth (inches)	Total SE Cu (ppm)	Extract A Cu (ppm)	% of Total in Extract A	Extract B Cu (ppm)	% of Total in Extract B	Extract C Cu (ppm)	% of Total in Extract C	Extract D Cu (ppm)	% of Total in Extract D
Oh	110.2	29.4	26.7	31.8	28.9	22.0	20.0	27.0	24.5
0-1	31.0	8.8	28.4	8.4	27.1	5.1	16.5	8.7	28.1
1-2	16.1	4.9	30.4	5.1	31.7	<5.0	--	6.1	37.9
2-3	5.2	<4.0	--	<4.0	--	<5.0	--	5.2	100.0
3-4	18.4	5.2	28.3	5.0	27.2	<5.0	--	8.2	44.6
4-5	5.5	<4.0	--	<4.0	--	<5.0	--	5.5	100.0
5-6	5.4	<4.0	--	<4.0	--	<5.0	--	5.4	100.0
6-7	6.5	<4.0	--	<4.0	--	<5.0	--	6.5	100.0
8-9	8.3	<4.0	--	<4.0	--	<5.0	--	8.3	100.0
10-11	27.6	<4.0	--	<4.0	--	<5.0	--	27.6	100.0
12-13	31.6	<4.0	--	<4.0	--	<5.0	--	31.6	100.0
14-15	53.1	<4.0	--	<4.0	--	<5.0	--	53.1	100.0

Table C-12. Breakdown of lead distribution between extracts in core 4.

Depth (inches)	Total SE Pb (ppm)	Extract A Pb (ppm)	% of Total in Extract A	Extract B Pb (ppm)	% of Total in Extract B	Extract C Pb (ppm)	% of Total in Extract C	Extract D Pb (ppm)	% of Total in Extract D
Oh	4260	138	3.2	3451	81.0	569	13.4	102	2.4
0-1	3123.7	389	12.5	2476	79.3	224	7.2	34.7	1.1
1-2	585	184	31.5	362	61.9	39.0	6.7	<5.0	--
2-4	71.1	13.3	18.7	50.5	71.0	7.3	10.3	<5.0	--
4-5	21.8	5.4	24.8	16.4	75.2	<5.0	--	<5.0	--
5-6	50.5	14.8	29.3	28.0	55.4	7.7	15.2	<5.0	--
6-7	28.8	6.4	22.2	16.2	56.3	6.5	22.6	<5.0	--
8-9	74.7	18.4	24.6	45.0	60.2	11.3	15.1	<5.0	--
10-11	4.9	<4.0	--	<4.0	--	4.9	100.0	<5.0	--
12-13	7.5	<4.0	--	7.5	100.0	<5.0	--	<5.0	--
14-15	--	<4.0	--	<4.0	--	<5.0	--	<5.0	--

Table C-13. Breakdown of zinc distribution between extracts in core 4.

Depth (inches)	Total SE Zn (ppm)	Extract A Zn (ppm)	% of Total in Extract A	Extract B Zn (ppm)	% of Total in Extract B	Extract C Zn (ppm)	% of Total in Extract C	Extract D Zn (ppm)	% of Total in Extract D
Oh	275.7	43.6	15.8	51.3	18.6	100.3	36.4	80.5	29.2
0-1	193.1	40.7	21.1	20.9	10.8	51.8	26.8	79.7	41.3
1-2	88.3	12.7	14.4	6.7	7.6	39.5	44.7	29.4	33.3
2-4	78.1	6.2	7.9	4.0	5.1	29.1	37.3	38.8	49.7
4-5	67.6	4.1	6.1	<4.0	--	28.4	42.0	35.1	51.9
5-6	57.4	5.5	9.6	<4.0	--	28.7	50.0	23.2	40.4
6-7	65.2	5.7	8.7	<4.0	--	33.7	51.7	25.8	39.6
8-9	71	7.1	10.0	<4.0	--	32.7	46.1	31.2	43.9
10-11	73.3	5.5	7.5	<4.0	--	31.0	42.3	36.8	50.2
12-13	54	<4.0	--	<4.0	--	31.0	57.4	23.0	42.6
14-15	41.4	<4.0	--	<4.0	--	26.6	64.3	14.8	35.7

Table C-14. Breakdown of copper distribution between extracts in core 4.

Depth (inches)	Total SE Cu (ppm)	Extract A Cu (ppm)	% of Total in Extract A	Extract B Cu (ppm)	% of Total in Extract B	Extract C Cu (ppm)	% of Total in Extract C	Extract D Cu (ppm)	% of Total in Extract D
Oh	92.3	<4.0	--	6.1	6.6	63.1	68.4	23.1	25.0
0-1	56	<4.0	--	12.8	22.9	18.3	32.7	24.9	44.5
1-2	19.1	4.4	23.0	7.5	39.3	<5.0	--	7.2	37.7
2-4	--	<4.0	--	<4.0	--	<5.0	--	<5.0	--
4-5	--	<4.0	--	<4.0	--	<5.0	--	<5.0	--
5-6	5.1	<4.0	--	<4.0	--	<5.0	--	5.1	100.0
6-7	6.3	<4.0	--	<4.0	--	<5.0	--	6.3	100.0
8-9	8	<4.0	--	<4.0	--	<5.0	--	8.0	100.0
10-11	9.2	<4.0	--	<4.0	--	<5.0	--	9.2	100.0
12-13	6.5	<4.0	--	<4.0	--	<5.0	--	6.5	100.0
14-15	5.1	<4.0	--	<4.0	--	<5.0	--	5.1	100.0

APPENDIX D.

TOTAL DIGESTION DATASETS

Table D-1. Soil weight and dilution corrected dataset for Core 2 Total Digestions (in ppm). Red values indicate values that can reflect error due to manganese quality control results.

Depth (in.)	Zn	Fe	Co	Ni	Cu	Cd	Sb	Pb	As	P	Mn
Oh	184	5939	<10	13.0	103	<10	<10	4743	42.0	186	95.3
0-1	43.2	6121	<10	<10	29.6	<10	<10	971	19.2	96.0	61.8
1-2	27.7	6319	<10	<10	17.4	<10	13.2	473	19.4	80.3	48.8
2-3	26.0	7368	<10	<10	10.5	<10	<10	212	<10	89.2	70.2
3-4	45.2	7295	<10	<10	19.5	<10	<10	673	<10	110	128
4-5	29.7	8227	<10	<10	<10	<10	<10	40.3	<10	90.3	73.6
5-6	19.6	9536	<10	<10	<10	<10	<10	13.3	<10	79.7	39.5
6-7	16.8	10,247	<10	<10	<10	<10	<10	35.4	<10	93.6	47.5
7-8	17.4	12,488	<10	<10	10.1	<10	<10	20.3	<10	95.7	47.0
8-9	19.4	13,182	<10	<10	10.8	<10	<10	40.9	<10	94.9	70.1
9-10	20.2	17,176	<10	11.8	15.7	<10	<10	26.8	<10	105	65.1
10-11	28.7	31,836	<10	25.0	31.8	<10	<10	17.2	<10	126	115
11-12	24.4	25,769	<10	19.6	25.4	<10	<10	<10	<10	116	95.0
12-13	26.8	35,679	<10	31.2	36.2	<10	<10	<10	<10	123	124
13-14	24.5	40,487	<10	30.5	40.1	<10	<10	<10	<10	113	157
14-15	22.9	61,951	<10	41.8	58.9	<10	<10	<10	<10	121	255
15-16	12.3	48,951	<10	24.7	42.5	<10	<10	<10	<10	94.2	68.7

Table D-2. Soil weight and dilution corrected dataset for Core 4 Total Digestions (in ppm). Red values indicate values that can reflect error due to manganese quality control results.

Depth (in.)	Zn	Fe	Co	Ni	Cu	Cd	Sb	Pb	As	P	Mn
Oh	239	7159	<20	16.2	93.3	11.5	16.1	4303	36.1	410	N/A
0-1	145	8037	<10	11.3	62.7	<10	<10	3235	31.5	310	457
1-2	51.1	7700	<10	<10	22.8	<10	<10	577	10.4	145	360
2-4	34.6	8475	<10	<10	<10	<10	<10	74.0	18.5	116	360
4-5	24.4	8815	<10	<10	<10	<10	<10	25.5	<10	104	191
5-6	28.4	11,482	<10	<10	<10	<10	<10	49.9	<10	113	111
6-7	32.6	14,891	<10	<10	<10	<10	<10	22.1	<10	126	85.0
7-8	37.6	19,096	<10	<10	13.0	<10	<10	44.8	<10	159	114
8-9	36.2	17,946	<10	<10	13.0	<10	<10	64.6	<10	163	184
9-10	37.1	21,800	<10	<10	13.4	<10	<10	32.9	<10	178	149
10-11	37.1	23,914	<10	13.4	13.5	<10	<10	<10	<10	170	108
11-12	35.7	22,714	<10	<10	12.5	<10	<10	<10	<10	161	101
12-13	23.3	16,976	<10	<10	<10	<10	<10	<10	<10	119	75.3
13-14	12.5	13,208	<10	<10	<10	<10	<10	<10	<10	59.4	53.6
14-15	15.2	14,955	<10	<10	<10	<10	<10	<10	<10	59.5	73.7

APPENDIX E.

X-RAY DIFFRACTION (XRD) RESULTS

XRD Quantification Equations (Laboratory Procedure)

$$\text{Illite} = \frac{I_{(1G)}}{T} \times 10$$

$$\text{Montmorillonite} = \frac{M_{(1)}}{4T} \times 10$$

$$\text{Chlorite} = \frac{C_{(3)}}{I_{(2)}} \times \frac{I_{(1G)}}{T} \times 10$$

$$\text{Mixed-layer clay minerals} = \frac{I_{(1H)} - \left[I_{(1G)} + \frac{M_{(1)}}{4} \right]}{T} \times 10$$

$$\text{Kaolinite} = \frac{K_{(1)}}{T} \times 10$$

or, if chlorite present

$$= \frac{K_{(2)}}{2C_{(4)}} \times \frac{C_{(3)}}{I_{(2)}} \times \frac{I_{(1G)}}{T} \times 10$$

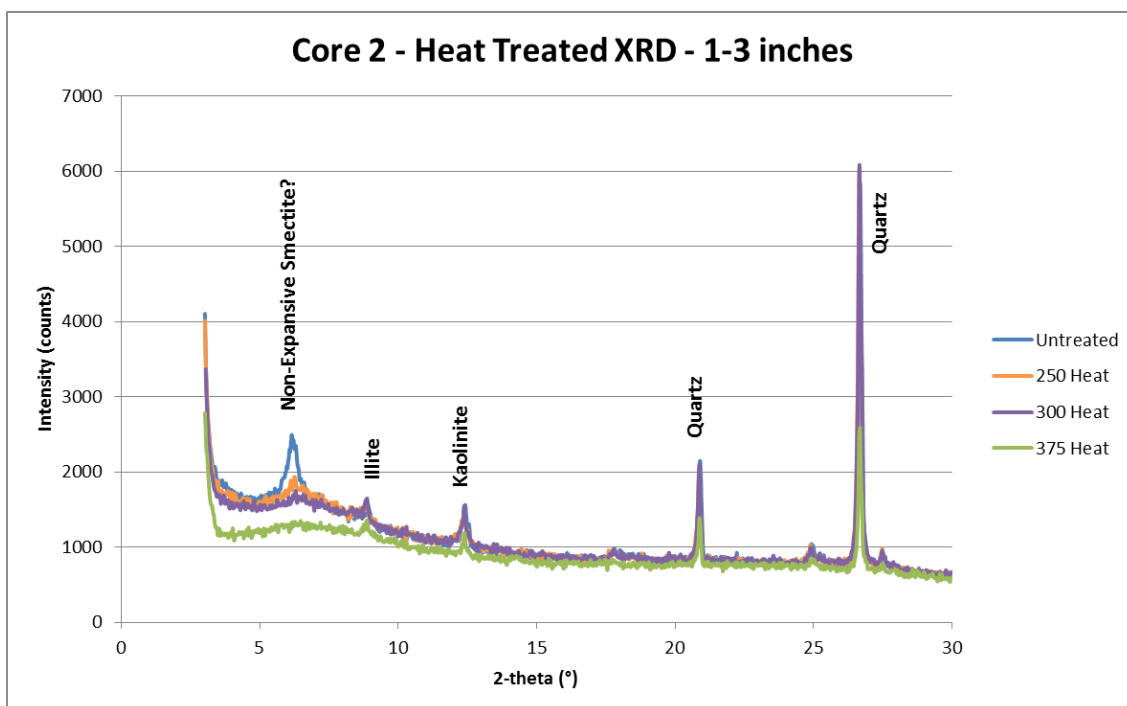
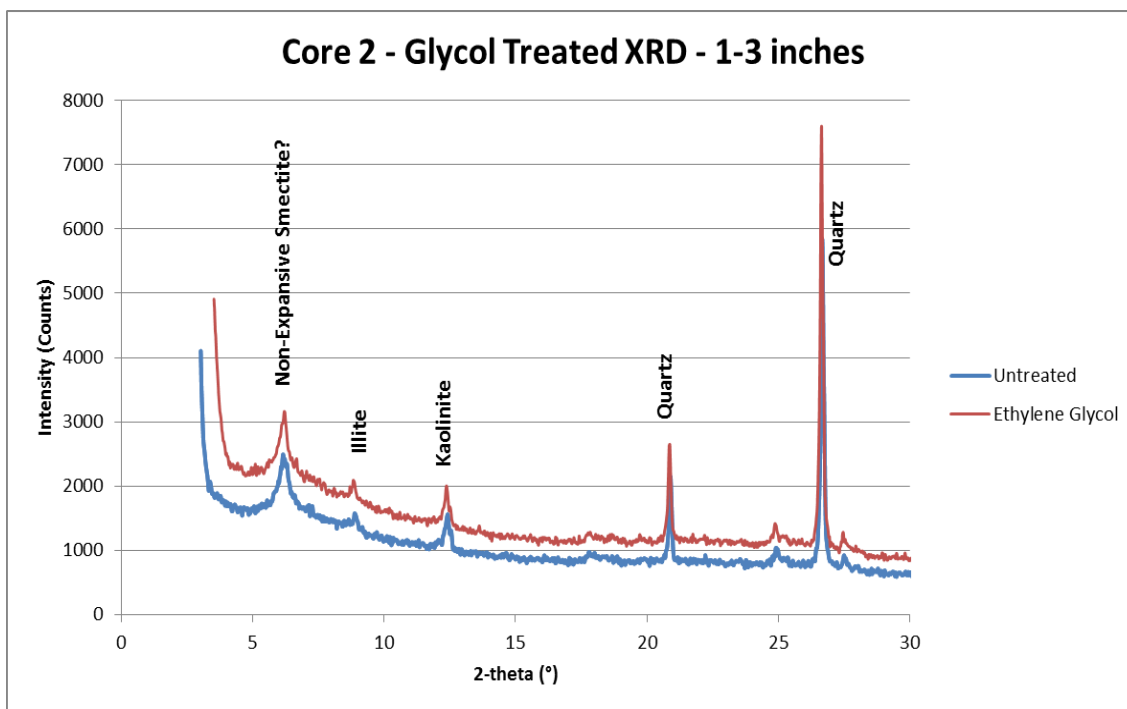
where T is equal to "total counts"

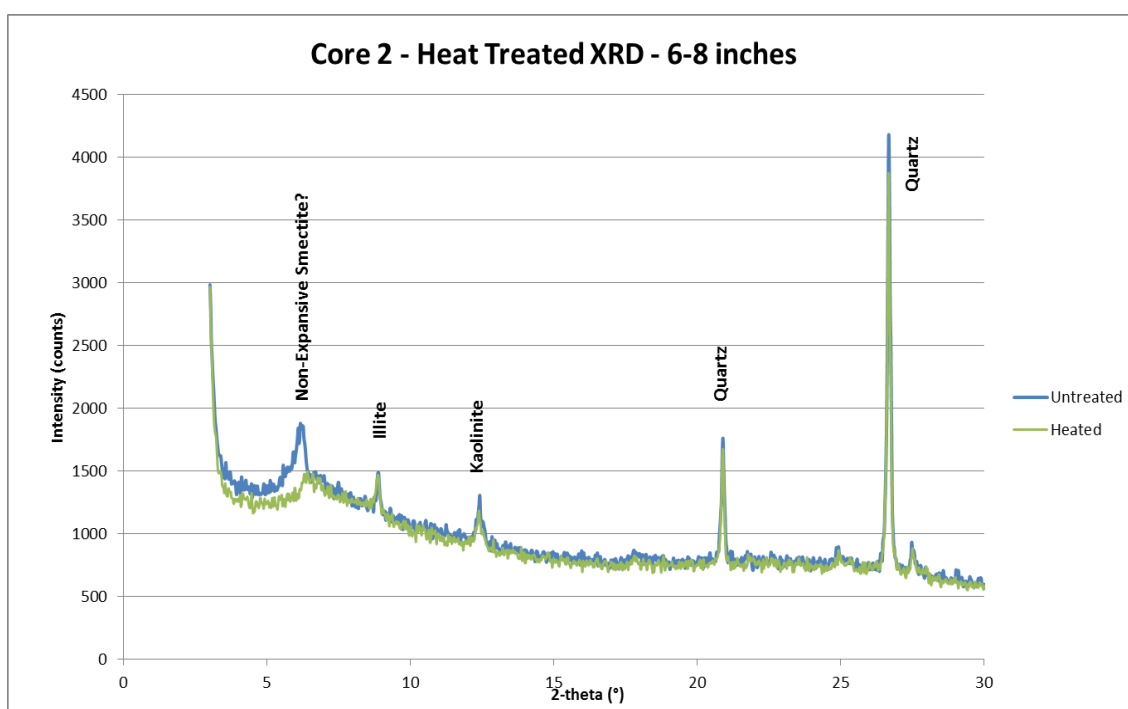
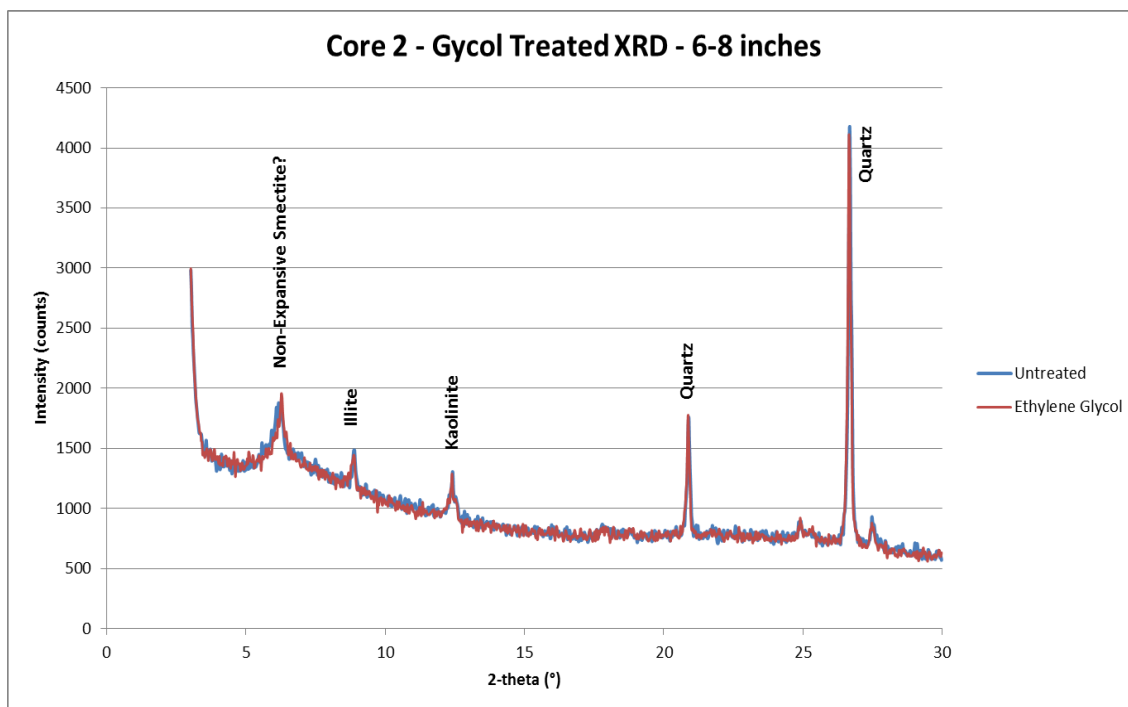
$$T = I_{(1H)} + K_{(1)}$$

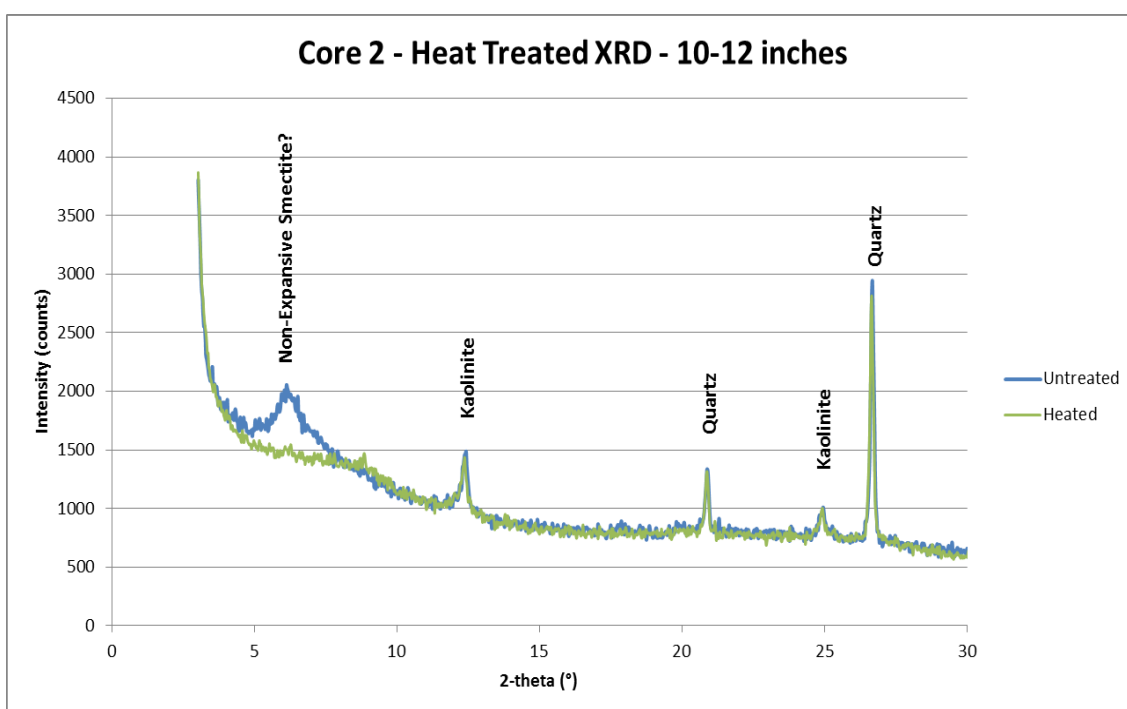
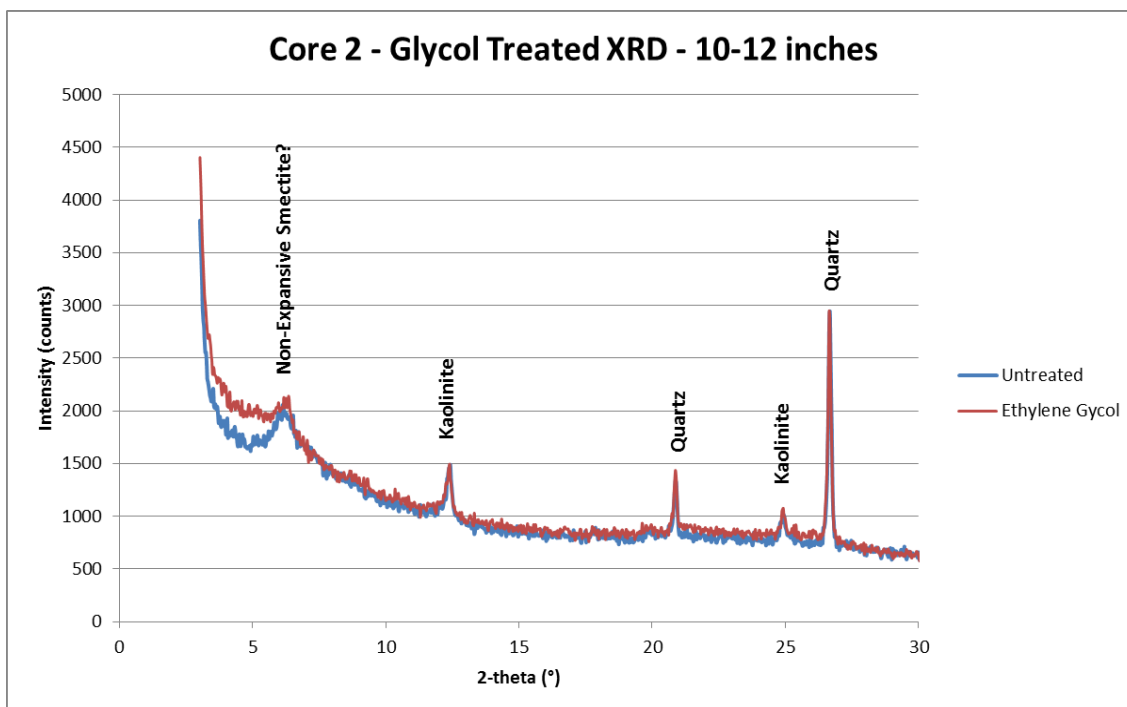
or, if chlorite present

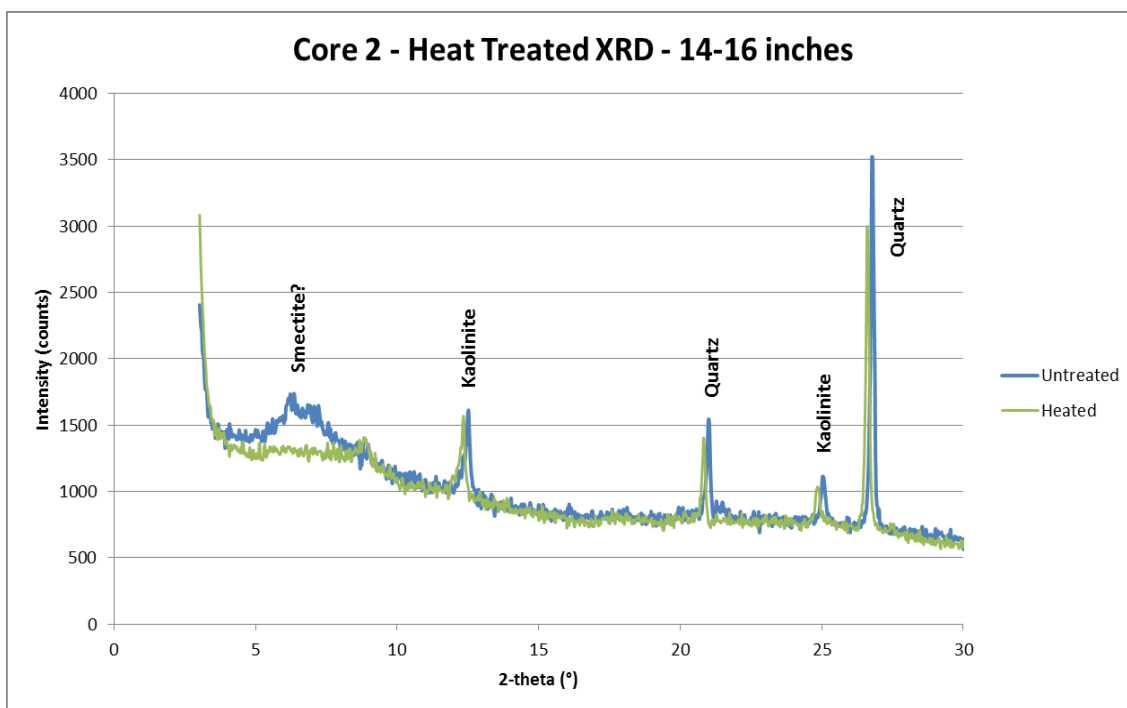
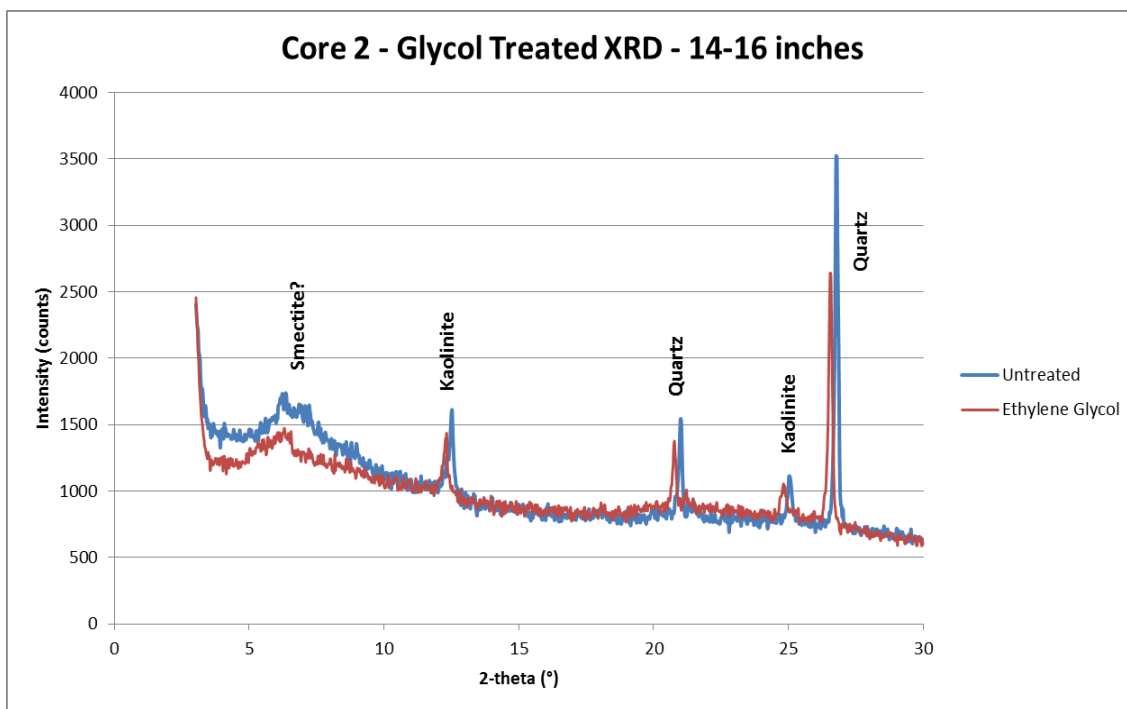
$$T = I_{(1H)} + \left\{ \frac{[C_{(3)}][I_{(1G)}]}{I_{(2)}} \right\} + \left\{ \frac{[K_{(2)}][C_{(3)}][I_{(1G)}]}{[2C_{(4)}][I_{(2)}]} \right\}$$

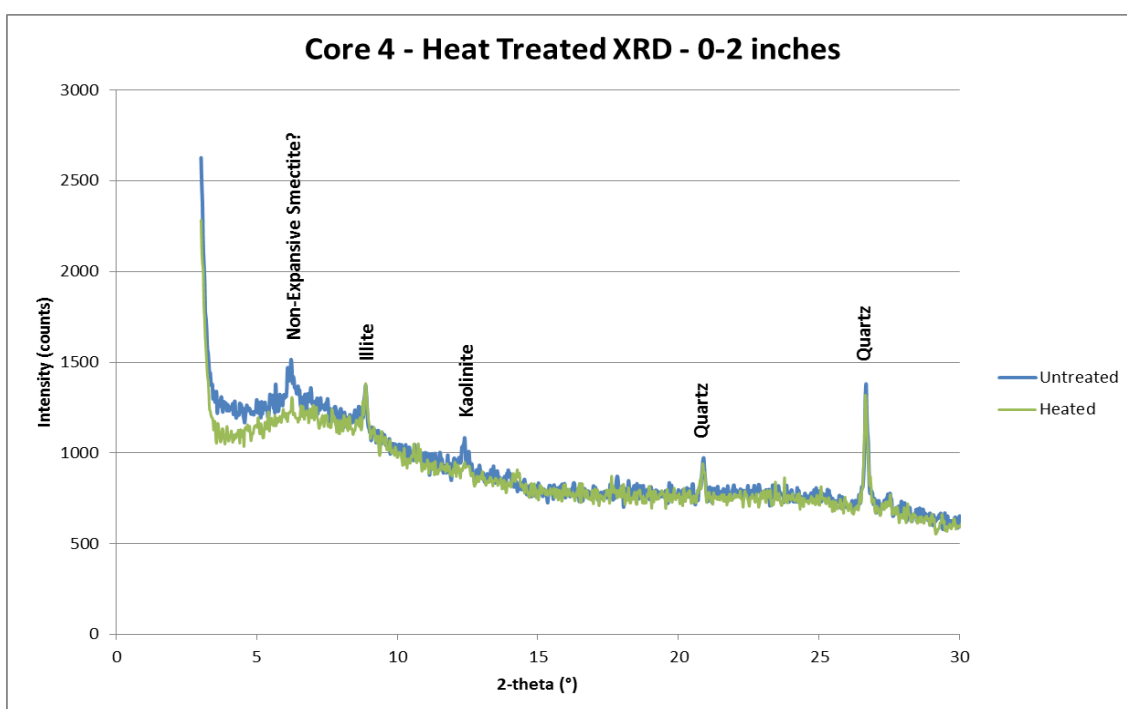
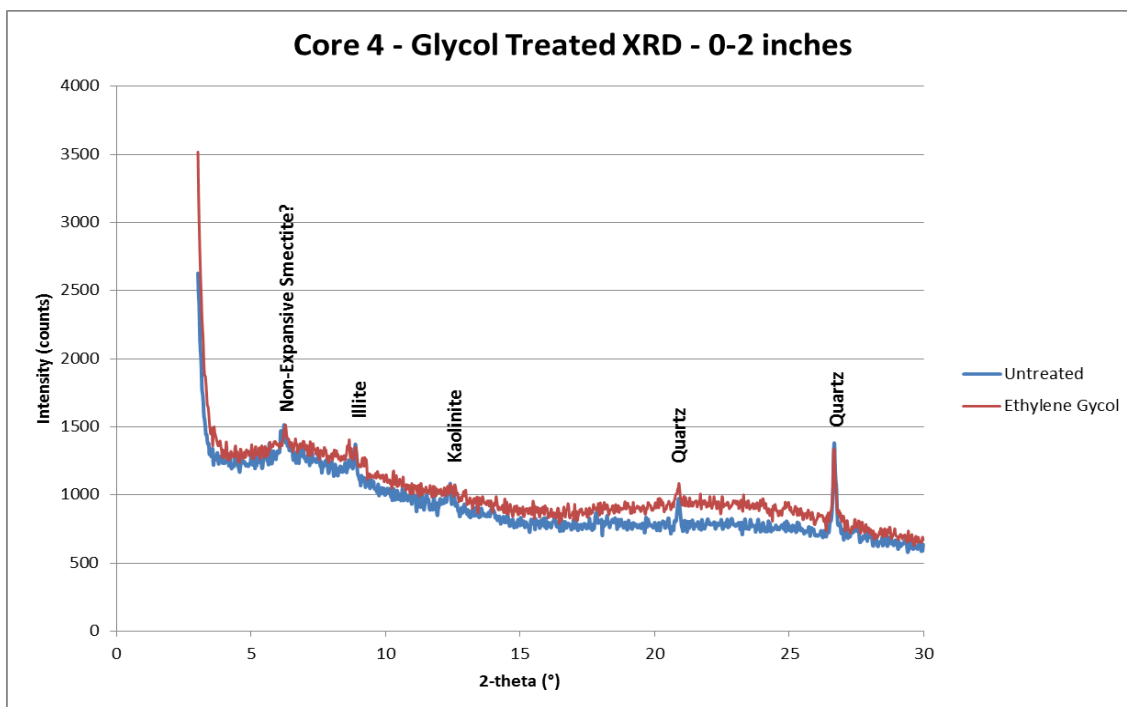
- 1) No treatment rapid scan run at $12.4^\circ 2\theta - K_{(1)}$,
- 2) No treatment rapid scan run $17.8^\circ 2\theta - I_{(2)}$,
- 3) No treatment rapid scan run 18.4° to $18.9^\circ 2\theta - C_{(3)}$;
- 4) No treatment slow scan run at $24.9^\circ 2\theta - K_{(2)}$
- 5) No treatment slow scan run at $25.1^\circ 2\theta - C_{(4)}$;
- 6) Ethylene glycol treated run at $5.2^\circ 2\theta - M_{(1)}$
- 7) Ethylene glycol treated run at $8.8^\circ 2\theta - I_{(1G)}$;
- 8) Heated run at $8.8^\circ 2\theta - I_{(1H)}$.

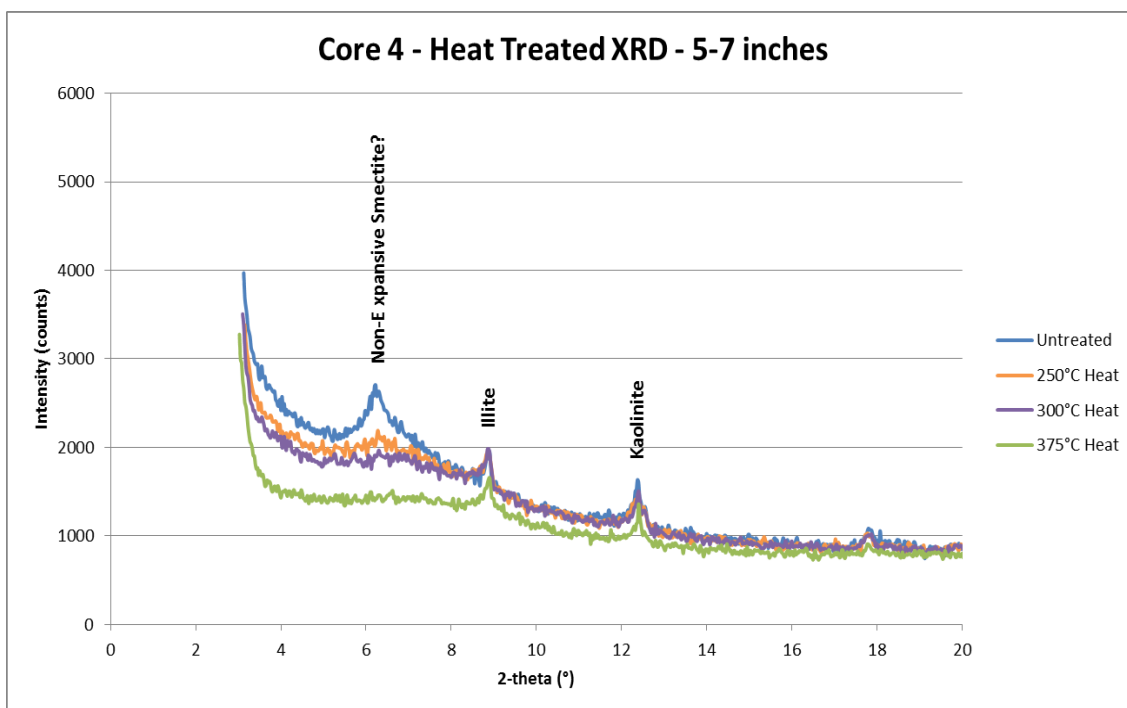
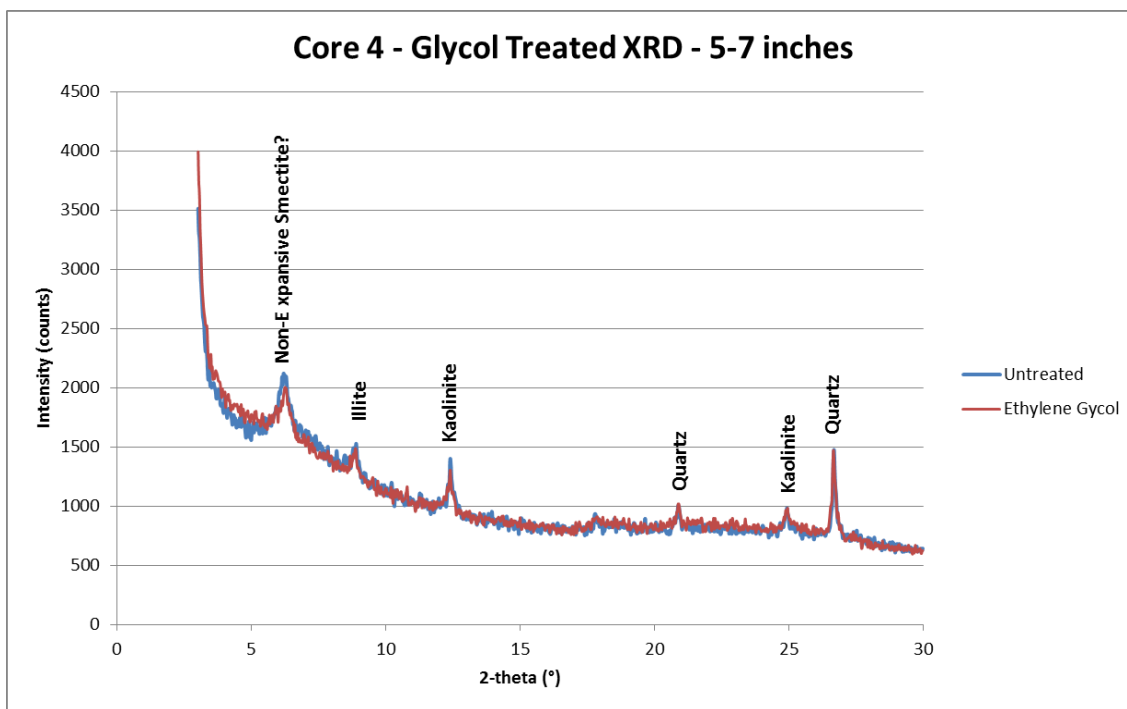


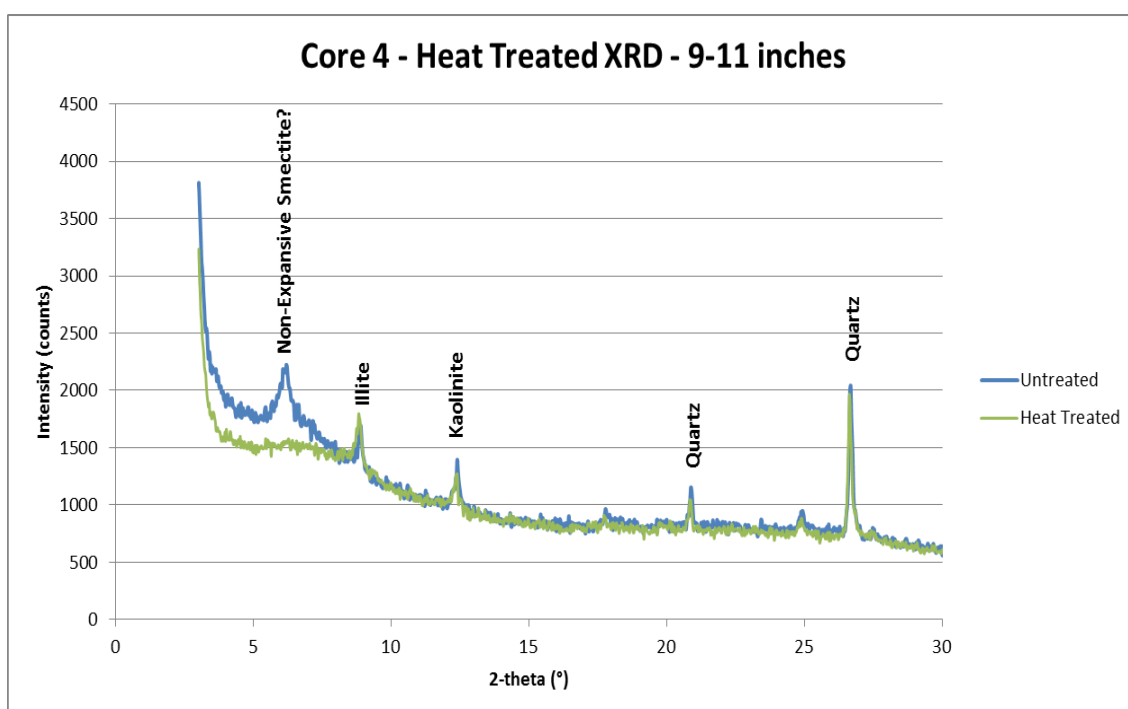
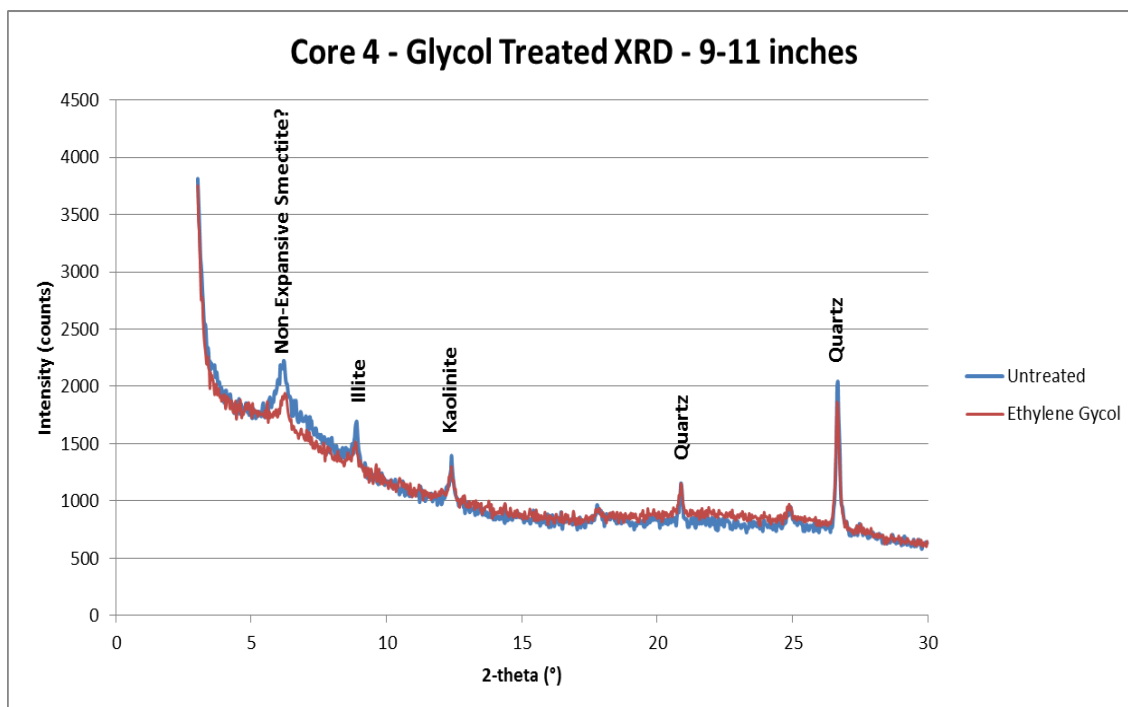


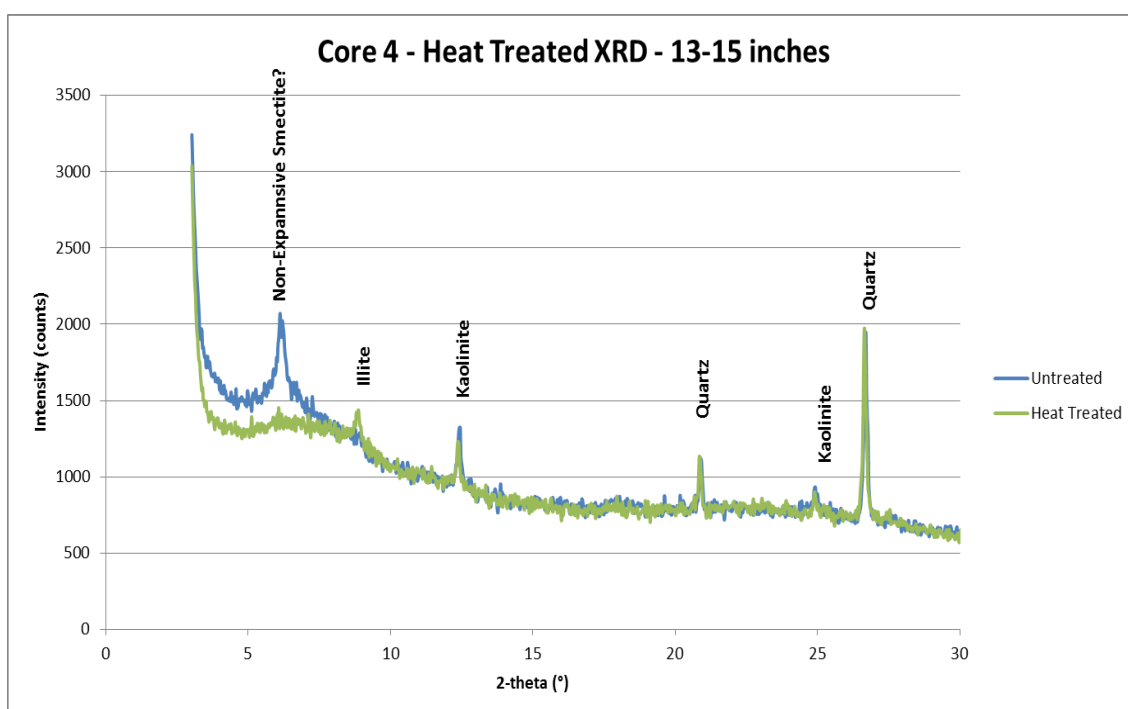
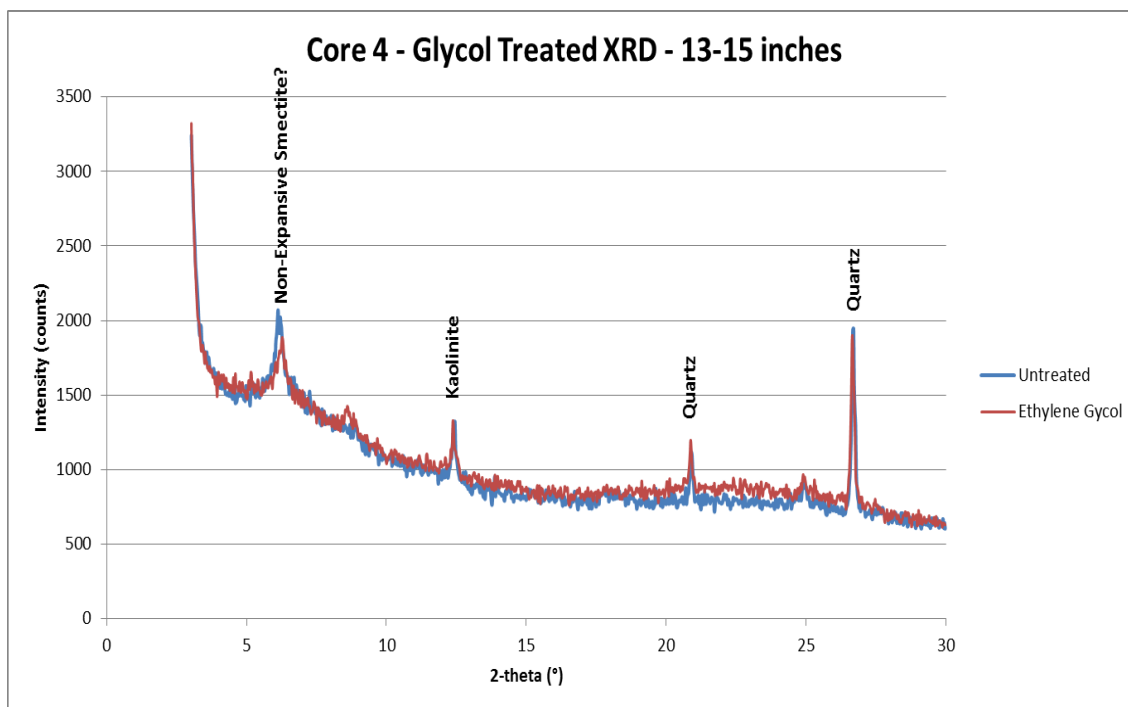












APPENDIX F.

pH DATASET AND QUALITY CONTROL

Table F-1. Table of pH values.

Sample ID	Day 1	Day 2	Day 3	Day 4	Day 5	Day 6	Day 7	Day 8	Average pH of Days 6-8
Core 2, 0h-1"	4.98	5.20	5.12	5.09	5.15	5.20	5.18	5.23	5.20
Core 2, 3-5"	4.47	4.43	4.50	4.42	4.32	4.29	4.29	4.36	4.31
Core 2, 7-9"	4.21	3.98	3.96	3.92	3.82	3.82	3.78	3.85	3.82
Core 2, 11-13"	4.29	4.17	4.11	3.99	3.84	3.80	3.77	3.83	3.80
Core 2, 14-16"	3.85	4.01	3.96	3.95	3.89	3.87	3.91	3.90	3.89
Core 4, 0-2"	4.80	4.94	4.93	5.21	5.45	5.93	5.89	6.02	5.95
Core 4, 4-6"	4.22	4.16	3.94	3.92	3.93	3.88	3.94	3.96	3.93
Core 4, 7-9"	3.97	4.04	3.90	3.87	3.91	3.86	3.91	3.91	3.89
Core 4, 10-12"	4.34	4.29	3.85	3.81	3.80	3.82	3.80	3.86	3.83
Core 4, 13-15"	3.95	4.06	3.91	3.88	3.83	3.89	3.86	3.93	3.89
DIW Blank	6.77	5.30	5.58	5.32	5.48	6.34	6.64	7.03	6.67

Table F-2. Quality Control for pH testing.

									AVG
pH Standard Average (4)*	3.98	4.00	3.98	3.98	3.98	4.01	4.00	4.00	3.99
pH Standard Average (7)*	6.94	6.99	6.96	6.95	6.95	7.00	6.99	6.99	6.97

* Standards were run before and after the soil samples. These values reflect the average of the two.

Standard Deviation of pH Standards (Days 1-8)	4.00	±	0.01
	7.00	±	0.02

Standard Deviation of pH Standards (1 Day)	4.00	±	0.00
	7.00	±	0.01

	Day 1	Day 2	Day 3	Day 4	Day 5	Day 6	Day 7	Day 8
pH Before (4)	4.01	4.01	4.00	3.99	3.98	4.00	4.00	4.02
pH After (4)	3.95	3.99	3.96	3.97	3.98	4.01	3.99	3.98
pH Before (7)	6.97	7.00	6.98	6.97	6.96	7.00	7.00	6.97
pH After (7)	6.90	6.98	6.94	6.92	6.93	7.00	6.97	7.01

BIBLIOGRAPHY

- Adriano, D.C. *Trace elements in terrestrial environments: biogeochemistry, bioavailability, and risks of metals*. Springer, 2001.
- Bolter, E., Wixson, B.G., Butherus, D.L., and Jennett, J.C., 1974, "Distribution of Heavy Metals in Soils Near an Active Lead Smelter." Mining Symposium, University of Minnesota, Duluth, Minnesota, Jan. 17.
- Bornstein, R.E. "Long Term Geochemical Effects of Lead Smelting Within the New Lead Belt, Southeast Missouri." M.S. Thesis. University of Missouri-Rolla, Rolla, Missouri, 1989.
- Bradl, H.B. "Adsorption of heavy metal ions on soils and soils constituents." *Journal of Colloid and Interface Science*. 2004, 277.1, 1-18 and references therein.
- Buchauer, M.J. "Contamination of soil and vegetation near a zinc smelter by zinc, cadmium, copper, and lead." *Environmental Science & Technology*. 1973, 7.2, 131-135.
- Butherus, D.L. "Heavy Metal Contamination in Soils Around a Lead Smelter in Southeast Missouri." M.S. Thesis. University of Missouri-Rolla, Rolla, Missouri, 1975.
- Deer, W.A., Howie R.A., and Zussman, J. *An introduction to the rock-forming minerals*. 2nd ed. Pearson Prentice Hall, 1966.
- The Doe Run Company, 2012 Sustainability Report published online by The Doe Run Company.
- Google Maps, 2014. Accessed online: January 14, 2014.
- Hammel, W., Debus, R., and Steubing, L. "Mobility of antimony in soil and its availability to plants." *Chemosphere*. 2000, 41.11, 1791-1798.
- Hettiarachchi, G.M., and Pierzynski, G.M. "Soil lead bioavailability and in situ remediation of lead-contaminated soils: A review." *Environmental progress*. 2004, 23.1, 78-93 and references therein.
- Jackson, D. R., and Watson A.P. "Disruption of nutrient pools and transport of heavy metals in a forested watershed near a lead smelter." *Journal of Environmental Quality*. 1977, 6.4, 331-338.
- Lindsay, W.L. *Chemical equilibria in soils*. John Wiley and Sons Ltd., 1979.

- Martinez, C. E., and Motto, H.L. "Solubility of lead, zinc and copper added to mineral soils." *Environmental Pollution*. 2000, 107.1, 153-158.
- Martinez-Villegas, N., Flores-Vélez, L.Ma., and Dominguez, O. "Sorption of lead in soil as a function of pH: a study case in México." *Chemosphere*. 2004, 57.10, 1537-1542.
- McBride, M.B. *Environmental Chemistry of Soils*. Oxford University Press, 1994.
- McKenzie, R. M. "The adsorption of lead and other heavy metals on oxides of manganese and iron." *Australian Journal of Soil Research*. 1980, 18.1, 61-73.
- Mulvany, P.S. and Thompson, T.L., editors. "Paleozoic Succession in Missouri, Part 1 (Revised) – Cambrian System: Missouri Department of Natural Resources" *Missouri Geological Survey*. 2013, Report of Investigations 70 part 1 Revised.
- National Institute for Occupational Safety and Health (NIOSH). "NIOSH Pocket Guide to Chemical Hazards, Department of Health and Human Resources (2007)."
- National Weather Service (NWS). *Unique Local Climate Data (for St. Louis area)*. National Oceanic and Atmospheric Administration (NOAA). Unpublished raw data. Accessed online January 28, 2014.
- Nedwed, T. and Clifford, D.A. "A Survey of Lead Battery Recycling Sites and Soil Remediation Processes." *Waste Management*. 1997, 17.4, 257-269 and references therein.
- Prapaipong, P., Enssle, C.W., Morris, J.D., Shock, E.L., and Lindvall, R.E. "Rapid transport of anthropogenic lead through soils in southeast Missouri." *Applied Geochemistry*. 2008, 23.8, 2156-2170.
- Prokop, Z., Cupr, P., Zlevorova-Zlamalikova, V., Komarek, J., Dusek, L., and Holoubek, I. "Mobility, bioavailability, and toxic effects of cadmium in soil samples." *Environmental Research*. 2003, 91.2, 119-126.
- Ragaini, R. C., Ralston, H.R., and Roberts, N. "Environmental trace metal contamination in Kellogg, Idaho, near a lead smelting complex." *Environmental Science & Technology*. 1977, 11.8, 773-781.
- Rauret, G., López-Sánchez, J.F., Lück, D., Yli-Halla, M. Muntau, H., and Quevauviller, P. "BCR Information, Reference Materials, The certification of the extractable contents (mass fractions) of Cd, Cr, Cu, Ni, Pb and Zn in freshwater sediment following a sequential extraction procedure, BCR-701." European Commission, Directorate-General for Research, EUR 19775 EN, 2001.

- Rogers, R. K., and Davis, J.H. "Geology of the Buick Mine, Viburnum Trend, Southeast Missouri." *Economic Geology*. 1977, 72.3, 372-380.
- Ruby, M.V., Davis, A., and Nicholson, A. "In situ formation of lead phosphates in soils as a method to immobilize lead." *Environmental Science & Technology*. 1994, 28.4, 646-654 and references therein.
- Rucker, B.A. *An Investigation of Lead and Other Metal Contaminants in Soil Near the Buick Lead Recycling Smelter, Iron County, Missouri*. M.S. Thesis. University of Missouri-Rolla, Rolla, Missouri, 2000.
- Stevenson, F.J., and Welch, L.F. "Migration of applied lead in a field soil." *Environmental Science & Technology*. 1979, 13.10, 1255-1259.
- Street, J.J., Sabey B.R., and Lindsay, W.L. "Influence of pH, phosphorus, cadmium, sewage sludge, and incubation time on the solubility and plant uptake of cadmium." *Journal of environmental quality*. 1978, 7.2, 286-290.
- Tarbuck, E.J. and Lutgens, F.K. *Earth: An Introduction to Physical Geology*. 9th ed. Pearson Prentice Hall, 2008.
- Taylor, R. M., and McKenzie, R.M. "The association of trace elements with manganese minerals in Australian soils." *Australian Journal of Soil Research*. 1966, 4.1, 29-39.
- Thompson, T.L. "The stratigraphic succession in Missouri – Revised: Missouri Department of Natural Resources." *Division of Geology and Land Survey*. 1995, Volume 40 (2nd Series).
- Tidball, R.R. *Geography of Soil Geochemistry of Missouri Agricultural Soils*. Geochemical Survey of Missouri: U. S. Geological Survey Professional Paper 954 – H, 1 United States Government Printing Office, Washington: 1984.
- United States Department of Agriculture (U.S.D.A), Natural Resources Conservation Service, Soil Survey Staff. Web Soil Survey. Available online at <http://websoilsurvey.nrcs.usda.gov/>. Accessed June 19, 2013.
- United States Department of Agriculture. *Soil Survey of Iron County, Missouri*, U.S.D.A. Soil Conservation Service and Forest Service published report, 1991.
- United States Environmental Protection Agency (USEPA). Standard operating procedure for the digestion of aqueous and solid samples using Method 200.2 Hotblock Digestion Technique Method 200.2, Metal Methods 025, Region 5, Chicago, IL, 2003.

- Witt III, E.C., Wronkiewicz, D.J., Pavlowsky, R.T., and Shi, H. "Trace metals in fugitive dust from unsurfaced roads in the Viburnum Trend resource mining District of Missouri—Implementation of a direct-suspension sampling methodology." *Chemosphere*. 2013, 92.11, 1506-1512.
- Witt III, E.C., Shi, H., Wronkiewicz, D.J., and Pavlowsky, R.T. "Phase portioning and bioaccessibility of Pb in suspended dust from unsurfaced roads in Missouri –A potential tool for determining mitigation response." *Atmospheric environment*. 2014, 88, 90-98.
- Wong, C.S.C., and Li, X.D. "Pb contamination and isotopic composition of urban soils in Hong Kong." *Science of the total environment*. 2004, 319.1, 185-195.
- Wu, J., and Boyle, E.A. "Lead in the western North Atlantic Ocean: Completed response to leaded gasoline phaseout." *Geochimica et Cosmochimica Acta*. 1997, 61.15, 3279-3283.
- Zimdahl, R.L., and Skogerboe, R.K. "Behavior of Lead in Soil." *Environmental Science & Technology*. 1977, 11.13, 1202-1207.

VITA

Krista Nicole Rybacki was born and raised in Nashville, Illinois. In May of 2012, Krista earned a Bachelor of Science degree in Geology and Geophysics from Missouri University of Science and Technology. She graduated Summa Cum Laude with a 4.0 GPA. Additionally, during her time as an undergraduate student, Krista was inducted into the Mines and Metallurgy Academy as an Academy Scholar and awarded the 2012 O.R. Grawe Award by the Association of Missouri Geologists. In May of 2014, she earned her Master's of Science degree in Geology and Geophysics from Missouri University of Science and Technology. During her master's, Krista was a Chancellor's Fellow and was supported by the Chancellor's Fellowship.

Krista plays violin in her spare time, enjoys baking, photography, traveling, weather watching, and hanging out with friends and family. She has one older brother who is also a geologist.

Krista has held a geoscience policy internship at American Geosciences Institute in Alexandria, Virginia. She spent the summer splitting her time working at the office and also on Capitol Hill in Washington D.C. covering U.S. Senate and U.S. House of Representative hearings dealing with the geoscience issues. Through this experience she met and talked with several policy makers and important geoscientists in government agencies.